Development of Novel Methods for Municipal Water Main Infrastructure Integrity Management

by

© Hieu Chi Phan

A thesis submitted to the

School of Graduate Studies

in partial fulfillment of the requirement for the degree of

Doctor of Philosophy (Civil Engineering)

Faculty of Engineering & Applied Science

Memorial University of Newfoundland

May 2019

St. John's, Newfoundland, Canada

Abstract

Water Distribution Network (WDN) is an important component of municipal infrastructure. Many municipal water distribution systems are exposed to harsh environment and subjected to corrosion with age. Many of the water mains in North America are close to or have exceeded their design life and are experiencing a number of issues associated with leaks and breakage of the water mains. Maintaining structural integrity of the water infrastructure with the limited municipal budget has been a challenge. Under this circumstance, the municipalities are focusing on prioritizing their infrastructure for maintenance with optimum utilization of the resources. In this regard, an effective method for prioritizing is required for optimally maintaining the infrastructure integrity. The proposed research focuses on developing risk/reliability based prioritizing methods for water main infrastructure maintenance.

Historic water main break data (i.e. number of breaks per km) is often used to identify breakage patterns in the attempts to reliability assessments of deteriorating water mains. This statistical modelling approach is unable to identify the failure mechanism and have limited use. Physical/mechanistic models are therefore desired for better understanding of the failure mechanisms and reliability assessment of WDN. In the proposed research, mechanics-based model is developed for the reliability assessment of water mains. Existing models for remaining strength assessment of the deteriorating pipelines are first examined to develop improved models. Pipe stress analysis is then performed for the reliability assessment of the pipes based on a stochastic analysis using Monte Carlo simulation.

For prioritizing water mains, system reliability and risk assessment methods are employed. For small WDN, the system failure of the pipeline network is modeled using Fault-Tree Analysis (FTA). The FTA is however tedious for large complex network. For large WDN, a complex network analysis method is employed to determine the potential of network disconnection due to water main break. Algebraic Connectivity (AC) of a complex network analysis is found to effectively represent the robustness and redundancy of WDN. The fluctuation in AC due to water main break could be used to assess the criticality of each pipe segment to the overall structure of the network. The AC then used as a part of overall consequence of the network due to water main breaks. A Fuzzy Inference System is proposed to combine network consequence with other consequence for risk assessment of complex WDN.

In summary, a novel risk/reliability-based method for maintenance of water distribution system is developed in this thesis. In developing this method, mechanics-based failure is considered for reliability assessment and AC from graph theory is used for the consequence assessment of water main break on the overall network. A framework is developed for risk assessment considering the reliability and various consequences.

This dissertation is dedicated to:

My parents, Hien Nhat Phan and Hoi Thi Ngo

My wife, Thuy Thi Hoang

My daughter, Han Tam Phan

My sister, Hien Diu Phan

for their endless love.

Acknowledgement

I would like to acknowledge the support of many individuals, without which, I could not finish this thesis. I indeed wanted to express the thankfulness from depth of my heart to my supervisor, **Dr. Ashutosh Sutra Dhar**, who gave me a chance to start the journey and who was always there to listen, answer, help, sympathize and much more. His guidance throughout my PhD program was valuable not only for the thesis but also for my further work. It was an extreme luck for me when **Dr. Bipul Chandra Hawlader** introduced me to my supervisor back in 2014.

I would like to express my gratefulness to my supervisory committee members, **Dr. Faisal Khan** and **Dr. Premkumar Thodi**, for their valuable comments. I also had valuable instruction and guidance from **Dr. Rehan Sadiq** from The University of British Columbia. My fellow PhD student **Bipul Chandra Mondal** provided helpful support when we collaborated.

The financial support for this thesis had been provided by the Natural Sciences and Engineering Research Council of Canada (NSERC) through its Collaborative Research and Development Grants and the city of Mount Pearl in the province of Newfoundland and Labrador. The city of Mount Pearl provided necessary information regarding their Water Distribution Network along with the past water main break records.

I would like to dedicate this thesis to my mother, **Mrs. Hoi Thi Ngo**, and my father, **Dir. Hien Nhat Phan** who always inspired me to higher study that they did not have the opportunity. I was indebted to my wife who always waiting for me, my sister whose

unceasing support was essential to complete this thesis. And finally, I dedicated this work to my daughter, **Han Tam Phan**.

Contributions from this research

The major contributions of the research in this thesis are listed below:

- A framework has been developed for mechanics-based failure probability/ risk assessment of water distribution network for maintenance prioritization;

- For the mechanics-based failure assessment to use in the above framework, a new stress -based failure assessment model has been developed for Cast Iron watermains using finite element analysis;

- A method has been developed for assessing effect of water main break on the overall network by using the Algebraic Connectivity, a parameter of complex network analysis using graph theory;

- A risk assessment method has been developed aggregating different consequences using a fuzzy inference system and an overall maintenance prioritization framework for water distribution network has been developed considering reliability and risk.

List of Publication[1]

- **Phan, H. C**. and Dhar, A. S., 2016. Pipeline Maintenance Prioritization Considering Reliability and Risk: A Concept Methodology. Journal of Advances in Civil and Environmental Engineering. 3(1): 13-30.

- **Phan, H. C**., Dhar, A. S. and Sadiq, R., 2017. Complex network analysis for water distribution systems by incorporating the reliability of individual pipes. 6th CSCECRC International Construction Specialty Conference, CSCE 2017 Annual General Conference. Vancouver, BC, May 31 - June 3, 2017.

- **Phan, H. C**., Dhar, A. S. and Mondal, B. C., 2017. Revisiting burst pressure models for corroded pipelines. Canadian Journal of Civil Engineering, 44(7), pp.485-494.

- **Phan, H. C**., Dhar, A. S., Thodi, P. and Sadiq, R., 2018. Probability of network disconnection of water distribution system for maintenance prioritization. Journal of Water Supply: Research and Technology-Aqua, 67(3), pp.252-269.

- **Phan, H. C**., Dhar, A. S. and Sadiq, R., 2018. Prioritizing Water Mains for Inspection and Maintenance Considering System Reliability and Risk. ASCE Journal of Pipeline Systems Engineering and Practice. 18:9(3):04018009.

- **Phan, H. C.**, Dhar, A. S., Sadiq, R. and Hu, G., 2018. Managing Water Main Breaks in Distribution Networks – A Risk-Based Decision Making. Under review.

[1] The author of this thesis, Hieu Chi Phan, hold a primary author status for all the studies listed.

Table of Contents

List of Figures

List of Tables

CHAPTER 1. INTRODUCTION

1.1 Background

Municipal water mains are essential infrastructure in modern society, which have been used to supply portable water to city dwellers. Historically, many different pipe materials were developed and used to transport drinking water. Ductile iron and cast iron pipe cover a significant volume of current municipal distribution network. Cast iron pipes and ductile iron pipes account for 56% of total pipe length in US and Canada, which were mostly installed more than 50 years ago (Folkman, 2018). The water distribution systems are aging and subjected to deterioration, causing water main breaks. Cast iron and ductile iron pipes have highest break rates compared to other pipe materials (Folkman, 2018). This led to the use of alternative pipe material such as PVC pipes.

While the alternative materials, which have better resistance properties against corrosion, are gradually used for replacing existing deteriorated pipe or for new installation, most of existing cast iron pipes are in danger because of their high corrosion rate. Municipal investments to maintain the integrity of these water mains are very significant. In this regard, a risk/reliability-based prioritizing of water mains can provide effective utilization of municipal budget for maintaining integrity of WDNs. The risk/reliability-based prioritization process faces various challenges as briefly outlined below.

1. There is lack of data for development of risk and reliability assessment models. Many of the municipalities do not have data collection program. Although the municipality

can keep record of incidents using modern computational system, the leakage or breakage only recorded from a given time, when the incidents are reported or observed. Many technical metrics such as soil resistivity for predicting corrosion are not available in the database.

2. Widely acceptable models are not available for reliability and risk assessment of water mains.

3. WDN failures can lead to different types of consequences such as economic, safety or environment. A proper method is not available to combine these consequences for risk assessment.

4. A pipe failure is commonly considered as an independent event, however, there are interactions between pipe failure events. An acceptable method is currently not available to describe the interaction between the pipe failure events.

5. Even though the risk can sometime be estimated, an acceptable prioritizing plan is difficult to obtain because of it requires a hybrid subjective-objective decision process. Decision makers thus need various tools for helping them to obtain an acceptable maintenance plan.

1.2. Reliability of Water Mains

The reliability or failure probability of infrastructure with age can be represented by the well-known bathtub curve (Fig.1.1) where the failure rate initially decreases as the handing and installation errors are overcome, followed by a constant rate of random

failures during the service life and then an increase of failure rate at the wear out period. The decreasing failure rate period could be ignored for the service life of pipes. The failure process during the constant failure rate period can be assumed as a time-independent Poisson process (Watson et al., 2004). However, the failure process in the wear out period depends on the deterioration of the pipe and the resulting failure mechanisms. Corrosion is considered as the major form of water main deterioration for ductile iron and cast iron water mains that cover majority of water distribution pipes (Folkman, 2018).

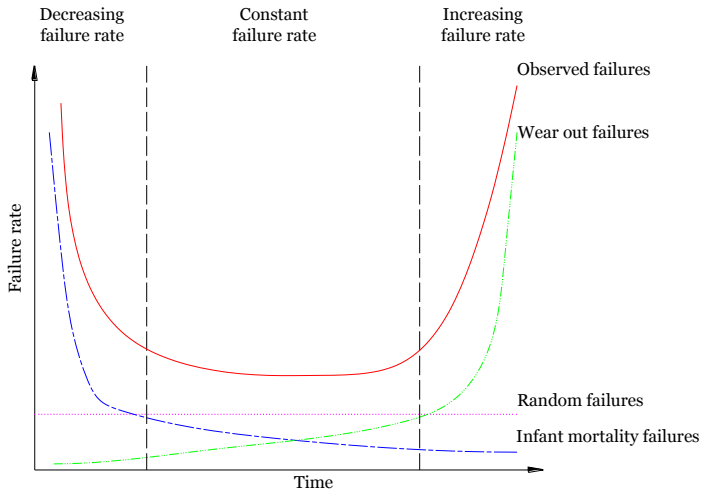

Figure 1.1. The bathtub curve hazard functions of the pipe

(After Watson et al., 2004)

The degradation of water pipe due to corrosion is generally modelled using statistical approach based on prior break data (Kleiner and Rajani 2010). However, the statistical modelling approach does not account for the mechanism of failure of the pipe and have very limited use (Nishiyama and Filion, 2013). Nishiyama and Filion (2013) recommended considering physical/mechanics-based models. Several mechanical models have been

available in literature. Sadiq et al. (2004) and Tee et al (2013) developed models for corroded water mains considering pipe wall stresses. Ji et al (2016) applied fracture mechanics model for probabilistic analysis of pipe with corrosion defects. Fahimi et al. (2016) also conducted fracture mechanics analysis for establishing interaction diagram of buried piped under complex bending condition. The mechanics-based model development requires a proper corrosion propagation model based on long-term observation data and a stress assessment method for corroded pipe. Currently, no simplified method is available for the stress and failure assessment of corroded municipal water main. On the other hand, municipalities often lack resources to collect data that are required for the development of the corrosion models. A combination of mechanics-based and statistic-based techniques along with the Bayesian updating process could be used to deal with municipal water mains.

1.3. Risk Assessment of Water Distribution Network

Various risk assessment methods are available in literature, which can be classified as matrix, probabilistic and indexing approaches, Muhlbauer (2004). The risk models can be either overly simplified or overly complicated. While using less available inputs may result in missing of important information, a model with unnecessary variables may lead to a too complicated model and repeating information. An acceptable model is the one that can thoroughly mine all the data available but use as less inputs as possible.

The risk of overall WDN is sometimes estimated by system reliability (Tung, 1985), which provides a metric to generally evaluate the condition of the network. This metric can

be used for comparison of the conditions of a network with the others. However, it is complicated to calculate system reliability without a proper simplification. Furthermore, prioritizing planning, a major focus of the stakeholder, cannot be performed with the system risk only.

1.4. Motivation of the Research

Due to widespread concerns with the aging municipal water mains, municipalities are moving toward adoption of an advanced reliability/risk-based management practice. The reliability of the overall system can be calculated from the component failure probabilities as a combinatorial problem. The difficulties of defining system failure probability or reliability for real water main network is however well-recognized due to the complexity of the problem. A balance is therefore sought for the reliability assessment that is practical to compute with the one that is expected (Wagner et al., 1988). Several techniques including Fault Tree Analysis (FTA), minimal cut sets, and conditional probability approach were used to examine the pipeline networks references. However, for large networks, these require complex calculation process, huge computational time and idealizing assumptions. In this regard, complex network analysis of graph theory could be used to avoid the large computation while assessing the robustness and redundancy of the networks (Phan et al., 2018a).

Furthermore, consequence estimation for risk assessment is a challenging task for WDN. Amongst the various types of consequences such as economic, environment, etc., the important level of a particular pipe to the well-connectedness of the system is rarely

discussed in literature. There are individual or combination of pipes in the network whose failure may lead to severe disconnection of a part of the network from the water source, or to the reduction of the redundancy of the network. These pipes needed to be identified for effectively maintaining the water mains in WDN. However, no method is currently available for prioritizing pipe in WDN considering the combined effects of network well-connectedness and other consequences of water main break. The author is motivated to address the limitations of the reliability and risk assessment methods and develop improved methods for maintenance of municipal water main infrastructure.

1.5. Research Objectives and Scope

The municipalities commonly employ a reactive approach for maintaining the aging water main infrastructure where a component of the infrastructure is repaired or replaced after failure of the component. This reactive maintenance approach results in an expensive solution as it requires emergency mobilization of crews, causes loss of water due to the water main breaks and may damage nearby facilities by the flowing water. Environment Canada revealed that proactive actions to prevent failure of water mains can provide significant benefits estimated as $3 of saving for every $1 on the proactive actions (Harvey, 2015). For a rational basis of infrastructure maintenance, the Canadian Network of Asset Managers recommends an Asset Management Plan (AMP) that includes a recommendation for establishment of 10 year and long-term renewal plans and strategies to reduce the cost of rehabilitation (Harvey, 2015). In this regard, a risk method is employed through evaluating the risks associated with the failure of infrastructure components. However, it recognizes the considerable uncertainty in quantifying both the probability of failure and

the consequence of water main failure for the risk assessment. With the limitations in mind, a risk-based screening tool is developed with support from Water Research Foundation (WRF), Water Environment Research Foundation (WERF) and U.S. Environmental Protection Agency (EPA) (Grigg et al. 2013). This tool employs an overall likelihood index of failure and an overall consequence score for the risk assessment. It does not account for physical deterioration of the water mains in the failure likelihood (probability of failure) assessment. The effect of water main failure on overall network is not considered for the failure consequence assessment. Therefore, the developed tool is only applicable for investment planning and is not suitable for maintenance planning of aging infrastructure components.

This research focuses on developing a risk-based method for maintenance of water main infrastructure through addressing the limitations in existing methods of failure probability and consequence assessments. A mechanics-based failure assessment model is developed to account for the physical deterioration of the water mains for failure probability assessment. A method of complex network analysis is developed for the assessment of the consequence of water main failure on the overall network.

The following present the specific objectives and scopes of the research.

1. Develop a framework for mechanics-based reliability/risk assessment method for reliability and risk-based maintenance prioritization of WDN.

2. Develop a mechanics-based failure assessment model for reliability assessment of water mains stated in the above objective.

3. Develop a method for the assessment of the effects of water main failure on the overall WDN.

4. Develop risk based prioritizing planning techniques for water main inspection and maintenance combining the effects on overall network with other consequences.

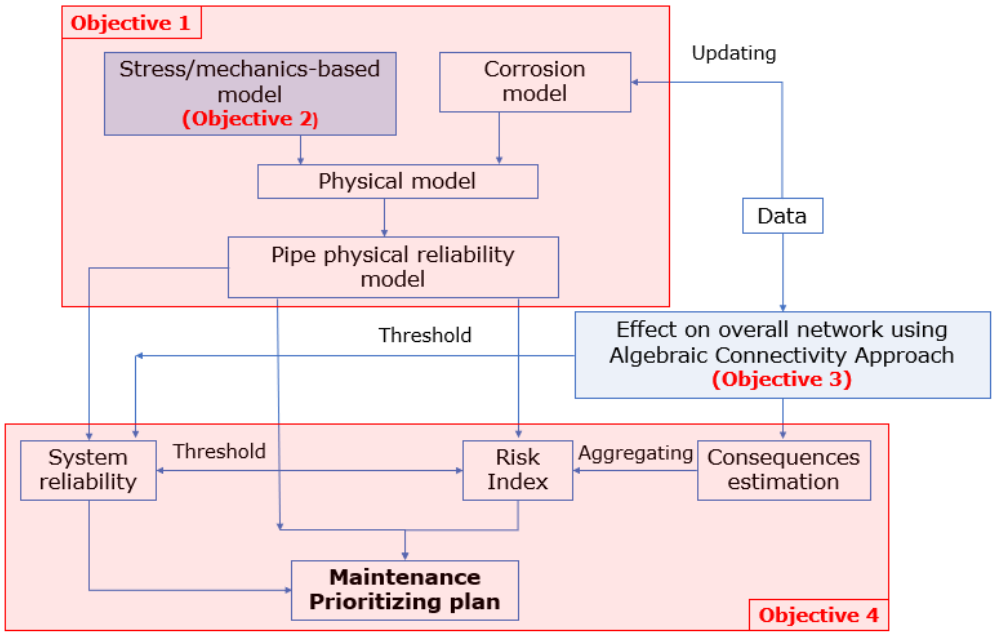

Figure 1.2. Framework of proposed prioritizing plan for WDN

This research develops to advance the risk-based method for maintenance prioritization planning of water distribution network through developing improved methods of failure probability and consequence assessments. The methodology of using the developed failure probability and consequence assessment methods is demonstrated through application to hypothetical and a real water distribution system. The overall risk-based method for maintenance prioritization using the developed methodology is illustrated in Figure 1.2.

As seen in Figure 1.2, a mechanics-based reliability/risk assessment framework is first developed in Objective 1. For the mechanics-based reliability assessment, a failure assessment model for corroded pipes, available for energy pipelines, is employed since a failure assessment model for corroded water main is not available. In Objective 2, a failure assessment model for corroded cast iron water main is developed through a detailed finite element analysis. The research in Objective 3 focuses on developing a method for assessment of consequence on overall water distribution system due to water main breaks. Then, a framework is developed in Objective 4 to combine the consequence on overall water distribution system with other consequences for risk assessment for a reliability/risk-based maintenance program of water distribution system.

1.6. Outline of the Research Methodology

The following presents a brief outline of the methodologies undertaken to achieve the above objectives. A more detail discussion on the research methodologies and results are provided in the subsequent chapters.

Develop a framework for mechanics-based reliability/risk assessment for WDN (Objective 1):

A framework for mechanics-based failure probability assessment is developed through calculation of pipe wall stresses and stochastic degradation. Pipe stress due to external load is calculated using the recommendation of AWWA M45 (2014). The stress due to internal pressure of corroded pipe is calculated using burst pressure model in modified ASME B31G equation (ASME B31G, 2012). It is however recognized that the

modified ASME B31G equation was developed for steel energy pipelines. A burst pressure model applicable for water mains is later developed. The proposed framework is demonstrated through application to reliability and risk assessment of small WDN using conventional Fault Tree Analysis, FTA, for maintenance prioritization. A version of the work has been published in ASCE journal of pipeline system engineering and practice (Phan et al., 2018b).

Development of a mechanics-based failure assessment model for water mains (Objective 2):

As discussed above, the mechanic-based failure assessment of water mains requires stress calculation due to external loads and internal pressure. Currently, no simplified method exists for calculation of stress for corroded pipes. A number of different design equations exists for failure assessment for energy pipeline under internal pressure. However, the equations were reported to be unsuccessful in predicting the burst pressure for energy pipeline. In the current study, the existing burst pressure models for energy pipelines is first revisited using data from Finite Element Analysis (FEA) with application for Differential Evolution (DE) algorithm. The study is then extended through detailed FEA for cast iron water mains to develop simplified equation for burst pressure prediction. A portion of the work has been published in Canadian Journal of Civil Engineering (Phan et al., 2017b).

Effects of water main breaks on overall network (Objective 3):

Considering that the application of conventional FTA method for overall impact assessment on the network is difficult for large WDN, the method of complex network analysis is examined for reliability assessment of WDN. Algebraic Connectivity (AC) of Complex Network Analysis is found to successfully define the network disconnection and robustness. A methodology is developed for reliability assessment of WDN using AC and identifying the critical pipes in the network. The work has been published in Journal of Water supply: Research and Technology (Aqua), Phan et al. (2018a) and in 2017 CSCE annual conference (Phan et al., 2017a).

Risk assessment of WDN due to water main breaks (Objective 4):

Risk assessment for WDN requires quantification of consequence of water main breaks. Water main break results in different economic, environment and social consequences. A Fuzzy Inference System (FIS) is proposed to aggregate different consequences for risk assessment of WDN for maintenance prioritization. The properties of AC are used to assess the topological consequence accounting for the change in redundancy of the network. It is proposed to use consequence parameters for other consequences. This work has been submitted for publication in a journal.

1.7. Organization of the Thesis

This thesis is organized in seven chapters.

Chapter 1 provides a discussion on the research background, objectives of the research and an outline of the methodology.

Chapter 2 provides a discussion on the literature review relevant to the research.

Chapter 3 presents a framework developed for reliability and risk-based prioritization of considering physical deterioration of pipes.

Chapter 4 presents the development of failure assessment model for using in the mechanics-based failure probability assessment of water mains to be used in the framework developed in Chapter 3.

Chapter 5 presents a method for considering the effects of water main breaks on overall WDN.

Chapter 6 introduces a method for risk-based prioritizing of WDN combining difference consequences.

Chapter 7 presents the overall conclusion of the thesis and the recommendations for future work.

CHAPTER 2. LITERATURE REVIEW

2.1. Introduction

Maintaining integrity for WDN has been a concern for the municipalities as water main breaks are increasing with aging water distribution system. Over the last few decades, a number of different approaches were developed for effectively assessing the effects of water main breaks in an attempt to develop a maintenance plan for WDN. Many studies (e.g. Ross, 1985; Cullinane, 1986; Cullinane et al., 1992; Zhuang et al., 2012; Yannopoulos, and Spiliotis, 2013) focused on reliability assessment based on hydraulic availability of the network which is defined as the percentage of time a system can supply water with sufficient hydraulic pressure. The other studies estimated reliability in terms of structural failure probability (e.g. Tung, 1985; Bao and Mays,1990; Sadiq et al., 2004; Deuerlein et al., 2009; Tee and Khan., 2012; Gheisi and Naser., 2013; Barone and Frangopol, 2014). In these approaches, reliability of the overall network distribution system (system reliability) was used to evaluate the well connectedness of the network (Tung, 1985; Cullinane et al., 1992 Lindhe 2008; Yannopoulos and Spiliotis, 2013). It is however difficult to assess reliability of large WDN which contains loops and large number of pipes. Other approach employed is the development of risk/failure probability model for each individual pipe and then total risk/failure probability is obtained using a summation (Kleiner and Rajani 2010, Rogers, 2011). In this approach, pipe failures are assumed to be independent events.

Prior water main break data are often used to develop reliability model for different groups of water mains. However, sufficient data is generally not available to the municipalities to develop the model. The limitations of the pipe break data for statistical model are well recognized, as discussed in more detail in Nishiyama and Filion (2013). A mechanics-based failure modelling approach is recommended to overcome the break data-based model.

2.2. Mechanics-based Failure Modeling

Failure models of water mains are generally developed by using statistical or physical approaches. The statistical approach attempts to mine the break records and other inputs (e.g. age, length, diameter, freezing index, corrosion resistance, soil type etc.) to establish a model based on statistics models. The physical approach employs the mechanism of failure considering the type of loads and the corrosion propagation process. Rajani and Kleiner (2001) suggested that physical models have not been fully developed due to the lack of knowledge of the physical mechanism and limitation of the available data. However, physical or mechanics-based model provides a rational method of failure modelling through understanding the failure mechanisms of pipe.

2.2.1. Physical Failure Mechanisms

Physical failure of pipeline occurs when the wall stress exceeds the capacity of pipe material. Fig.2.1 shows the failure modes of water pipe summarized in Rajani and Kleiner (2001). It can be seen that water pipes suffer from various failure mechanisms depending

on the types of loads and effects such as internal pressure, soil weight, frost load, thermal change, etc.

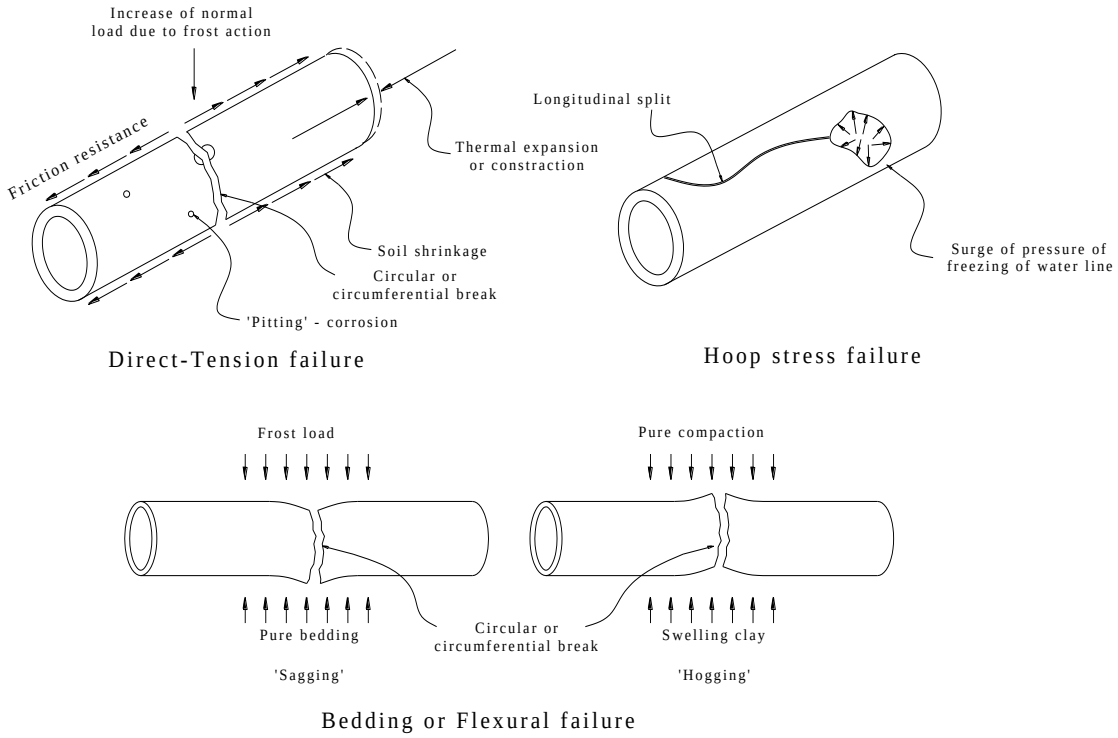

Figure 2.1. Failure modes for buried pipes (After Rajani and Kleiner, 2001)

AWWA (2014) recommends assessing the pipe wall stresses due to the internal pressure and external loads. The combined stress, σ_c, is thus calculated as:

$$\sigma_c = \sigma_0 + \sigma_b \tag{2.1}$$

Where: σ_o is the wall stress due to internal pressure and σ_b is the wall stress caused by ring bending due to external loads.

The pipe wall stress calculated using Eq.2.1 provides the maximum circumferential stress, which would lead to longitudinal cracking on the wall. The equations for pipe wall

stresses in the design code (e.g. Eq. 2.1) are based on uniform thickness of the pipe wall. A uniform corrosion depth over the entire length and the circumference of the pipe is therefore commonly assumed for the failure probability assessment of water mains using the equation for wall stresses (Sadiq et al., 2004, Tee et al., 2013). The remaining thickness of the wall, calculated as the difference between the pipe wall thickness and the corrosion depth, is used in calculation of the pipe wall stress. However, corrosion generally causes thickness reduction within localized (corroded) areas, resulting in the non-uniform wall thickness. The effect of localized wall thickness reduction on the failure probability assessment is considered in the current study.

Fig.2.2 shows localized corrosion defects on the exterior surface of a water main exhumed from the city of Mount Pearl in the province of Newfoundland and Labrador in Canada. The localized corroded area causes stress concentration, resulting in higher stress in vicinity of corrosion that cannot be predicted using the equations proposed in AWWA M45 (2014). However, design codes for energy pipelines (i.e. DNV, 2010, ASME, 2012) account for the stress concentration due to corrosion under internal pressure and provides equation for burst pressure of corroded pipes. The burst pressure models for energy pipes are developed for high strength steel pipes subjected to high internal pressure and therefore may not be applicable for cast iron and ductile iron water pipes having much lower strength than high strength steel. The internal pressures for water mains are also less.

Figure 2.2. Pipe sample exhumed from the city of Mount Pearl showing multiple corroded defects

However, researchers have identified some limitations of the existing burst pressure models for energy pipeline. Hasan et al. (2011) demonstrated through a probabilistic assessment of the remaining strength of corroded pipes that different burst pressure models available in the literature (e.g. ASME B31G, 2012; CSA Z662, 2015 and DNV RP-F101, 2010) provided significantly different failure strengths even with the same defect sizes for particular pipes. Swankie et al. (2012) found the modified ASME (2012) method to provide overestimation of the burst pressure for 35% of the pipes and underestimation for 50% of the pipes they tested. The model error in several existing models was found to affect the burst probability assessment by several order of magnitudes (Zhou and Zhang, 2015). An

improved burst pressure model is therefore desired for accurate failure assessment of the pipelines.

As oil and gas pipelines are operated at high internal pressure, the bursting may occur before the corrosion propagates too deep. For water main, the corrosion depth can be significant before bursting of the pipe occurs since the operating pressure is less. However, if pipe wall is too thin, the minor load from on pipe as concentration load from surrounding soil (e.g. rock pieces) could lead to leakage. The AWWA (2014) standard thus defines the wall thickness less than 20% of original thickness as failure. For assessment of both types of failure the corrosion propagation model is required.

2.2.2. Corrosion Propagation Models

Prediction of the propagation of corrosion with age is required for consideration of the wall thickness reduction for failure probability assessment of pipelines. Rossum (1969) proposed power function models for the prediction of corrosion depth and corrosion rate with time (Eq.2.2 and 2.3, respectively).

$$d(t) = Kt^n \tag{2.2}$$

$$Cr(t) = Knt^{n-1} \tag{2.3}$$

Where d(t) is corrosion depth at time t; Cr(t) is corrosion rate at time t; K and n are constants.

These equations model a fade-out process which has high value magnitude initially and slows down gradually. Corrosion process is generally slowed down with time due to formation of a micro film that acts as a protection layer for the metal. Rossum (1969) has

developed the basic model in Eq.2.3 with the effect of cell potential (E), pH and soil resistivity (ρ) as in Eq.2.4.

$$d(t) = K\left[\frac{(10-pH)t}{\rho}\right]^n \quad (2.4)$$

The self-inhibiting characteristic of corrosion in Rossum (1969) is widely accepted and developed in literature (Mughabghab and Sullivan 1989). Mughabghab and Sullivan (1989) demonstrated that the environment surrounding metal influences the corrosion process. For example, the presence of oxygen accelerates the corrosion rate initially, however, the corrosion rate slows down with time due to formation of $Fe(OH)_3$. They defined the parameters in Eq.2.2 as below:

$K_a = 5.75(9.87 - pH)$ For acidic pH value (2.5)

$K_b = 5.05(2pH - 10.26)$ For basic pH value (2.6)

$n = A_1\theta + A_2CL + A_3$ (2.7)

Where: K_a and K_b are the K constants in Eq.2.3, θ is the moisture content in soil, CL is the clay content in soil, A1, A2, A3 are constant depends on the aeration (Table 2.1).

Table 2.1. Value of A1, A2, A3 in Eq.2.7 (After Mughabghab and Sullivan, 1989).

Aeration	A1	A2	A3
Good	0.57	-0.22	0.02
Fair	2.4	-1.66	0.24
Poor	0.22	-0.48	0.57

Rajani et al (2000 and 2007) proposed two-phase model where the first phase refers to the exponential growing of the defects and the second phase refers to the self-inhibiting of the corrosion process, as in Eq.2.8 and Eq.2.9. Corrosion parameters for the two-phase model are provided in Table 2.2.

$$dt(t) = at + k(1 - e^{-ct}) \quad (2.8)$$

$$Cr(t) = a + kce^{-ct} \quad (2.9)$$

Where: a is the minimum constant rate, c is the inhibition factor, and (a+kc) is the maximum corrosion rate

Table 2.2. Corrosion parameters for two-phase model (After Rajani, 2007)

Soil corrosivity	Corrosion parameter for two-phase model			
	a (mm/year)	k (mm)	c (1/year)	a+kc (mm/year)
Very low (VLC)	0.0042	1.95	0.058	0.1173
Low (LC)	0.0210	9.75	0.058	0.5856
Moderate (MC)	0.0252	11.7	0.058	0.7038
High (HC)	0.0294	13.65	0.058	0.8211
Very high (VHC)	0.0336	15.60	0.058	0.9384

Velazquez et al (2009) allowed a corrosion-free period of time t_0 and defined the corrosion process using Eqs (2.10) and (2.11). The initial time, t_0, is reported to be 3 years, meaning that within the first 3 years, no corrosion will occur.

$$dt(t) = k(t - t_0)^n \quad (2.10)$$

$$Cr(t) = kn(t)^{n-1} \quad (2.11)$$

The constants K and n depend on soil type such as clay, clay loam or sandy clay loam. Pipes in clay and sandy clay loam appeared to have the highest and lowest corrosion rate, respectively. The constants proposed in Velazquez et al (2009) are included in Table 2.3.

Table 2.3. Corrosion parameters (After Velazquez et al., 2009)

Soil type	K	n	t_0
Clay	0.178	0.829	3
Sandy clay loam	0.144	0.734	2.6
Clay loam	0.163	0.793	3.1

Doyle et al (2003) proposed a constant corrosion rate, Cr, depending on the soil characteristics (Eq.2.12). Though soil characteristics (i.e. resistivity, pH, Redox potential, sulfides and moisture) are considered in the analysis, only pH and soil resistivity are found to influence significantly. The constant corrosion rate is commonly considered when long term observation data is not available (Mohebbi and Li, 2011).

$$Cr = 0.6874 - 0.037pH - 0.0887\rho \quad (2.12)$$

Although models were developed for corrosion assessment, as discussed above, it is difficult to obtain a general model applicable for all area because the corrosion process is unique for a particular area corresponding to unique environment. A practical approach is to establish corrosion model for each area or community using the break records within the

area to adjust the parameters in existing models. This process is well-known as Bayesian updating where the posterior distribution of interest (i.e. parameters of corrosion model in this case) is updated based on the prior belief using collected data from WDN.

The Bayesian updating process has been widely applied for various fields including water distribution system (e.g. Watson et al., 2004; Bromley et al., 2005; Wang et al., 2010). Thodi et al. (2010) employed a simplifying approach of estimating the normalizing factor in the basic Bayes's theorem and provided alternative solutions using a Markov chain Monte Carlo (MCMC) method and the Metropolis–Hastings (M-H) algorithm to obtain the posterior distribution of the input variables. Kabir et al. (2016) developed Bayesian Weibull Propositional Hazard Model by periodically using posterior distribution of the previous period as the prior for the next. The updating process is conducted after four periods and then compared with the Cox proportional hazard and Poisson model. The Bayesian inference is commonly incorporated with an optimization algorithm to obtain posterior distribution and the coefficients for the model (Scheidegger et al., 2015).

2.3. Reliability Evaluation of Overall Network

Reliability and risk of WDN system are of great interests for risk and reliability-based maintenance prioritization. However, municipal WDN is a complex system containing thousands of nodes and pipes, leading to the difficulties in evaluating system reliability. The complexity arises from large number of demand nodes, multiple-sources, complex connectivity and inter-dependent components. Consequently, the WDN reliability analyses are commonly performed through simplification incorporating certain basic

assumptions. A common assumption is to ignore the interaction and dependency of the components. Thus, the network failures can be estimated through the failure assessment of individual pipes (e.g. Moglia et al., 2006; Kleiner et al., 2010; Rogers, 2011). Even though this assumption eases the computational process, it may overly simplify the high-density network which contains loops and provides redundancy of supplying water to a given demand node or ignore the important of crucial pipes that their failure can lead to the disconnection of many other pipes.

To model the interaction among pipes, Complex Network Analysis (CNA) of graph theory can be conducted. Complex network analysis was applied in various areas including WDNs for reliability assessment of overall system (Yazdani and Jeffrey, 2010, 2011a, 2011b; Nazempour et al., 2016). Yazdani and Jeffrey (2010) observed metrics of the CNA to evaluate the robustness and vulnerable characteristic of WDN. Nazempour et al. (2016) employed CNA method for optimizing the contaminated sensor locations. Among several metrics provided by CNA, an Algebraic Connectivity (AC) is found to describe network connectivity. The AC is a well-known measure for evaluating the well-connectedness of the graph (Fiedler, 1973; Capocci et al., 2005; Ghosh and Boyd, 2006; Newman, 2006, Yazdani and Jeffrey, 2011a, b). The network with higher AC is more robust or more tolerant to the breakage of links.

2.4. Consequence of Water Main Break

Different approaches are employed to identify the consequence of water main break. NIPP (2013) divided the consequences in to four categories: i) public health and safety, ii)

economic, iii) psychological, and iv) governance/mission impacts. St. Clair and Sinha (2014) pointed out that there are 8 groups of impacts arise from a breakage of a water main. These are environmental, traffic flow, service disruption, time, financial, financial on private property, public health, and other impacts. Baah et al. (2015) employed the relationship of consequences to 11 detailed factors such as road way type, intersecting a railway track, pipe size, pipe burial depth, located downtown, proximity to hospital, distance to building, proximity to river, proximity to park or recreation areas, proximity to bad storm water pipe.

To quantify the failure consequence, both objective and subjective based approaches are used. The subjective approach is carried out based on the evaluation of expert knowledge to score impact factors and then normalize them to have an overall consequence of a pipe failure (Baah et al. 2015, Alidoosti et al. 2012). The objective approach focuses on evaluating specific consequence of the failure. The overall consequence of failure is generally expressed in term of costs. The component costs may vary depending on the purpose of assessment. Sahraoui et al. (2013) and Tee and Khan (2012) modelled the consequence as the cost for inspection, repair and cost of monetary loss if failures occur. Barone and Frangopol (2014) considered consequence as a combination of direct and indirect costs.

In most of the approaches for assessing consequence, the relative topological importance of pipes is not considered. However, the topological important level of a pipe in a network should be considered for the consequence assessment for water main break. If a pipe is broken, it affects the surrounding pipes, demand nodes and to the overall

network. Severity of the effects depends on the location of pipe in the network. Walski (1993) employed hydraulic approach to investigate the effect of water main break on neighboring pipes. To account for the hydraulic effect on neighboring pipes due to water main break, researchers suggest of using hydraulic importance factor for reliability analysis of WDN by topologically decomposing the network (Jun et al., 2008, Yoo et al., 2014, Deuerlein et al., 2009). The topological importance of a pipe is discussed with conducting CNA in Yazdani and Jeffrey (2011) by highlighting the bridge pipes connecting water mains of two communities of a city. Phan et al. (2017a) has observed the critical properties of AC from CNA and then discussed the relationship of importance level with the change of AC due to failure of a particular pipe. They demonstrated that the change in AC can be effectively used for topological importance or topological consequence of water main break, which requires further development.

2.5. Risk Assessment and Decision Planning

Risk is a measure of the probability and the consequence of undesired events to represent human, environmental or economic values. It is commonly expressed as the probability of occurrence times the consequence. In a system, the risk could be for each component, and for the overall system. The system risk can be calculated as the sum of the component risks when the system components behave independently. Due to the complexity with dependent system components, it is a common practice to idealize the components in water main networks to be statistically independent (Tung, 1985; Wagner et al, 1988; Quimpo and Shamsi, 1991).

Muhlbauer (2004) summarized that there are three types of risk models, which are (1) matrix (2) probabilistic and (3) indexing models. The matrix model breakdown risk problem into probability and consequence. A matrix is created with rows and columns corresponding to occurrence probability and consequence of the failure. Then each cell in the matrix is assigned to have a risk evaluation level such as low, medium or high according to its location in the matrix. This approach is overly subjective and not appropriate if there are various factors related to the risk. However, the advantage of this approach is the separation of risk into consequence and probability (Muhlbauer, 2004). This method is being adjusted by incorporating fuzzy techniques. For instance, Tchorzewska-Cieslak (2011) and Wu et al. (2013) developed the traditional risk matrix model by using the Fuzzy Inference System to obtain the risk aggregated from consequence and likelihood.

The probabilistic models attempt to assess all possible failure events through rigorous mathematical and statistical models. This approach requires intensive data and depends heavily on event-tree or fault-tree results, which can be affected by human perception (Muhlbauer, 2004). However, these drawbacks can be improved with the development of data mining techniques, the application of fuzzy method to deal with uncertainty and development of understanding of the failure mechanism. Sadiq et al., (2008) evaluated the risk (e.g. likelihood of failure) of water quality failure by FTA. Hu et al. (2018) used FTA with the application of fuzzy techniques to obtain failure probability/risk of the system.

The indexing models are commonly used in literature where scores and relative weights for items are employed in the risk assessment. The risk index of each pipe segment can be found based on its attributes. A pipe risk index is useful for prioritizing pipe for

maintenance work through highlighting the most significant pipes based on ranking (Muhlbauer, 2004). Researchers employed different risk indexing method for WDN. Fares and Zayed (2010) used 16 risk-of-failure factors with a Fuzzy Inference System to obtain the equivalent impact value for pipe prioritizing plan. Kabir et al. (2015) proposed to use the Bayesian Believe Network along with the updating process to obtain the aggregated risk indexes of each pipes in the system. Kleiner and Rajani (2010) developed a computational tool, an Individual Water mAin Renewal Planner (i.e. I-Warp), which is a risk indexing model, to predict the water main breaks within a given period, then the cost of replacement for a particular pipe is used to optimize the minimum budget for replacement.

2.6. Summary

In this chapter, various research methods employed toward maintaining the integrity of municipal water distribution network are briefly discussed. Researchers employed different approaches of reliability and risk assessments for water main maintenance planning. It is revealed that water main break data is mostly used for structural reliability assessment of water mains. The limitations of this method in reliability assessment are however identified and the use of a mechanics-based method is recommended.

Another challenge is the assessment of effects water main breaks have on the overall network and on the individual pipe segment. Different risk assessment methods accounting for the water main breaks were proposed based on various simplifying assumptions.

In the current research, a framework for reliability assessment method for WDN using mechanics-based method is developed. An innovative risk assessment method is also developed using CNA and Fuzzy Inference System for complex WDN.

CHAPTER 3. A FRAMEWORK FOR MECHANICS-BASED RELIABILITY/RISK ASSESSMENT FOR WDN[2]

3.1. Introduction

Water main infrastructure is a high-value municipal asset that requires regular maintenance in order to ensure optimum performance. However, the municipal budget is often not sufficient to meet investment levels, needed for maintaining the integrity of the deteriorating water mains. Under the circumstances, municipalities focus on prioritizing the assets for maintenance with optimum utilization of resources. Therefore, a rational method is required for prioritizing the infrastructure for inspection and maintenance considering reliability and risk of the pipeline network. Reliability assessment for pipeline network has been used for decades for optimization of water main system. Hydraulic reliability, defined as the probability of providing the demand flow rates at a given point, is employed to design water distribution network and to determine the optimum pipe sizes (Fujiwara and De Silva, 1990; Wagner et al, 1988, Atkinson et al, 2014). Redundancy in the network (increase of connectivity with additional pipe segments) is often used to increase the hydraulic reliability. A reliability assessment with respect to the structural condition of the pipe (i.e., structural reliability) is used for structural integrity assessment of the pipelines. The structural reliability of water main system for inspection and

[2] This chapter is based on the published work in a peer-reviewed journal: Hieu Chi Phan, Ashutosh Sutra Dhar, Rehan Sadiq (2018), "Prioritizing Water Mains for Inspection and Maintenance Considering System Reliability and Risk", Journal of Pipeline Systems Engineering and Practice, ASCE, 9(3), p.04018009 (https://doi.org/10.1061/(ASCE)PS.1949-1204.0000324). The work was carried out, and the paper was drafted by the first author. The work was supervised, and the paper was reviewed by the co-authors.

maintenance planning is the major focus of this chapter and is intended for structural integrity management of the water main network. The presence of redundancy in the water distribution system is thus assumed to have no influence on the structural reliability of a pipe segment or the network.

Historical pipe break data is often used for structural reliability assessment of a pipeline to prioritize water mains for renewal. With the historic data, statistical models are developed to identify the breakage pattern for different types of pipes under various environments. The records of pipe failures or repair events maintained by many water utilities are used in the development of the models. The statistical model avoids the complexity and can be used when data is not available for physical pipe deterioration. A number of research publications exist on reliability and/or risk assessments of the water main infrastructure using this approach (e.g., Rajani et al., 2001; Hu et al., 2013). In most of these publications, statistical deterministic and/or probabilistic models have been developed using historic break data to predict future break rate or failure probability of the pipeline. However, relatively low coefficients of determination are often observed with these models in various regression analyses (e.g., Kleiner and Rajani 2010; Hu et al., 2013). The other challenge with these models is complexity in model structure and unavailability of necessary data required for development of the models. Municipalities often lack resources to collect data that are required for the development of many of the models. Even if the data are available, these may not be perfect for the development of the prediction models. As a result, most of these models are not implemented in the municipal pipeline maintenance planning (Jenkins et al., 2015). Besides, the models assess the risk and/or

reliability for a group of infrastructure asset based on the failure data on similar infrastructure. The approach may be suitable for budget allocation or asset management planning but is not applicable for the maintenance of a specific pipe component in the network since the physical condition/deterioration of the component is not considered. A physical deterioration-based model would usually provide the service lifetime of a specific pipe component.

Rogers (2011) proposed a failure model to apply for specific pipe components using the previous break record of the particular components. Weibull distribution function was employed to determine the time to next failure of the pipe component. A minimum of three break records for a pipe component are required to develop the model. Jenkin et al. (2015) proposed a Weibull hazard rate model for water distribution network that is applicable even if the available data are incomplete. In their model, the expert opinion of a utility professional was elicited to fill the data gap in order to develop and validate the model. The model parameters are determined based on limited data and filling data gaps. A similar approach of using limited data and expert judgement is proposed for failure probability assessment of city gas transmission and distribution system when data information is limited in Liu et al. (2016). This approach thus predominantly employs pipe break data for the development of failure prediction model and does not account for the pipe's mechanical reliability.

However, it is challenging to assess the failure probability of the infrastructure for municipalities with no record of pipe break data. Park et al. (2015) developed a procedural framework for modelling the likelihood of failure for underground pipelines where they

proposed to use a non-probabilistic analysis and/or establish data collection strategy when no data is available to the municipality. Sadiq et al. (2004) and Tee et al. (2013) employed a stochastic method to determine the failure probability of pipeline through assessment of pipe wall stresses considering different established failure modes. The time-dependent reduction of pipe wall thickness is considered deterministically and/or stochastically in the development of the model.

The failure probability of a pipeline can be expressed using either parametric or nonparametric models (Park et al., 2015). The parametric model is generally preferred since it assumes a probability distribution (e.g., Weibull, gamma, exponential etc.) of the reliability, which can be developed with a small sample size. Although the suitability of a distribution function depends on the type of assets and the environmental and operational conditions, Weibull distribution is widely used for infrastructure deterioration modeling including underground pipes (Park et al., 2015, Chookah et al. 2011). Sadiq et al. (2004) examined several distributions such as normal, lognormal, exponential, Weibull, and Hertz distributions to define the failure probability for a water main simulated using Monte Carlo (MC) simulation. The lognormal, Hertz, and Weibull distributions were found to fit well with the simulated data. The Weibull function has been considered in this chapter due to the versatility of the model in characterizing the life cycle of a component using a single equation. The Weibull model also has the flexibility to represent one of the other distribution types using suitable parameters.

In this chapter, a stochastic approach using MC simulation is employed to predict corrosion as an input for the mechanics-based model to assess failure probability. The

failure modes established in the water main design codes (i.e., AWWA 2014) is used for physical assessment of the pipes for the development of the model. It is proposed that a Weibull model be used for each pipe component (based on available information and/or stochastic analysis), which could be updated with the availability of data in the future. A new reliability and risk management approach is proposed for prioritizing water mains for inspection and maintenance. Mechanical failure modes of the pipes are considered for the development of reliability model. The term "reliability" here thus corresponds to "mechanical reliability"

3.2. Weibull Function

A Weibull distribution function is proposed for failure prediction modelling of each pipe component in the network. The probability density function of failure according to Weibull distribution is given by (Eq.3.1):

$$f_i(t) = \frac{\beta_i}{\eta_i}\left(\frac{t-\gamma_i}{\eta_i}\right)^{\beta_i - 1} e^{-\left(\frac{t-\gamma_i}{\eta_i}\right)^{\beta_i}} \tag{3.1}$$

From the Weibull model, reliability function and failure function are defined using Eq.3.2 and Eq.3.3, respectively:

$$R_i(t) = e^{-\left(\frac{t-\gamma_i}{\eta_i}\right)^{\beta_i}} \tag{3.2}$$

$$F_i(t) = 1 - e^{-\left(\frac{t-\gamma_i}{\eta_i}\right)^{\beta_i}} \tag{3.3}$$

Where:

$R_i(t)$: Reliability, at time *t*

$F_i(t)$: Failure probability,

β_i: Shape parameter,

η_i Scale parameter, and

γ_i: Location parameter.

In this model, the location parameter (γ) is proposed to be a variable that could be updated based on future inspection data or expert opinions on the pipe condition when available. For example, if the inspection data or expert opinion indicates a failure probability of a pipe (say "*p*"), the time (t_E) corresponding to the failure probability is first determined from the Weibull function with γ=0. Then, the location parameter, γ corresponding to the pipe condition can be estimated from the relation, $t - \gamma_i = t_E$, where '*t*' is the actual age of the pipe. The location parameter will be negative if the observed failure probability (p) is greater than the failure probability calculated using the initial Weibull function and vice versa. The Weibull function with the new location parameter can be used for subsequent prediction of the failure probability or reliability. Similarly, after undertaking any inspection or maintenance work on a pipe component, the component failure probability can be defined based on the actual pipe condition and the corresponding location parameter can be determined. Thus, the model can be used for future maintenance planning of the existing and the repaired/renewed components. The model parameters of the Weibull model can also be updated when sufficient data would be available. The use

of the model with a mathematical function (Weibull function) would make it easier for use by the water companies, since the failure function can be described using a single variable (i.e., time).

3.3. Failure Function Development

The failure function predicts the probability of failure of a pipeline over a period of time (i.e., with age). The cumulative probability distribution function (CDF) is often used to define the failure probability over time.

The development of the failure function starts with identification of failure modes for a given class of pipeline under an operating environment. Three separate groups of factors leading to asset failure are identified as intrinsic factors, operational factors and operating environment (Park et al., 2015). The intrinsic factors include the pipe structural properties, material type, pipe-soil interaction, and the quality of installation. The operational factors include operating pressure (internal load) as well as the maintenance program undertaken by the municipalities. The operating environment includes temperature, corrosivity, and burial depth. However, it is very difficult to obtain data of these factors and establish relationships to calculate the reliability of the pipes using the factors. Under this situation, a deterministic approach for mechanical failure assessment in combination with a probabilistic method can be used for reliability assessment, which could be updated when information will be available. In this regard, selection of the significant factors leading to pipe failure and identification of the failure modes are required for the determination of the failure function. For metal pipes, corrosion is

considered as the most significant factor contributing to pipe failure. The corrosion can be due to steady and continuous deterioration mechanism of pipe material that may be triggered by the corrosive operating environment. Pipe wall thickness loss due to corrosion may lead to different modes of pipe failure.

Tee and Khan (2013) investigated corrosion-induced failure modes for flexible non-pressure metal pipes that included excessive deflection, buckling, wall thrust and bending stress. They revealed that failure due to wall stress from the thrust and/or bending is the most dominating failure mode. The pipe stress is considered as the major design criteria for water mains (AWWA 2014). AWWA (2014) recommend assessing the pipe wall stresses due to the internal pressure and external load. The stress due to the internal pressure can be expressed as (AWWA 2014):

$$\sigma_0 = \frac{P_{op} D}{2t_w} \tag{3.4}$$

Where:

P_{op}: Internal pressure,

σ_0: Wall stress due to internal pressure P_{op},

D: Pipe diameter, and

t_w: Pipe wall thickness.

The stress due to external load (i.e., earth load and vehicle load) is calculated in terms of ring bending stress, σ_b. The AWWA (2014) recommend calculating the ring bending stress as:

$$\sigma_b = D_f E_p \left(\frac{\left(D_L W_c + W_L\right) K_x}{\frac{E_p I_p}{r^3} + 0.061 M_s} \right) \left(\frac{t_w}{D} \right) \tag{3.5}$$

Where:

σ_b: Wall stress due to bending,

D_f: Shape factor,

D_L: Deflection lag factor,

W_c: Vertical soil load on pipe, calculated as $W_c = \gamma_s H$,

γ_s: Unit weight of soil overburden,

H: Burial depth to top of pipe,

W_L: Live load on pipe, calculated as $W_L = \frac{M_p P I_f}{L_1 L_2}$,

M_p: Multiple presence factor,

P: Wheel load,

I_f: Impact factor,

L_1, L_2: Load width parallel and perpendicular to direction of travel,

K_x: Bedding coefficient,

E_p: Young modulus of pipe material,

I_p: Moment of inertia of unit length of pipe,

M_s: Soil constrained modulus,

r: Radius of pipe,

The combined stress is thus calculated as:

$$\sigma_c = \sigma_0 + \sigma_b \tag{3.6}$$

The pipe wall stress calculated using Eq.3.6 provides the maximum circumferential stress, which would lead to longitudinal cracking on the wall. However, ring fracture is the most common mode of failure generally observed for water mains, particularly for small diameter pipes. It is sometimes assumed that the ring fracture for a small diameter pipe is due to longitudinal bending stress resulting from low moment of inertia of the pipe cross-section. The assumption, however, is not proven. On the other hand, analysis of small diameter pipe with lack of bedding support using finite element analysis indicated higher circumferential stress than the longitudinal stress (Balkaya et al., 2011). Understanding the mechanism of the ring fracture in buried pipe is a subject of further research with the mechanics of soil-pipe interaction. The failure modes recommended in the design code (i.e., AWWA 2014) is considered here for the development of failure function.

The equations for pipe wall stresses in the design code (e.g. Eq.3.4 and Eq.3.5) are based on uniform thickness of the pipe wall. A uniform corrosion depth over the entire length and the circumference of the pipe is therefore assumed for the failure probability assessment of water mains using the equation for wall stresses (Sadiq et al., 2004, Tee et al., 2013). The remaining thickness of the wall, calculated as the difference between the pipe wall thickness and the corrosion depth, is used in the calculation of pipe wall stress. However, corrosion generally causes thickness reduction within localized (corroded) areas,

resulting in the non-uniform wall thickness. The effect of localized wall thickness reduction on the failure probability assessment is considered here as discussed below.

ASME (2012) expresses the remaining strength of corroded pipe with localized corroded area in terms of burst pressure, as:

$$P = P_0 \times \left[\frac{1 - \frac{2}{3}\frac{d}{t_w}}{1 - \frac{2}{3}\frac{d}{t_w}\frac{1}{M}} \right] \tag{3.7}$$

Where:

P_0: Burst pressure of intact pipe,

t_w: Wall thickness,

d: Corrosion depth,

l: Corrosion length,

M: Folias factor, which is given by

$$M = \sqrt{1 + 0.6275\frac{l^2}{Dt_w} - 0.003375\frac{l^4}{D^2 t_w^2}} \qquad For\ \frac{l^2}{Dt_w} \le 50, \quad \text{or}$$

$$M = 0.032\frac{l^2}{Dt_w} + 3.30 \qquad For\ \frac{l^2}{Dt_w} > 50$$

The burst pressure apparently accounts for the pipe wall stress due to the internal pressure. With Eq.3.4, Eq.3.7 can be rearranged to calculate the time-dependent pipe wall stress due to internal pressure, as:

$$\sigma_0(t) = \left[\frac{1 - \frac{2}{3}\frac{d(t)}{t_{w0}}\frac{1}{M(t)}}{1 - \frac{2}{3}\frac{d(t)}{t_{w0}}} \right] \times \frac{P_{op} D}{2t_{w0}} \tag{3.8}$$

Where:

$\sigma_0(t)$: Wall stress in corroded pipe at time '*t*' due to internal pressure P_{op} (MPa),

t: Time (year),

d(t): Depth of corrosion at time t,

M(t): The Folias factor at time t

t_{w0}: Wall thickness before corrosion, at time t=0.

The time-dependent bending stress can be expresses, as:

$$\sigma_b(t) = D_f E_p \left(\frac{(D_L W_c + W_L) K_x}{PS + 0.061 M_s} \right) \left(\frac{t_w(t)}{D} \right) \tag{3.9}$$

$t_w(t)$: Remaining wall thickness at time t, calculate as $t_w(t) = t_{w0} - d(t)$

The time-dependent corrosion depth d(t) can be estimated from the corrosion rate, as:

$$d(t) = d(t - \Delta t) + C_r \Delta t \tag{3.10}$$

Where:

C_r: Corrosion rate (mm/year).

Total stress, $\sigma_c(t)$, calculated using Eq.3.6 is then compared with the maximum allowable stress of the material (generally the yield stress of the material) to define the limit state function as shown below:

$$z(t) = \sigma_y - \sigma_c(t) \tag{3.11}$$

Where:

σ_y : The maximum allowable stress or yield stress,

z(t): Failure function. A pipe is considered to have failed when $z(t) \leq 0$.

Monte Carlo simulation is employed considering the failure modes defined in Eq.3.11 to develop the failure function for each pipe component in the system. The random variables in MC simulation are the maximum allowable stress, corrosion depth, corrosion rate, corrosion length and pipe operating pressure. The depth of corrosion is a time-dependent variable and is used for calculating the pipe failure probability with time.

Fig.3.1 presents the flow chart used for the MC simulation process. In this algorithm, time *'t'* is expressed in year that increases from 1 to a given time *T*. The number of trials within a particular year (time or age) is denoted as *N*. In each trial, random variables of pipe sizes, material capacity, corrosion sizes are generated. Failure can occur if the depth of corrosion is over 80% of the wall thickness as required in AWWA M45 (2014) for leak control condition. If the depth of corrosion is less than 80% of the wall thickness, then the combined stress is calculated, and the magnitude of failure function is checked (i.e.

Eq.3.11). A failure is recorded if the failure function is negative. The probability of failure at that time *t* is determined by counting the number of failures in *N* simulation (Eq.3.12).

$$P(t) = \frac{N_{failure}(t)}{N} \tag{3.12}$$

Where, $P(t)$ is the failure probability of a pipe component at time "*t*", $N_{failure}(t)$ is the number of failure (i.e. number of trials with $z(t)<0$) at time '*t*' counted within *N* trials.

The CDF of failure probability of pipeline from the MC simulation (CDF-MC) is thus obtained against the time (i.e., pipe age). A three-parameter Weibull model (Eq.3.1) is then fitted with the data from CDF-MC using Least Square Error (LSE) method.

The failure probability of the overall system can then be calculated from the component failure probabilities as a combinatorial problem. The difficulties of defining system failure probability or reliability for real water main network is however well-recognized due to the complexity of the problem. A balance is therefore sought for the reliability that is practical to compute with the one that is expected (Wagner et al. 1988). In this regard, the system configuration must be examined individually to determine how the component failures can lead to the failure of the system. Several techniques including Fault Tree Analysis (FTA), minimal cut sets, and conditional probability approach can be used to examine the pipeline network. FTA is one of the methods extensively used for analyzing complex system including water main network (Wagner et al. 1988, Tung 1985). A complex network can be simplified using network reduction method (Quimpo and Shamsi, 1991) and analyzed using the FTA or other methods. Tung (1985) examined the

method of FTA along with other techniques for evaluating reliability of a simple looped water distribution system with independent system components. All of the methods were found to provide practically same system reliability. Tung (1985) however indicated that the FTA is not widely used for topological type of system. The present research focuses on the structural reliability assessment for pipeline inspection and maintenance and does not involve any topological assessment of the water main network. FTA is therefore considered suitable for the system reliability assessment presented here.

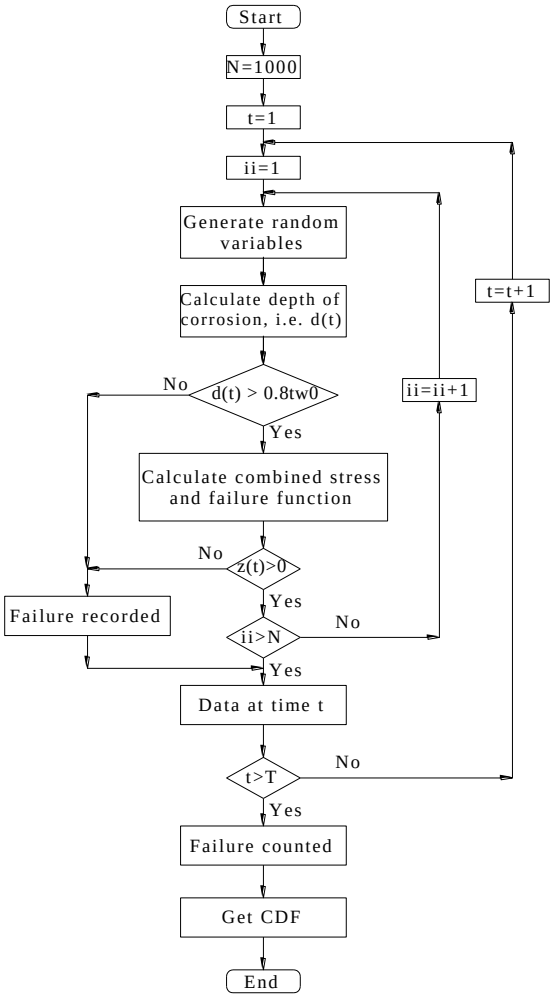

Figure 3.1. Flow chart for conducting Monte -Carlo simulations

3.4. Estimation of Risk

Risk is a measure of the probability and for the consequence of undesired events to represent human, environmental or economic values. It is commonly expressed as the probability of occurrence times the consequences.

In a system, the risk could be for each component, and for the overall system. The system risk can be calculated as the sum of the component risks when the system components behave independently. Due to the complexity with dependent system components, it is a common practice to idealize the components in water main networks to be statistically independent (Tung, 1985; Wagner et al, 1988; Quimpo and Shamsi, 1991). Independent water main components are also assumed in the current study for the system reliability and risk assessment. In real water main network, reliability and risk of pipeline components may be somewhat dependent on each other as the failure of one component may increase the loads to the others. However, the method based on the assumption of independent system components provides a practical basis for identification of critical pipe components for inspection and maintenance considering reliability and risk. In this regard, different reliability and risk acceptability criteria could be used for the system to compensate the error to some extent.

If the failure probability of the i^{th} component is $F_i(t)$ within time 't' and its consequences is denoted as $C_i(t)$, the risk of the i_{th} component can be calculated as (Eq.3.13):

$$Risk_i(t) = F_i(t) \times C_i(t) \tag{3.13}$$

The system risk, $Risk_{sys}(t)$, can be defined as the sum of the component risks (Eq.3.14):

$$Risk_{sys}(t) = \sum_{i=1}^{n} Risk_i(t) \quad (3.14)$$

The consequence of failure is quantified by analyzing the economic loss of failures. The total consequence could comprise direct consequence (i.e., cost for replacing or repairing of a component) and/or indirect consequence (i.e., environmental and/or health loss). However, the quantification of actual consequence of water main failure is very difficult, if not impossible.

Despite the challenges, the risk-based approach is gaining momentum in recent years for prioritization of water mains for inspection and maintenance. In this approach, a normalized cost is used to account for the consequence of failure. The normalized consequence method evaluates the relativity of each consequence with others, rather than quantifying any monetary value of the consequence. Park et al. (2010) employed rankings of the likelihood and the consequence of failure to develop a risk matrix for classifying potable water infrastructure into five priority groups. The likelihood of failure and the consequence for each asset were assigned a score ranging from 1 to 5. The assignment of the scores as well as the classification of infrastructure into the priority group requires subjective judgement. A similar approach is used in Baah et al (2015) for sanitary sewer pipe asset where more detailed impact factors were employed for the consequence (instead of using scores from 1 to 5). They provided up to 11 impact factors for different conditions/groups (Table 3.1). Each impact factor has a corresponding weight factor

depending on its importance. Pipeline impact scores are then summed up, after multiplying the impact factor by corresponding weight factor, to obtain a score of consequence (Eq.3.15).

$$C_{ofi} = \sum_{j=1}^{m} \left(S_{ij} \times w_j \right) \tag{3.15}$$

Where:

C_{ofi}: Consequence of failure (C_{of}) of pipe component 'i',

S_{ij}: Impact score of pipe component 'i' with impact factor 'j',

w_j: Weight of impact factor 'j',

m: Number of impact factor counted for consequence.

The C_{of} was then used to classify the failure consequence into five impact ratings that were used to develop a risk matrix (Baah et al., 2015). The risk matrix finally results in the subjective risk classification of a component or group of pipes (i.e. low risk, moderate risk, high risk etc.)

It is difficult, however, to implement the subjective risk classes for the risk assessment of multi-component systems. To this end, a risk assessment method is proposed here, as an alternative to the commonly used risk matrix approach. The normalized consequence method is applied for calculation of the risk. The impact factors in Table 3.1 (Baah et al., 2015) are assumed to be applicable for the failure consequence of water mains presented here.

The system risk is then calculated from the component failure probability and the consequences failure (Eq.3.16):

$$Risk_{sys}(t) = \sum_{i=1}^{n} F_i(t) \times C_{ofi} \quad (3.16)$$

Table 3.1. Consequence of failure (After Baah et al, 2015)

No.	Impact factor	Sub-criteria	Performance value	Weight factor
1	Road way type	Road Classes	1 - 3	0.2
2	Intersecting a railway track	Yes/No	3/0	0.2
3	Pipe size	Diameter $\leq$ 300mm 300mm < Diameter $\leq$ 600mm 600mm < Diameter $\leq$ 900mm 900mm < Diameter	1 1.5 2.25 3	0.16
4	Pipe burial depth	Depth $\leq$ 3m 3m < Depth $\leq$ 10m 10m < Depth	1 1.5 3	0.16
5	Located downtown	Yes/No	3/0	0.2
6	Proximity to hospital	Pipe distance $\leq$ 120m 120m < Pipe distance	3 0	0.2
7	Proximity to school	Pipe distance $\leq$ 200m 200m < Pipe distance	3 0	0.2
8	Distance to building	Distance $\leq$ 5m 5m < Distance $\leq$ 10m 10 < Distance	3 1.5 0	0.2
9	Proximity to park or recreation areas	Pipe distance $\leq$ 20m 20m < Pipe distance	3 0	0.16
10	Proximity to bad storm water pipe	Distance $\leq$ 10m 10m < Distance	3 0	0.2
11	Proximity to river	Pipe distance $\leq$ 15m 15m < Pipe distance	3 0	0.2

3.5. Procedure for Maintenance Decision

Fig.3.2 presents a flow chart for the procedure proposed for decision making considering risk and reliability. At a given time, failure probability and risk are calculated for each pipe component and the system based on the component failure functions (Weibull functions discussed earlier) and the consequences. These are then compared with the corresponding threshold values. Assuming that the components were constructed at different times and have different location parameters, component failure probabilities are different in each calculation step.

Whenever a system threshold (risk or reliability thresholds) is violated, an investigation is carried out to find out the component(s) (e.g., component(s) "*j*"), which has the most significant effect on the system reliability and risk. To identify a component influencing the system most significantly, the age of the component is first set such as to provide 100% reliability, while the other components are at their actual age. The reliability and risk are then calculated for the system. The procedure is continued for all the components. Subsequently, the components are ranked according to the calculated reliability and risk values. The component resulting in lowest system risk and highest system reliability corresponds to the one that has most significant influence on the system at that time.

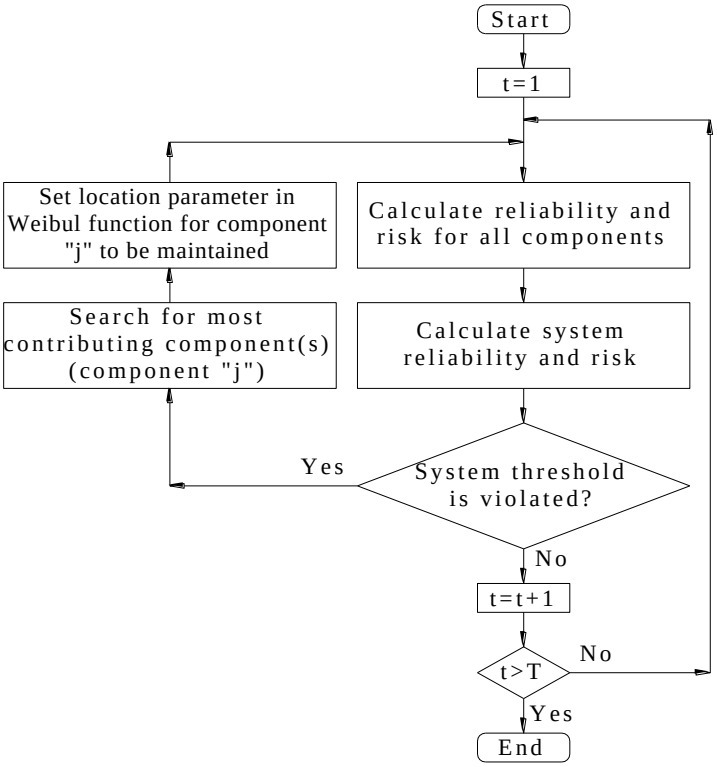

Figure 3.2. Flow charts for reliability and risk-based method approach for decision making

After ranking of the components, system reliability and associated risk are examined with consideration for repair/replacement of the component(s). Repair/replacement sequence is chosen from the most significantly influencing component, with subsequent addition of the next component according to the rank until the reliability and the risk criteria are met. The maintenance time and the identification of the "component(s) *j*" are then recorded and the location parameters for the components are set as discussed earlier.

The above steps are repeated to determine the life cycle maintenance plan for the pipeline network. The pipeline can be first inspected based on the maintenance plan and if it is necessary, the component is repaired. After each inspection and maintenance work,

the location parameter for the component is adjusted according to the condition of the pipe for the determination of next maintenance plan.

3.6. Modelling of Pipeline System

FTA method is proposed here for modelling the water main network. The method is useful for developing quantitative means to model the interaction between the events. Lindhe (2008) proposed an FTA method for probabilistic risk assessment of an entire drinking water system. In this method, the water supply failure (top event) is broken down into three subsystems namely raw water failure, treatment failure and distribution failure. An FTA is then constructed to model the system failure based on occurrence and non-occurrence of the subsystem failure using logic gates.

FTA is a top-down analysis process, which focuses on the development of the relationship between top event (i.e. system failure) and a series of lower-level events (basic events causing the system failure). The relationship of top and the basic events is constructed through the logical connection between them. Thus, logical branches from the top event to the basic events are deductively developed. For application of the method in a pipeline network system, the top event (i.e. the system failure) can be defined as a connectivity failure to a node i.e. connectivity to the nodes with specific consumers is lost. The failure of each pipe component in the network can be considered as a basic event. The OR-gate and AND-gate are two most commonly used logical gates in FTA to relate a higher-level event to lower-level events. The OR-gate is used if the higher-level event is

caused when any one of the several lower-level events occurs. The AND-gate is used when all the lower-events must occur simultaneously to cause a higher-level event.

For illustration purposes, a simple water main network consisting of seven pipe components is considered based on a small community water distribution system mentioned in Hickey (2008). The system is schematically shown in Fig.3.3. Water is supplied from the source to nodes A, B, C, and D through a network of pipelines. The pipelines of the system are assumed as independent. A fault tree illustrating the system failure is shown in Fig.3.4. The system failure is defined when the connectivity is lost to any of the nodes (A or B or C or D). Thus, any one of four events (i.e. connectivity loss to any of the nodes) would result in the system failure. Each of the events on the other hand is related to the failure of any of the pipeline components linked to the nodes. For example, connectivity to node A will be lost for failure of any of the components 1, 2 and 4 (Fig.3.3). The OR-gate is used to model this situation.

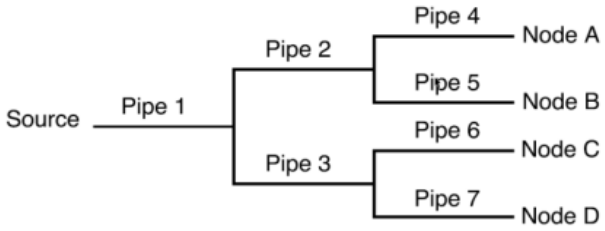

Figure 3.3. Schematic of a simple water pipeline system

Based on the system definition from FTA (Fig.3.4), the system failure probability can be defined as:

$$F_{sys}(t) = 1 - \left[\left(1 - F_A(t)\right) \times \left(1 - F_B(t)\right) \times \left(1 - F_C(t)\right) \times \left(1 - F_D(t)\right) \right] \qquad (3.17)$$

Where:

$F_{sys}(t)$ is the failure probability of the system at time *t*,

$F_A(t)$, $F_B(t)$, $F_C(t)$ and $F_D(t)$ are the failure probabilities of the events of connectivity loss to nodes A, B, C, and D, respectively, at time '*t*'.

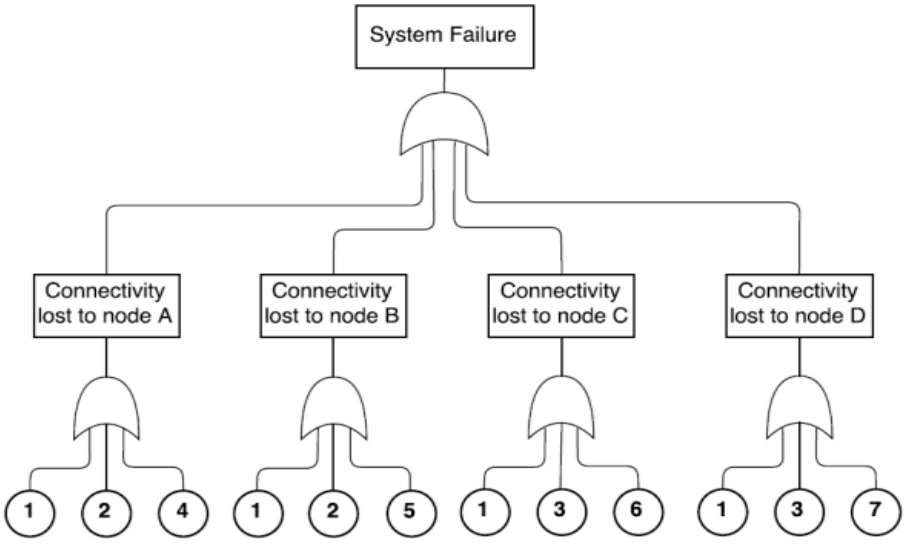

Figure 3.4. Fault tree analysis for system reliability

The failure probability of the events can be obtained from the failure probability of the related pipe components as shown below.

$$\begin{aligned} F_A(t) &= 1-\left[\left(1-F_1(t)\right)\times\left(1-F_2(t)\right)\times\left(1-F_4(t)\right)\right] \\ F_B(t) &= 1-\left[\left(1-F_1(t)\right)\times\left(1-F_2(t)\right)\times\left(1-F_5(t)\right)\right] \\ F_C(t) &= 1-\left[\left(1-F_1(t)\right)\times\left(1-F_3(t)\right)\times\left(1-F_6(t)\right)\right] \\ F_D(t) &= 1-\left[\left(1-F_1(t)\right)\times\left(1-F_3(t)\right)\times\left(1-F_7(t)\right)\right] \end{aligned} \tag{3.18}$$

Where: $F_i(t)$ is the failure probability of the i^{th} component at time *t*.

The method presented for the simple network (above) can be extended for more complex water distribution system through application of FTA and/or graph theory (i.e., Tung, 1985; Shinstine et al., 2002) as discussed in subsequent chapters.

3.7. Numerical Example

3.7.1. Calculations of Reliability and Risk

To illustrate a system analysis for pipeline maintenance prioritization, a numerical example is carried out in this section. A pipeline network consisting of the seven pipe components (Fig.3.3) is considered. Parameters for the MC simulation are assumed based on the typical values available in the literature. The deterministic parameters in the analysis are: E_p = 200 GPa, M_s = 19.3 MPa, K_x = 0.1, M_p = 1.2 and D_l= 1 (after AWWA, 2014). Pipes 1, 2, 3 are assumed to have 200 mm of diameter. All other pipes (pipe 4, 5, 6, 7) are assumed to have 150 mm of diameter. Table 3.2 provides the random input variables that include maximum allowable stress (yield stress) of pipe material (σ_y), wall thickness (t), operating pressure (P_{op}), length of corrosion defect (L_o) and corrosion depth rate (C_r). In Table 3.2, the mean values are taken as the typical values for the variables and the coefficient of variance (COV) are arbitrarily chosen since the specific information on the variables is not available. The mean corrosion rate is varied from 0.14 mm/year to 0.25 mm/year based on the information in Mohebbi and Li (2011) and Sridhar et al. (2001). The mean corrosion length is assumed to vary from 80 mm to 200 mm, estimated based on the information in Gajdoš and Šperl (2012) and Kleiner et al. (2012). A sensitivity analysis with these parameters was conducted and the sensitivity was found to be time-dependent

which is due to the use of a corrosion rate. In general, strength of the pipe material contributes most significantly followed by the wall thickness, loads and corrosion size.

Table 3.2. Input variables for Monte Carlo simulation

Input variable	Type of distribution		Pipe component Nos.						
			1	**2**	**3**	**4**	**5**	**6**	**7**
Yield stress (MPa)	Normal	Mean	150	150	150	150	150	150	150
		COV	0.5	0.5	0.5	0.5	0.5	0.5	0.5
Thickness (mm)	Normal	Mean	10	10	10	10	10	10	10
		COV	0.1	0.1	0.1	0.1	0.1	0.1	0.1
Internal pressure (MPa)	Normal	Mean	0.7	0.7	0.7	0.7	0.7	0.7	0.7
		COV	0.25	0.25	0.25	0.25	0.25	0.25	0.25
Corrosion length (mm)	Normal	Mean	150	100	120	180	150	80	200
		COV	0.5	0.5	0.3	0.35	0.2	0.5	0.15
Corrosion rate (mm/year)	Lognormal	Mean	0.25	0.15	0.18	0.16	0.2	0.14	0.19
		COV	0.25	0.2	0.2	0.25	0.12	0.15	0.2
Burial depth (m)	Normal	Mean	2.5	2	2.5	2	2.5	2	2.5
		COV	0.25	0.25	0.25	0.25	0.25	0.25	0.25
Unit weight of soil (kN/m^3)	Normal	Mean	18.8	18.8	18.8	18.8	18.8	18.8	18.8
		COV	0.2	0.2	0.2	0.2	0.2	0.2	0.2
Wheel load (kN)	Normal	Mean	71.3	71.3	71.3	71.3	71.3	71.3	71.3
		COV	0.2	0.2	0.2	0.2	0.2	0.2	0.2

Data from the MC simulation are then fitted with Weibull model, as discussed earlier. The resulting Weibull parameters and the coefficient of determination are included in Table 3.3. The location parameters (γ_i), representing the initial ages of components, are arbitrarily chosen for the example. Fig.3.5 compares the failure probability from MC simulation and the corresponding Weibull function. Comparisons over the full range of failure probabilities are shown in Fig.3.5 for overall demonstration, although the maintenance thresholds are set to low failure probability values. It is to be noted that over the lower

failure probability range (up to around 20%), the Weibull functions calculate higher failure probability with respect to MC simulation and thus provide conservative estimations.

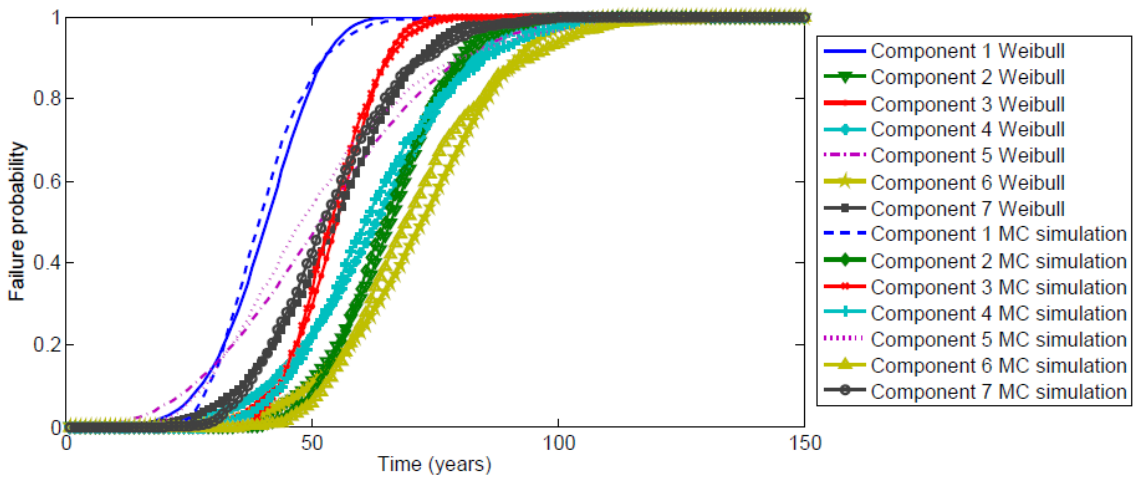

Figure 3.5. Failure probability of pipe components with Weibull functions

Table 3.3. Weibull parameters

Pipe component No. (i)	Parameter			Coefficient of determination, R^2
	Scale η_i	Shape β_i	Location γ_i	
1	44.252	4.690	-5	0.9994
2	72.125	6.027	-20	0.9995
3	58.173	7.007	-23	0.9996
4	70.188	3.914	-24	0.9991
5	57.249	2.919	-12	0.9984
6	79.587	4.998	-25	0.9978
7	58.748	4.081	-8	0.9992

Normalized consequences of the pipe components are estimated based on the impact factors in Baah et al. (2015) for calculation of risk. Table 3.4 shows the impact factors and

the weight factors chosen for each component and the resulting consequence calculated using Eq.3.15.

Table 3.4. Failure consequence estimation using Table 3.1

#	Impact factor	Weight factor	Component scores						
			1	**2**	**3**	**4**	**5**	**6**	**7**
1	Road way type	0.2	2.4	2.4	1	1	1	1	1
2	Intersecting a railway track	0.2	0	0	0	0	0	0	0
3	Pipe size	0.16	2.25	1.5	1.5	1	1	1	1
4	Pipe burial depth	0.16	3	1.5	1.5	1	1	1	1.5
5	Located downtown	0.2	0	0	0	0	3	0	3
6	Proximity to hospital	0.2	0	0	0	0	3	3	0
7	Proximity to school	0.2	0	0	0	0	0	0	0
8	Distance to building	0.2	1.5	0	0	1.5	1.5	1.5	3
9	Proximity to river	0.2	3	0	0	0	0	0	0
10	Proximity to park or recreation areas	0.16	0	0	0	3	3	3	3
11	Proximity to bad storm water pipe	0.2	3	3	3	0	0	0	0
	Normalized Consequence		**2.82**	**1.56**	**1.28**	**1.3**	**2.5**	**1.9**	**2.28**

3.7.2. Decision Making for Maintenance

Decision making using reliability and/or risk-based method requires selection of thresholds. Alternatively, the risk minimization approach can be applied through analysis of risks for different selected inspection/repair intervals. The second approach is applicable for preventive maintenance policy where a unit is maintained at fixed time intervals. Cheng

and Pandey (2012), however, demonstrated multiple local minimums in the expected cost rate plotted against inspection intervals. The multiple local minimums are due to the fact that the selected interval may miss any maintenance requirement within the interval. On the other hand, the fixed time interval approach is applicable for a single component system. It is difficult to select one maintenance interval for a multi-component system. Therefore, use of reliability and risk thresholds is considered suitable for the maintenance of pipeline network. However, the selection of the thresholds is a major challenge for application of this method. To this end, a relationship between the risk and reliability can be established for the system through calculation of failure probabilities and the corresponding risks. Fig.3.6 shows a nonlinear relationship between the risk and failure probability developed for the system considered in this example. It is to note that the relationship of risk and failure probability of a pipe is usually linear when the consequence is constant. However, the system risk presented here is the summation of risks of components and the system failure probability is obtained from a nonlinear function of failure probability of components in Eq.3.17. This explains the nonlinear relationship obtained in Fig.3.6.

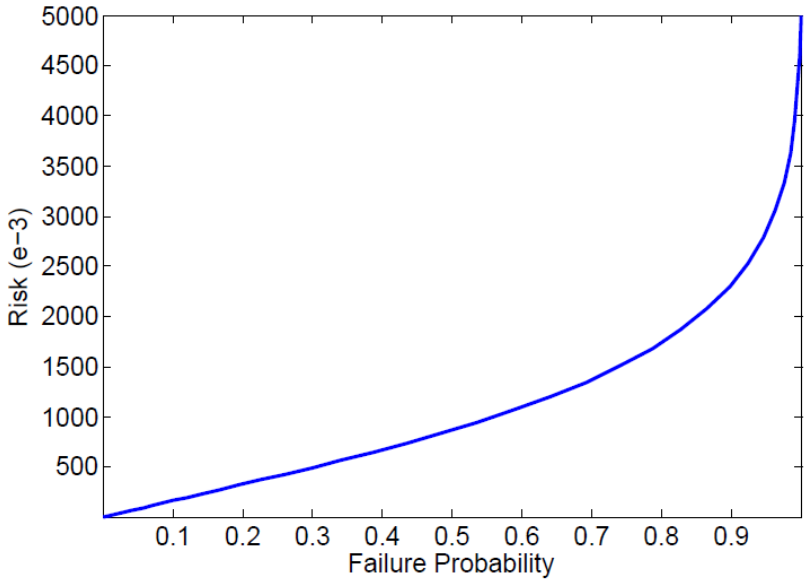

Figure 3.6. Relationship between system failure probability and system risk without maintenance

The risk thresholds can be chosen from the relation that corresponds to a desired failure probability or reliability. The acceptable failure probability (i.e., the failure probability threshold) may vary from system to system depending on the system type. A failure probability threshold of 5% (reliability threshold of 95%) is often interpreted as "high" potential of occurrence for a system (Ebeling, 2010). The risk corresponding to this failure probability threshold of 5% is around 84.9×10^{-3} in Fig.3.6.

An analysis of failure probability (reliability) based maintenance program with a failure probability threshold of 5% for the system (Fig.3.3) is presented in Fig.3.7. Fig.3.7 presents the calculated results of failure probability with age for the components and the system. The failure probability of the system is always higher than that of the components. Thus, the system failure probability appears to control the maintenance program for this

case. The component failure probabilities are consistently below the threshold (i.e. 5%) in Fig.3.7.

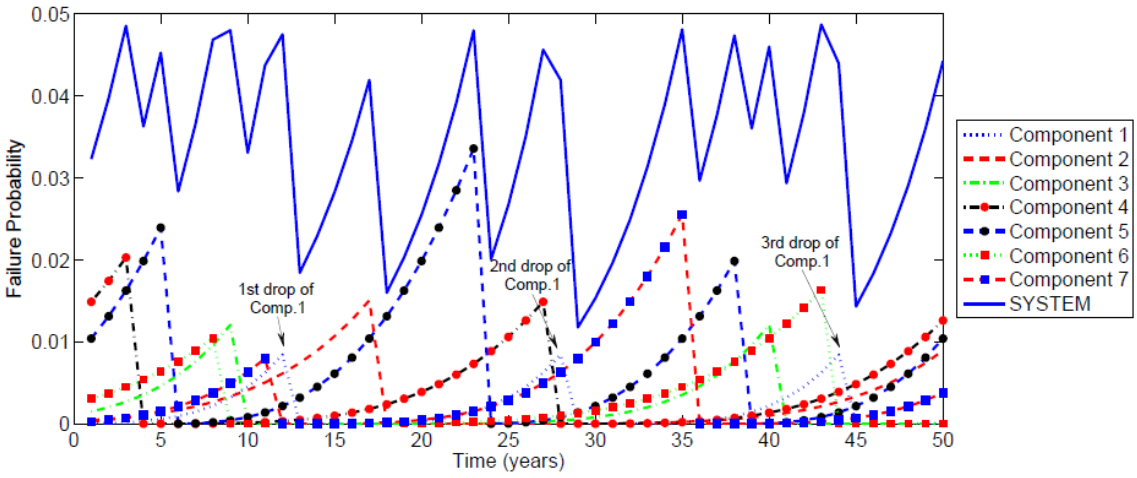

Figure 3.7. Failure probability in reliability-based method (failure probability threshold is 0.05)

When the system threshold is reached or exceeded, a repair/maintenance is assumed for this component and a new location parameter is assigned to the component (as discussed earlier). A location parameter corresponding to 0% failure probability is used after each repair/maintenance identification for the examples presented here. This is indicated by the drops in the failure functions in Fig.3.7. Every drop for each component corresponds to a maintenance that also results in a drop to the system failure probability. The maintenance schedule and the number of maintenance requirements for the components can thus be obtained from Fig.3.7 using the elapsed time and the number of drops, respectively. For example, component 1 has 3 drops, shown in Fig.3.7, at the time (age) of year 12, 28 and 44, respectively. A total of three maintenance actions are therefore

expected for the component at the ages of year 12, 28 and 44, respectively, within the lifetime of 50 years. This lifetime maintenance schedule is developed based on the assumption that each maintenance work would bring the pipe component to the state of 0% failure probability (the location parameter selected to provide 0% failure probability). However, a different location parameter can be selected when the actual condition of the pipe after each inspection/maintenance work is known. The estimated maintenance schedule for the pipeline components for this system is summarized in Table 3.5, including the year to repair/maintain and the components to be repaired/ maintained. A total of 15 maintenance counts are estimated over the period of 50 year for the system considered in this example. The risk for the system to be maintained using the reliability-based approach is also calculated as plotted in Fig.3.8. The maximum risk of the system is calculated to be 101.6×10^{-3} at year 23. This risk magnitude is higher than the risk corresponding to the 5% failure probability in Fig.3.6 (i.e., 84.9×10^{-3}). The difference is attributed to the differences in the components that contribute to the system reliability. For example, at year 23 (Fig.3.8), component 5 contributes the most to the system reliability. The component (component 5) has a high consequence of failure (i.e., 2.5 in Table 3.4). A different component might contribute to the system reliability presented in Fig.3.6. Fig.3.6 thus provides only a guideline on the relationship between the system risk and system reliability when no maintenance is performed. The risk-reliability relationship could be somewhat different as the maintenance is performed throughout the lifetime of the system.

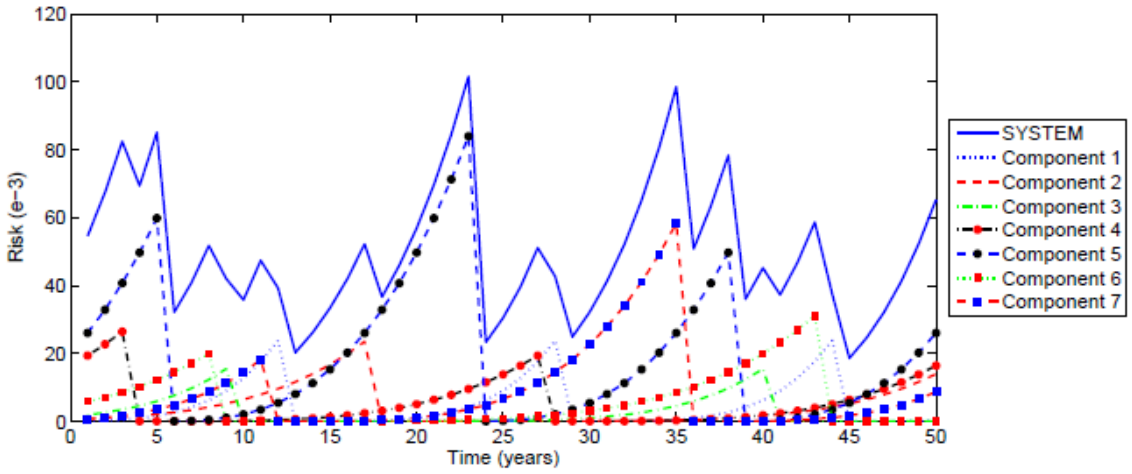

Figure 3.8. Risk in reliability-based method (failure probability threshold of 0.05)

Table 3.5. Maintenance schedule based on reliability-based method

Maintenance counts	Year to maintain	Component to maintain
1	3	4
2	5	5
3	8	6
4	9	3
5	11	7
6	12	1
7	17	2
8	23	5
9	27	4
10	28	1
11	35	7
12	38	5
13	40	3
14	43	6
15	44	1

A risk-based maintenance planning (prioritization) is also investigated for the pipeline network. A risk threshold of 101.6×10^{-3} is chosen based on the maximum risk calculated in the failure probability-based approach discussed above. The calculated risk and a summary of the maintenance program with the risk-based method is shown in Fig.3.9 and Table 3.6, respectively. The total number of maintenance requirement using risk-based method is 14, which is less than the maintenance requirement in the reliability-based method discussed above.

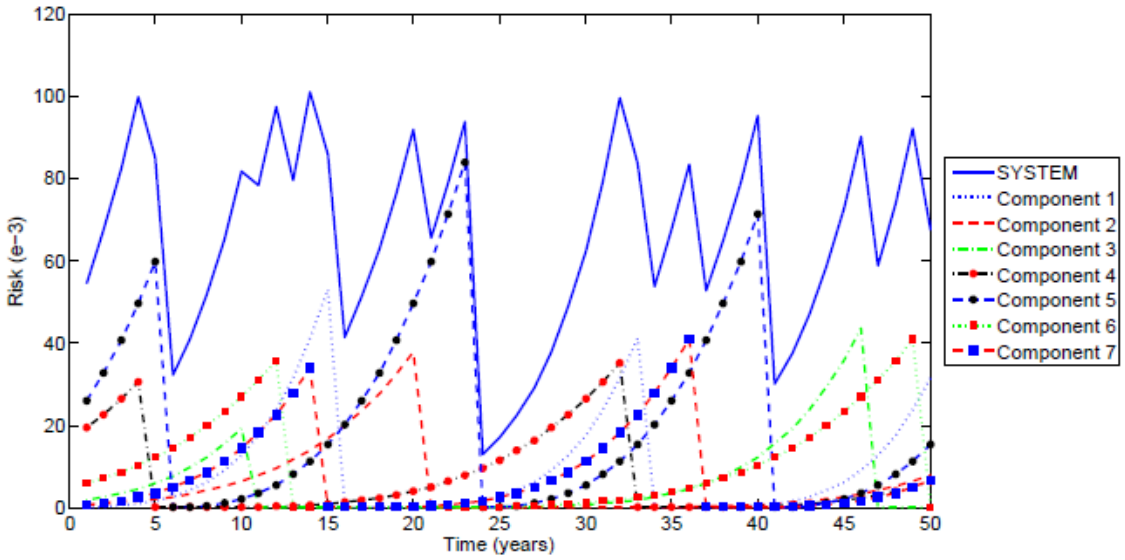

Figure 3.9. System risk and component risks with a risk threshold of 101.6×10^{-3}

The failure probability of the pipeline system and components corresponding to the risk-based maintenance is plotted in Fig.3.10. The maximum failure probability is calculated to be 9.9% (Fig.3.10), which is higher than the failure probability threshold assumed for the reliability-based maintenance program discussed above. This explains why

the number of maintenance requirements is found to be less (i.e., 14). A lower risk threshold could be chosen to develop a maintenance program for higher system reliability.

Table 3.6. Maintenance schedule based on risk-based method

Maintenance counts	Year to maintain	Component to maintain
1	4	4
2	5	5
3	10	3
4	12	6
5	14	7
6	15	1
7	20	2
8	23	5
9	32	4
10	33	1
11	36	7
12	40	5
13	46	3
14	49	6

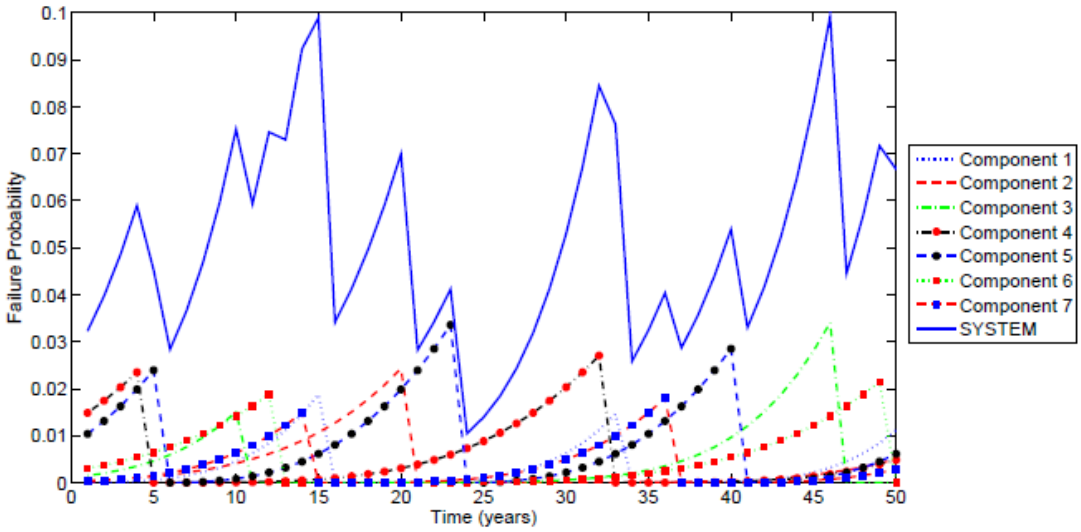

Figure 3.10. Failure probability with a risk threshold of 101.6×10^{-3}

3.8. Conclusion

A method for prioritizing water mains for maintenance considering failure probability and risk of pipeline system is developed here. The method can be used for municipalities with no available data for pipe failure probability assessment while the model could be updated when data would be available. In the proposed method, pipe failure probability is calculated based on a stochastic degradation analysis using MC simulation. The data from MC simulation is used to develop a simple Weibull function to model the failure probability. A method is proposed for expert opinions on the pipe conditions after an inspection and/or maintenance (repair/replacement) work without any requirement for data mining exercise. The model would thus be useful for existing and repaired/renewed pipe components. A risk assessment method is proposed, as an alternative to the commonly used risk matrix method, for calculation of risk for multi-component pipeline systems. The system failure of the pipeline network is defined using FTA.

Thresholds for the reliability and risk are found to govern the decision process in the reliability and risk-based approaches. In this regard, a careful determination of the thresholds is required to optimize the decision process considering both the reliability and the risk. To this end, a relation can be developed between the risk and the reliability for a system defined using FTA. The thresholds can rationally be chosen based on this relation.

The proposed method has been demonstrated through application to a simple water distribution network consisting of seven pipe components. Water main prioritization methods for more complex networks are presented in subsequent chapters.

CHAPTER 4. DEVELOPMENT OF A MECHANICS-BASED FAILURE ASSESSMENT MODEL[3]

4.1. Introduction

Water mains are important infrastructure that transport water for both industrial and household purposes. While metal pipes are popularly used with up to 56% of length of water mains made of cast iron and ductile iron, corrosion is reported as the major cause of water mains breaks of these pipes (Folkman, 2018). Additionally, the cast iron pipes, which was popularly used prior to 1970s, are in the end of their life cycle (i.e. 50 years, Folkman, 2018) indicating the need of replacing these pipes. Since pipeline deterioration is an inevitable process, it is desirable to optimize utilization of the structure through proper understanding of the remaining strength. In Chapter 3,5 and 6 of the thesis, the frameworks for risk and reliability assessment considering mechanical failure of the corroded pipes are presented. However, mechanical model for failure assessment of corroded water mains are not well developed. AWWA (2014) design code recommends evaluation of pipe wall strains due to internal pressure and bending, which are discussed in detail in Chapter 2 and 3. Pipe wall stress due to internal pressure is particularly responsible catastrophic failure such as bursting.

[3] This chapter is based on the published work in a peer-reviewed journal: Hieu Chi Phan, Ashutosh Sutra Dhar and Bipul Chandra Mondal (2016), "Revisiting burst pressure models for corroded pipelines", Canadian Journal of Civil Engineering, 44(7), pp.485-494. (https://doi.org/10.1139/cjce-2016-0519). The work was carried out, and the paper was drafted by the first author. The work was supervised, and the paper was reviewed by Dr. Ashutosh Sutra Dhar. Dr Bipul Chandra Mondal provided data from finite element modelling of energy pipelines.

Nevertheless, failure stress calculation method for corroded water main is currently not available. In the analysis presented in Chapter 3, a burst pressure model for energy pipelines is used to calculate the stress. This chapter focuses on developing a burst pressure model for cast iron water main. A number of predictive models for the burst pressure have been developed over the last 50 years, both for the intact (parent) pipes and the deteriorating energy pipes. However, no single model was found to be widely acceptable due to the limitations in predicting the burst pressures correctly (Zhu and Leis, 2012). Different models developed for burst pressure prediction of corroded pipes are described in the literature (i.e., Cosham and Hopkins 2004) and therefore not repeated here.

The models were commonly developed based on simplified analytical results and/or on empirical fits to limited experimental data. Hasan et al. (2011) demonstrated through a probabilistic assessment of the remaining strength of corroded pipes that different burst pressure models provide significantly different failure strengths even with the same defect sizes for particular pipes. An evaluation of several design models using finite element (FE) analysis and laboratory burst tests also provided both underestimation and overestimation of the burst pressures for corroded pipes (Chen et al., 2015, Swankie et al., 2012). For example, in 80 full-scale burst tests for pipes with diameters ranging from 88.9 mm to 168.3 mm, Swankie et al. (2012) found the modified ASME B31G method to provide overestimation of the burst pressure for 35% of the pipes and underestimation for 50% of the pipes tested. The model error in several existing models was found to affect the burst probability assessment by several order of magnitudes (Zhou and Zhang 2015). An

improved burst pressure model is therefore desired for accurate failure assessment of the pipelines.

Several experimental burst test results are available in the literature, which were used to develop or verify burst pressure models for corroded pipes (e.g., Coronin 2000, Swankie et al. 2012 and Zhou and Huang 2012). The burst tests for full-scale pipes are, however, very expensive and therefore avoided. Furthermore, the results from the burst tests could be affected by manufacturing defects in the test samples. The pipe samples could have non-homogeneous material properties and/or non-uniform wall thicknesses that could vary from sample to sample. As a result, the burst pressures of similar pipe samples may be different when tested independently. To this end, Finite Element (FE) analysis could be used to develop a database with known dimensions of the pipes, the corrosion defects, and the pipe material properties for the development of a burst pressure model.

FE analysis was used widely for the evaluation of the existing burst pressure models for pressure pipes (Chen et al., 2015, Swankie et al., 2012). Netto et al. (2005) employed FE analysis to develop a simplified equation for the burst pressure of corroded pipeline. They calculated the burst pressures for a 406.4 mm diameter pipe with various dimensions of the corrosion defects. A dimensional analysis was then performed with the FE results to develop the model. Wang and Zarghamee (2013) also used dimensional analysis and developed simplified burst pressure models for a wider range of pipe sizes, where the basic variables in the model are the same as those in Netto et al. (2005). However, two different equations were developed in Wang and Zarghamee (2013) for two ranges of pipe diameters (i.e., < 610 mm and ≥ 610 mm). The structure of the models developed from the

dimensional analysis (Netto et al. 2005, Wang and Zarghamee 2013) is different from the structures of the equations in the existing pipe design codes (e.g. ASME B31G 2012, CSA Z662 2015 and DNV RP-F101 2012) and the one yielded from a theoretical study (Gajdoš and Šperl, 2012). Wang and Zarghamee (2013) and Netto et al (2005) considered a particular type of steel pipe for the development of the burst pressure model. The applicability of the model for pipes made of steel with different grades was not investigated. Ma et al. (2013) revealed that the error in the burst pressure predictions using different models depend on the strength grade of the steel. The error was found to be the lowest for high-strength grade steel and highest for low-strength grade steel (Ma et al. 2013).

In this chapter, the structures of three existing models are employed to revisit the burst pressure models for corroded pipes considering a wide range of pipe sizes and material strength grade. Model for high strength steel and cast iron are developed separately to revise/develop the burst pressure models for corresponding type of materials. A series of FE analyses are conducted to develop a database for the burst pressures of corroded pipes with known pipe geometries and material parameters. The FE database is then used to determine different coefficients and exponents of the models (model constants). An optimization algorithm based on differential evolution (DE) method is developed to determine the model constants through error minimization. For high strength steel, pipes with diameters ranging from 324 mm (12.8 in.) to 914 mm (36 in.) are considered with the corrosion patches varying in lengths from 150 mm (6 in.) to 528 mm (20.8 in.) and depths from 20% to 70% of the wall thicknesses. For cast iron, pipe diameters

ranging from 127mm (5.0 in.) to 441mm (17.36 in.) with depth of defects varies from 0.25% to 90% of the wall thickness are considered.

4.2. Finite Element Analysis (FEA)

FE analysis is an effective tool for modelling complex mechanical problems including complex geometries and non-linear stress-strain behavior. A general-purpose FE code, ABAQUS 6.14 (Dassault Systemes 2014), is used in this study to calculate the burst pressure of corroded pipes. ABAQUS is one of the commonly used software that can be used to model the non-linear deformation during yielding of corroded pipelines under high pressures. ABAQUS/Explicit is used due to its capability of modelling highly non-linear problem effectively (Martin et al. 2007).

In the FE analysis, the corrosion on the pipe wall is modeled through the reduction of wall thickness over a rectangular patch. The length of the rectangle is in the longitudinal direction of the pipe, which is varied. A constant width is used for the patch. Earlier research has revealed that the width of the corrosion patch does not have a significant effect on the burst pressure of corroded pipes (Mondal and Dhar, 2015). The depth of corrosion is assumed to be uniform. Although the actual geometry of corrosion patches is very complex, existing literatures reveal that the failure behavior of corroded pipeline generally depends on the maximum depth and the longitudinal extent of the corroded area (Mondal and Dhar 2016a). Rectangular idealization with a uniform depth for the corrosion patch is therefore considered reasonable for the analysis of pipes with corrosion defects. For the sides of the rectangles, Mondal and Dhar (2016 a, b) investigated pipes subjected to wall

corrosions with both sharp and smooth edges (Fig.4.1). An ellipse with a ratio of the major to minor axis of 2 was fitted to produce the smooth edge. Calculated burst pressures with the two different edge conditions (sharp and smooth edges) were not found to vary significantly (Mondal and Dhar 2016a, b). This is due to the fact that the maximum von Mises stress and the maximum principle plastic strain at failure are not significantly affected by the edge conditions. Fig.4.2 shows the von Mises stresses around the corroded zone at the failure pressure of a pipe. However, the model development and analysis with smooth edge is complicated and time consuming. Sharp edge condition is therefore considered for the FE analysis presented here. The pipes under the loading of internal pressure are analyzed to calculate the burst pressure.

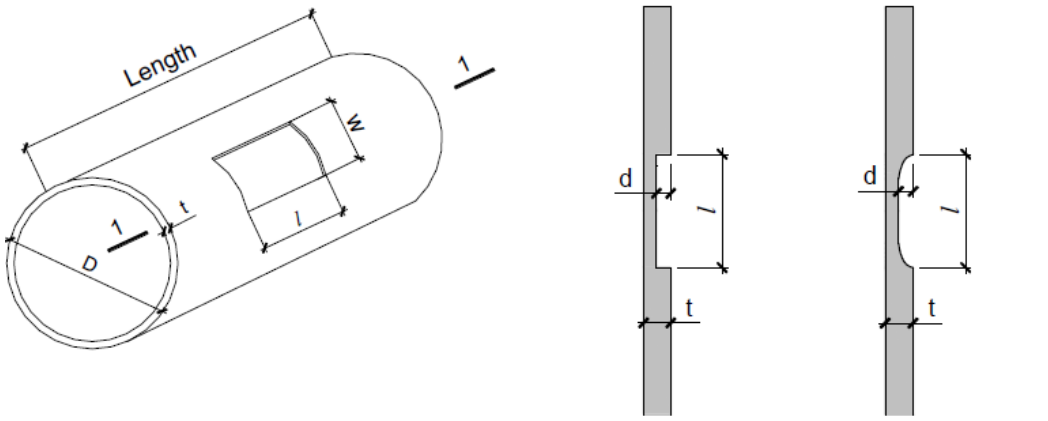

(a) Pipe with a corrosion patch (b) Sharp Edge (1-1) (c) Smooth Edge (1-1)

Figure 4.1. Edge conditions of corrosion patch, after Mondal and Dhar (2016b)

The pipe domain in the FE analysis is modelled using the eight-node continuum element (ABAQUS element "C3D8R"). A mesh sensitivity analysis was performed to determine the optimum mesh size. Fine mesh is applied within and around the corroded

area where stress concentration is expected. Coarse mesh is applied where uniform stress is expected. FE meshing around the corroded area for a pipe is shown in Fig.4.3. Fully restrained boundary conditions are used at the ends of the pipes. To avoid the effect of boundary conditions within the corroded zone, the length of the pipes is chosen to be longer than the minimum length recommended in Fekete and Varge (2012). The model lengths are 2500 mm, 3500 mm, 4500 mm and 3000 mm for pipes with diameters of 342 mm, 508 mm, 762 mm and 914 mm, respectively. The lengths are greater than 3 times the diameter of the pipes. Details of the FE modelling approach for corroded pipes are available elsewhere (Mondal and Dhar 2016 a, b).

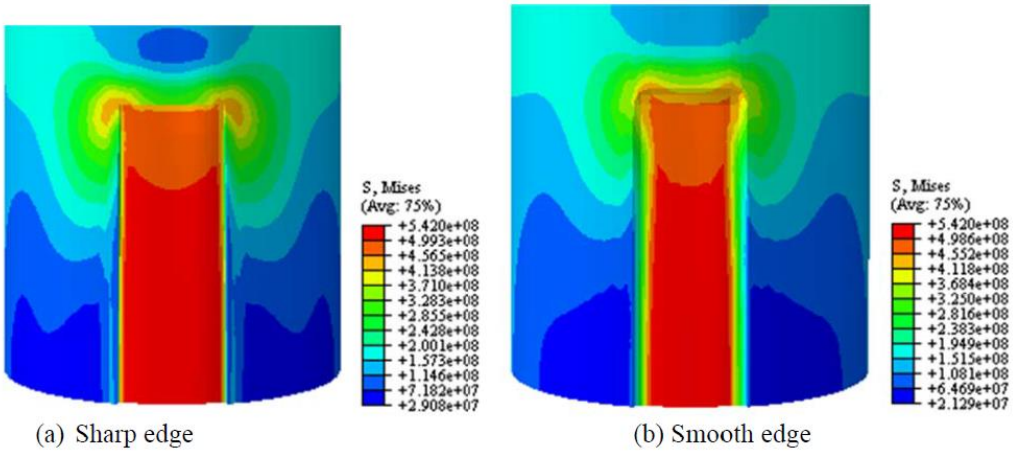

Figure 4.2. Contour of von Mises stresses around a corrosion patch for sharp and smooth edges (at the failure pressure of 11.43 MPa)

Figure 4.3. Typical FE meshing around a corrosion area

Mondal and Dhar (2016b) investigated the effects of using non-linear and bi-linear stress-strain relations of pipe materials on the predicted burst pressures of steel pipes. The burst pressures predicted using the two approaches were within 2% of each other. Therefore, a bi-linear stress-strain model is used in this research to avoid the additional computational time required for the non-linear model. Strain based criteria is used to define the failure in order to define the burst pressure (after Mondal and Dhar 2016b). The failure pressure (burst pressure) is considered as the minimum internal pressure at which the maximum principal plastic strain on the pipe wall reaches the failure strain of the materials. The failure strains of the materials are obtained as the plastic strains corresponding to the ultimate stress using the true stress-strain relations presented in Fekete and Varga (2012). Table 4.1 shows different input parameters used in the FE analysis along with the calculated burst pressures. Material properties of the steel are provided in Table 4.2. The

FE model was validated using the experimental burst pressure results of Diniz et al (2006) (Mondal and Dhar 2016b). Diniz et al, (2006) measures a burst pressure of 11.30 MPa for a 324 mm diameter pipe using full-scale laboratory tests. A burst pressure of 11.43 MPa is calculated using the FE analysis for the pipe (FEM No. 1, in Table 4.1), which is within 1.1% of the measured burst pressure. After the validation, 27 other analyses were performed with different pipe diameter, wall thickness and corrosion dimensions to produce a database.

Table 4.1. Pipe database for FE analysis for energy pipe

FEM No.	Diameter *D* (mm)	Wall thickness *t* (mm)	Corrosion depth *d* (mm)	Corrosion length *l* (mm)	Yield strength (MPa)	Ultimate strength (MPa)	Plastic strain at failure ε_u	Burst pressure *P* (MPa)
1	324	9.74	6.818	528	452[1]	542[1]	0.041	11.430
2	324	9.74	6.818	300	452	542	0.041	12.708
3	324	9.74	6.818	150	452	542	0.041	16.644
4	324	9.74	1.948	528	452	542	0.041	29.586
5	324	9.74	3.896	528	452	542	0.041	22.440
6	324	9.74	3.896	300	452	542	0.041	23.300
7	324	9.74	3.896	150	452	542	0.041	25.400
8	324	9.74	1.948	300	452	542	0.041	26.520
9	324	9.74	0	0	452	542	0.041	35.968
10	508	14.6	10.22	500	414[1]	600[1]	0.093	13.260
11	508	14.6	10.22	300	414	600	0.093	16.960
12	508	14.6	10.22	150	414	600	0.093	24.650
13	508	14.6	0	0	414	600	0.093	35.810
14	762	17.5	8.75	300	465[2]	564[2]	0.059	18.110
15	762	17.5	8.75	200	465	564	0.059	20.440
16	762	17.5	4.375	200	465	564	0.059	24.330
17	762	17.5	12.25	528	465	542	0.059	9.990
18	762	17.5	7	528	465	542	0.059	17.770
19	762	17.5	3.5	528	465	542	0.059	22.950
20	762	17.5	12.25	300	465	542	0.059	12.840

FEM No.	Diameter *D* (mm)	Wall thickness *t* (mm)	Corrosion depth *d* (mm)	Corrosion length *l* (mm)	Yield strength (MPa)	Ultimate strength (MPa)	Plastic strain at failure ε_u	Burst pressure *P* (MPa)
21	762	17.5	7	300	465	542	0.059	19.520
22	762	17.5	3.5	300	465	542	0.059	23.760
23	762	17.5	12.25	150	465	542	0.059	17.600
24	762	17.5	7	150	465	542	0.059	22.250
25	762	17.5	3.5	150	465	542	0.059	24.660
26	762	17.5	0	0	465	564	0.059	27.640
27	914	25.4	10.6	300	452[1]	542[1]	0.041	25.120
28	914	25.4	0	0	452	542	0.041	33.510

[1]Diniz et al. (2006), [2]Oh et al. (2007)

1 inch = 25.4 mm, 1 MPa = 145 psi

Table 4.2. Material properties of steel

Pipe Size (mm)	Steel Grade (API 5L/ CSA Z245.1)	Density (kg/m^3)	Modulus of Elasticity (GPa)	Yield strength (MPa)	Ultimate strength (MPa)	Poisson's Ratio	Total strain at failure
324	X65/448	7850	210.0	452	542	0.3	0.043
508	X60/414	7850	210.0	414	600	0.3	0.095
762	X65/448	7850	210.0	465	564	0.3	0.061
914	X65/448	7850	210.0	452	542	0.3	0.043

1 inch = 25.4 mm, 1 MPa = 145 psi

4.3. Burst Pressure Model Development

The existing burst pressure models employ a reduction factor to account for the corrosion defects. For the development of a burst pressure model, a mathematical model

is required for the reduction factor through identification of the variables influencing the factor. Researchers employed dimensional analysis (Buckingham's π theorem) in the development of the burst pressure model using data obtained from FE analyses (e.g., Netto et al. 2005, Wang and Zarghamee, 2013). The dimensional analysis provides a convenient tool to develop relationships between variables representing the physical phenomena when a mathematical model is not known. Netto et al. (2005) and Wang and Zarghamee (2013) determined the basic variables contributing to the reduction of burst pressure for corroded pipe as d/t and l/D, where d is the depth of corrosion, l is the length of corrosion, t is the pipe wall thickness, and D is the pipe outer diameter. Based on the analysis, Netto et al (2005) developed a burst pressure model for corroded pipeline (Eq.4.1):

$$P = P_0\left[1-0.9435\left(\frac{d}{t}\right)^{1.6}\left(\frac{l}{D}\right)^{0.4}\right] \tag{4.1}$$

The equations developed in Wang and Zarghamee (2013) are (Eq.4.2).

$$\frac{P}{P_0} = \begin{cases} 1-0.886\left(\frac{d}{t}\right)^{1.00}\left(\frac{l}{D}\right)^{0.3} & if \quad D < 610mm \\ 1-1.12\left(\frac{d}{t}\right)^{1.15}\left(\frac{l}{D}\right)^{0.3} & if \quad D \geq 610mm \end{cases} \tag{4.2}$$

The existing design codes, such as the modified ASME B31G (2012), CSA Z662 (2015) and DNV RP-F101 (2010) codes also use the defect depth and the defect length in the calculation of the burst pressure reduction for corroded pipe. However, the structure of the equations in the design codes is different from those developed from the dimensional analysis (discussed above). Each of the three design codes (i.e., ASME B31G, CSA Z662

and DNV RP-F101) adopted an equation of similar structure, which is consistent with the model known as RSTRENG (Kiefner and Vieth 1989). Mondal and Dhar (2016b) revealed that the burst pressure models in the design codes (i.e., ASME B31G, CSA Z662 and DNV RP-F101) are essentially the same when a uniform corrosion depth is considered. The burst pressure models from these design codes can be expressed in a general form (Eq.4.3):

$$P = P_0 \left[\frac{1 - \frac{d}{t}}{1 - \frac{d}{tM}} \right] \tag{4.3}$$

Where M is known as Folias factor, which is given as (ASME B31G, CSA Z662):

$$M = \sqrt{1 + 0.6275\frac{l^2}{Dt} - 0.003375\frac{l^4}{D^2t^2}} \qquad for\ \frac{l^2}{Dt} \leq 50 \text{ , and}$$

$$M = 0.032\frac{l^2}{Dt} + 3.3 \qquad for\ \frac{l^2}{Dt} > 50$$

The Folias factor in the DNV RP-F101 code is given by:

$$M = \sqrt{1 + 0.31 \cdot \left(\frac{l}{\sqrt{Dt}}\right)^2}$$

The burst pressure reduction factors in the design codes thus depended on d/t and l^2/Dt.

Gajdoš and Šperl (2012) developed a theoretical equation to calculate the maximum stress in a corroded pipe. The equation is expressed as (Eq.4.4):

$$\sigma = \frac{\sigma_H}{1 - \frac{\pi dl}{4t(t+l)}} \tag{4.4}$$

Where:

σ: The maximum stress in circumferential direction

σ_H: Hoop stress

$$\sigma_H = \frac{PD}{2t}$$

Eq.4.4 can be rearranged for the burst pressure as:

$$P = \left[\frac{2t\sigma_{flow}}{D}\right]\left[1 - \frac{\frac{\pi d}{4t}}{1+\frac{t}{l}}\right] \tag{4.5}$$

In Eq.4.5, parameters contributing to the burst pressure reduction appear to be *d*/*t* and *t*/*l*.

The structures of the equations discussed above (Eq.4.1, Eq.4.3 and Eq.4.5) for the burst pressure are different from each other, even though some of the parameters contributing to the burst pressure reduction are common. Each of the three model structures are evaluated here to revisit the models. The burst pressure equations are expressed in terms of the basic variables of the models, as shown in Eq.4.6, Eq.4.7 and Eq.4.8, keeping the similar structures of the equations as in Eq.4.1, Eq.4. 3 and Eq.4.5, respectively (called herein as Model 1, Model 2 and Model 3, respectively):

$$P = P_0 \times \left(1 + k_1 \left(\frac{d}{t} \right)^{k_2} \left(\frac{l}{D} \right)^{k_3} \right) \tag{4.6}$$

$$P = P_0 \times \left(\frac{1 + k_1 \frac{d}{t}}{1 + k_1 \frac{d}{t} \left(1 + k_2 \frac{l^2}{Dt} \right)^{k_3}} \right) = P_0 \times f \tag{4.7}$$

$$P = P_0 \times \left(1 - \frac{k_1 \frac{d}{t}}{1 + k_2 \frac{t}{l}} \right) \tag{4.8}$$

In Eq.4.6, Eq.4.7 and Eq.4.8 constants k_1, k_2, and k_3 (k_1 and k_2 for Model 3) are determined through fitting with the FE database (Table 4.1). The optimum values of the constants, k_i, are obtained through minimization of model errors.

4.4. Determination of Model Constants

The Sum of the Squares of Errors (SSE) is minimized to obtain the model parameters. The error is defined as the difference between the predicted data and the observed data. For a database with *n* observation data (*n* = 28 for 28 FE analysis performed in this study, in which, 4 are for un-corroded (intact) pipes and 24 are for corroded pipes) and each observation having *m* independent variables (basic variables identified for each model), the database can be expressed as (x_{ij}, x^*_i) (i = 1, 2,…n; j = 1, 2,…m). Here, x_{ij} are the independent variables and x^*_i are the dependent variables (the burst pressure from FE

analysis). In this study, the independent variables (basic variables) include pipe diameter, wall thickness, depth of defects, length of defects and so forth, as described in Table 4.1.

Consider a model relating the independent variables with the dependent variables as (Eq.4.9):

$$X'_i = f(x_{i1}, x_{i2\ldots}, x_{im} | k_1, k_2, \ldots, k_q) \quad (4.9)$$

where:

X'_i: The i^{th} predicted value of the dependent variable (i.e. the predicted burst pressure) with a set of 'q' model parameters (k_1, k_2,…, k_q) and '*m'* independent variables.

q: Number of parameters in the models (q = 3 for Model 1 and Model 2; q = 2 for Model 3).

The error in the i^{th} observation is given by (Eq.4.10):

$$e_i = x^*_i - X'_i \quad (4.10)$$

The sum of the squares of the error is (Eq.4.11)

$$SSE = \sum e_i^2 \quad (4.11)$$

Differential Evolution (DE) method (Storn and Price 1997) is used to determine of the model parameters with the minimum of the sum of the squares of the errors as the objective function. In this method, the material parameters are obtained through a direct search approach to improve the candidate solutions with regards to the objective function. The method is suitable for optimization of discontinuous function or problems with more

than one local minimum (Vincenzi et al. 2013). The algorithm used in the optimization using DE is presented as a flow chart in Fig.4.4. The variables used in Fig.4.4 are described in the following section. For the optimization, the Sum Squares of Error (SSE) is the objective function and the parameters $k_1,\ldots,k_q$ are the optimization variables. The method involves several steps of evolution simulating process to generate and adjust population through generations, as discussed below.

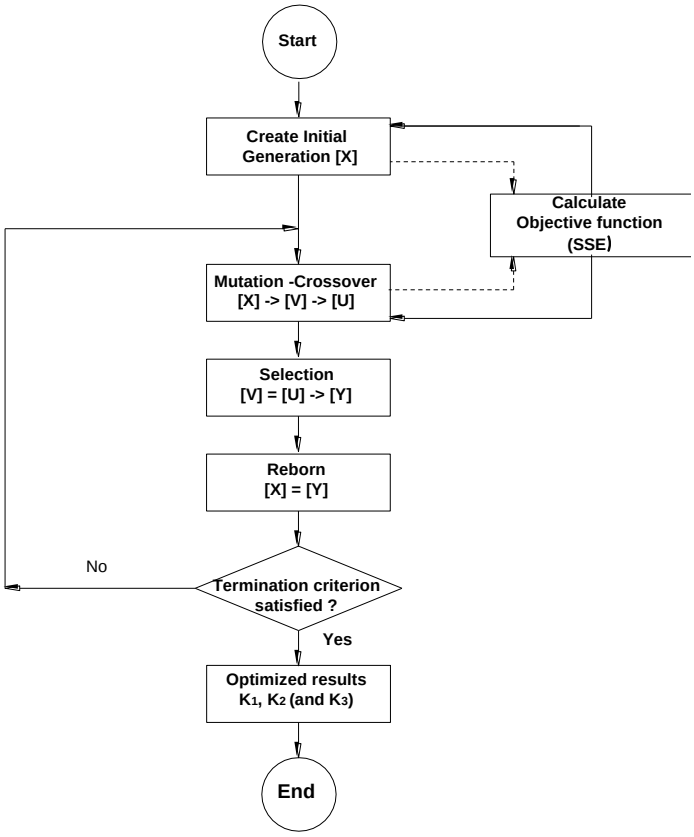

Figure 4.4. The flow chart of the optimization

4.4.1. Generating the Initial Generation

Let us assume that the main population $[X]_g$ is composed from *NP* individuals. Each individual contains 'n' observations (in this study, n = 24). The population of the g^{th} generation with NP individuals is defined as (Eq.4.12):

$$[X]_g = (x_{i1}, \ldots, x_{im}, x^*_i, k_{1sg}, \ldots, k_{qsg}, \ x'_{isg}) \quad (4.12)$$

Where:

i= 1, 2, …, n (the i^{th} observation of the database);

s=1, 2, …, NP (the s^{th} individual of the population);

In the initial step (first generation) g = 1, and then the initial population is (Eq.4.13):

$$[X]_1 = (x_{i1}, \ldots, x_{im}, x^*_i, k_{1s1}, \ldots, k_{qs1}, \ x'_{is1}) \quad (4.13)$$

The first part of the expression (x_{i1},…, x_{im}, x^*_i) is the FE database and is constant during the optimization process. The second part (k_{1sg},…, k_{qsg}) contain the vector of the parameters to be optimized (k_{1sg},…, k_{qsg}), which changes from individual to individual within a generation but remains constant within observations of each individual. The last part is the predicted values (i.e. predicted burst pressure, x'_{isg}) that changes from observation to observation. These predicted values are obtained from Eq.4.9.

The vector of the variables to be optimized (k_{1s1},…, k_{qs1}) is randomly chosen for '*n*' observations in the first generation. As mentioned above, x'_{is1} is the predicted value of the

dependent variable x^*_i, which is obtained from a model with a vector of ($k_{1s1},\ldots, k_{qs1}$). The objective function or the SSE_{sg} corresponds to g^{th} generation and s^{th} individual is then calculated as (Eq.4.14):

$$SSE_{sg} = \sum_{i=1}^{n}\left[x^*_i - x'_{isg}\right]^2 = \sum_{i=1}^{n}\left[x^*_i - f\left(x_{i,1,\ldots}, x_{i,m} \mid k_{1,s,g},\ ...,\ k_{q,s,g}\right)\right]^2 \qquad (4.14)$$

Where: q = 3, 3, and 2 for model 1, 2 and 3, respectively.

For the 1st generation the SSE is (Eq.4.15):

$$SSE_{s1} = \sum_{i=1}^{n}\left[x^*_i - x'_{is1}\right]^2 = \sum_{i=1}^{n}\left[x^*_i - f\left(x_{i1,\ldots}, x_{im} \mid k_{1s1},\ ...,\ k_{qs1}\right)\right]^2 \qquad (4.15)$$

Storn (2008) suggests the NP to be approximately equal to 10q as a rule of thumb. While the choice of NP/q would depend on the type of problem, a value between 5 and 10 is "a reasonable choice" (Qing, 2009). NP = 30 is chosen for the three models discussed here. The initial k_1 k_2 and k_3 are randomly chosen from -5 to 5 with a uniform distribution.

4.4.2. Mutation and Crossover

In g^{th} generation, the mutation step is carried out by randomly choosing three optimized vectors within the main population $[X]_g$, such as:

$$\overrightarrow{KV}_{r_1 g} = (k_{1r_1 g}, ..., k_{qr_1 g});$$

$$\overrightarrow{KV}_{r_2 g} = (k_{1r_2 g}, ..., k_{qr_2 g});$$

$$\overrightarrow{KV}_{r_3 g} = (k_{1r_3 g}, ..., k_{qr_3 g})$$

Where: r_1, r_2, r_3 are the integer random numbers chosen between [1: NP].

The mutation vector of the variables (to be optimized) is then defined as (Eq.4.16):

$$\overrightarrow{KV}_{sg} = (\mathrm{kv}_{1sg}, \ldots, \mathrm{kv}_{qsg}) = \overrightarrow{KV}_{r_1 g} + F \times (\overrightarrow{KV}_{r_2 g} - \overrightarrow{KV}_{r_3 g}) \quad (4.16)$$

The factor F is the mutation scale factor, commonly ranging from 0.5 to 1 (Storn, 2008). In this study, F = 0.75 is considered.

The $\overrightarrow{KV}_{sg}$ is used to calculate the corresponding predicted value xv'_{isg} and Sum Squares of Error SSE_{sg} of the mutation population $[V]_g$. The mutation population $[V]_g$ can be written as:

$$[V]_g = (x_{i1}, \ldots, x_{im}, x^*_i, kv_{1sg}, \ldots, kv_{qsg}, xv'_{isg})$$

Consequently, the crossover step takes place by generating a crossover population $[U]_g$ from randomly combining the main population $[X]_g$ and the mutation population $[V]_g$, as in Eq.4.17:

$$[U]_g = \begin{cases} [U]_{sg} = [X]_{sg} & if\ r_s > Cr \\ [U]_{sg} = [V]_{sg} & if\ r_s \le Cr \end{cases} \quad (4.17)$$

Where:

$[U]_{sg}$: The s^{th} individual of the crossover population $[U]_g$

$[X]_{sg}$: The s^{th} individual of the main population $[X]_g$

$[V]_{sg}$: The s^{th} individual of the mutation population $[V]_g$

r_s: Random number corresponding to s^{th} individual, chosen from 0 to 1.

Cr: The cross over probability, ranging from 0 to 1 (Storn, 2008). Cr = 0.9 is used here.

4.4.3. Selection and Reborn

From the selected individuals of crossover population $[U]_g$ and the main population $[X]_g$, the population $[Y]_g$ can be found using Eq.4.18:

$$[Y]_g = \begin{cases} [Y]_{sg} = [X]_{sg} & if\ SSEU_{sg} > SSE_{sg} \\ [Y]_{sg} = [U]_{sg} & if\ SSEU_{sg} \le SSE_{sg} \end{cases} \quad (4.18)$$

Where: $SSEU_{sg}$: The objective function (Sum Squares of Error) corresponding to g^{th} generation and s^{th} observation of the crossover population $[U]_g$

The population is then used as the main population $[X]_{g+1}$ in the next generation (g+1):

$[X]_{g+1} = [Y]_g$

These steps (mutation, crossover, selection and reborn) are repeated until the difference of SSE_{sg} in the main population $[X]_g$ is less than the terminal criterion ε (Eq.4.19).

$$\left| SSE_{g,min} - \frac{\sum_{s=1}^{NP} SSE_{sg}}{NP} \right| \le \varepsilon \quad (4.19)$$

ε : The termination criterion ($\varepsilon = 0.001$ is used);

$SSE_{g,min}$: The minimum value of SSE among *NP* individuals of the g^{th} main population

4.5. Results and Validation

Table 4.3 shows the model constants (parameters) obtained using the optimization method, along with the coefficient of determination (R-squares). The coefficients of determination are very high (greater that 99%) for each of the models, indicating that the models fit very well with the FE database.

Table 4.3. The results of optimization for the model parameters for high strength steel

Model	k_1	k_2	k_3	Generation	R^2
1	-0.88555	0.98077	0.31053	164	0.99490
2	-0.92126	0.06361	-2.75485	379	0.99577
3	1.24678	12.67390	-	73	0.99698

It reveals that the optimization method for model parameter determination provides a useful tool for the development of the burst pressure model. Each of the models investigated here (Model 1, Model 2 and Model 3, respectively) are found to be reasonable with the parameters estimated using the optimization method. Model 3, with the structure of the model of Gajdoš and Šperl (2012), provided the highest value of the coefficient of

determination. The resulting burst pressure models obtained from the investigation are shown in Eq.4.20, 4.21 and 4.22, respectively.

Model 1:

$$P = P_0 \times \left(1 - 0.88555 \left(\frac{d}{t} \right)^{0.98077} \left(\frac{l}{D} \right)^{0.31053} \right) \tag{4.20}$$

Model 2:

$$P = P_0 \times \left(\frac{1 - 0.92126 \frac{d}{t}}{1 - 0.92126 \frac{d}{t} \left(1 + 0.06361 \frac{l^2}{Dt} \right)^{-2.75485}} \right) \tag{4.21}$$

Model 3:

$$P = P_0 \times \left(1 - \frac{1.24678 \frac{d}{t}}{1 + 12.6739 \frac{t}{l}} \right) \tag{4.22}$$

The burst pressure reduction factors calculated using the developed models (Model 1, 2 and 3) are compared with those calculated using the FE analysis in Fig.4.5. The data coalesce around the 1:1 line in the figure, indicating a good correlation between the predictions using the models and the FE calculations. Each of the model provides some un-conservative estimation (overestimation) for lower values of the factor (<0.5). For the higher values of the factors, Model 1 (with the structure based on the dimensional analysis of Netto et al., 2005) and Model 2 (with the structure based on ASME B31G code) provided

both conservative and un-conservative estimations. Model 3 (with the structure based on the theoretical model of Gajdoš and Šperl, 2012) provided the most reasonable estimation.

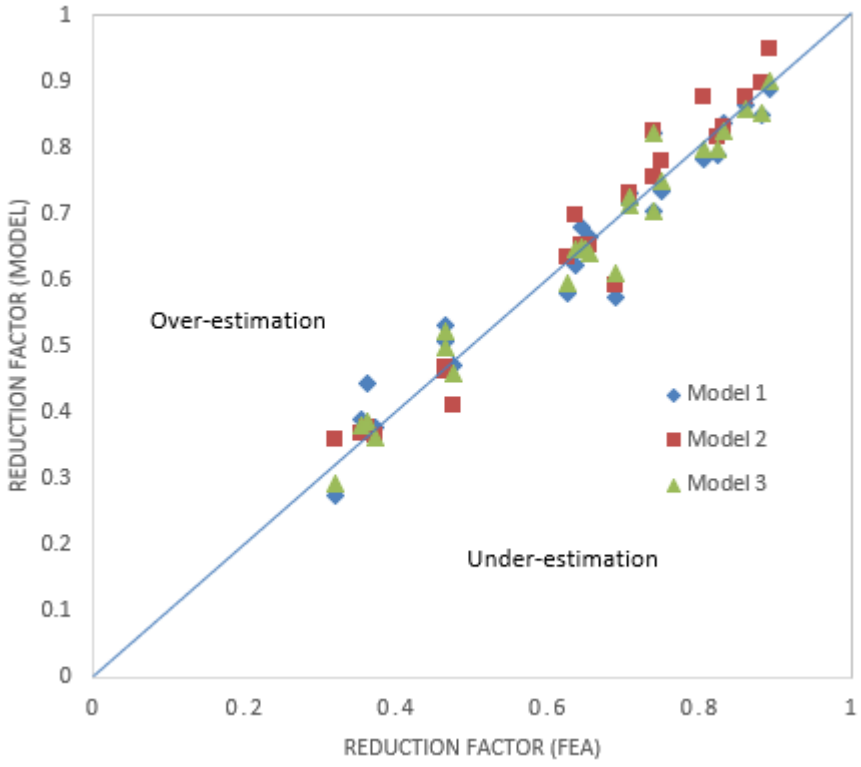

Figure 4.5. Comparison of the burst pressure models (Model 1, 2 and 3) with FE data for high strength steel

Fig.4.6 compares the burst pressure reduction factors calculated using the existing models such as Netto et al. (2005), ASME B31G (2012) and Gajdoš and Šperl (2012) with those from FE calculations. The data points in Fig.4.6 are widely scattered about the 1:1 line. Netto et al. (2005) and ASME B31G models generally provided over-estimations of the factor. The model of Gajdoš and Šperl (2012) generally provided underestimation of the factors (except for a few points).

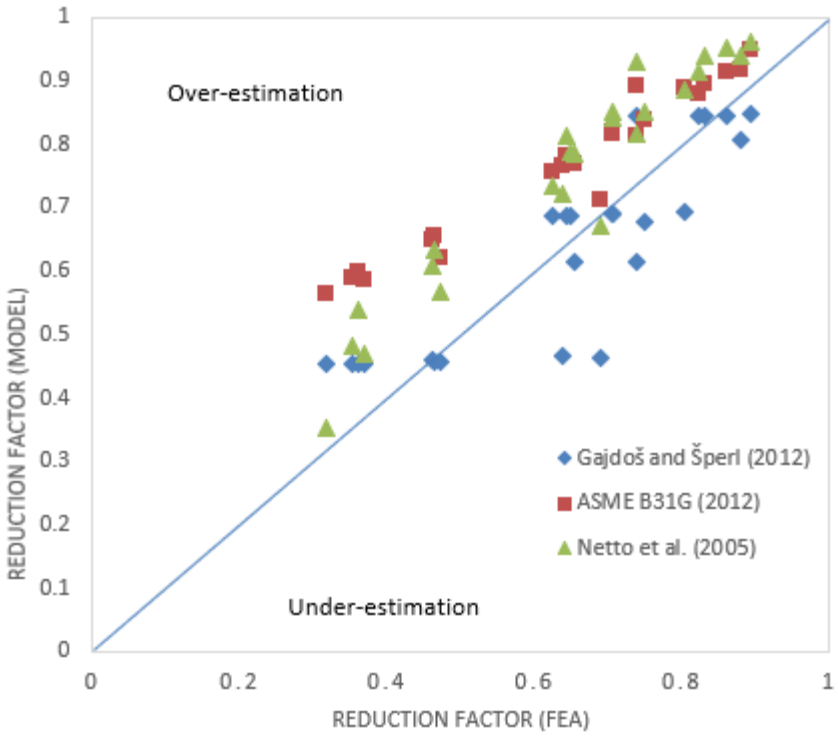

Figure 4.6. Comparison of the existing burst pressure models with FE data for high strength steel

The comparison in Fig.4.3 and 4.4 reveals that the model developed in this research based on the structures of the existing models provided an improvement to the models. The calculated results based on the developed models match with the FE data more closely than the calculations using the existing models.

The models are then evaluated with a number of burst test results available in the literature. Ma et al (2013) collected 79 burst test data from different sources. The database collected in Ma et al (2013) is used to evaluate the burst pressure models. Fig.4.7 plots the burst pressures from the tests against the burst pressures calculated using Models 1, 2 and

3, respectively. Since the test database does not include the burst pressure of intact pipes (P_0) for all cases, the burst pressures for intact pipes are estimated assuming the hoop stress as the ultimate strength of the material ($\sigma_H = \sigma_u$). The tests without defects are removed (i.e. 8 data points), and only defected pipes are focused.

In Fig.4.7, most of the data points are below 1:1 line (55, 48, 71 out of 71 data points for model 1, 2 and 3, respectively), indicating that the models provide the lower bound values. The models thus under-estimate the burst pressures with respect to the test results. It is to be noted that the experimental test results may be affected by various uncertainties including those with the defect shape, material non-homogeneity and/or other manufacturing defects, which may be the cause of overestimation by the models for a few cases. However, the models predict the experimental burst pressure reasonably.

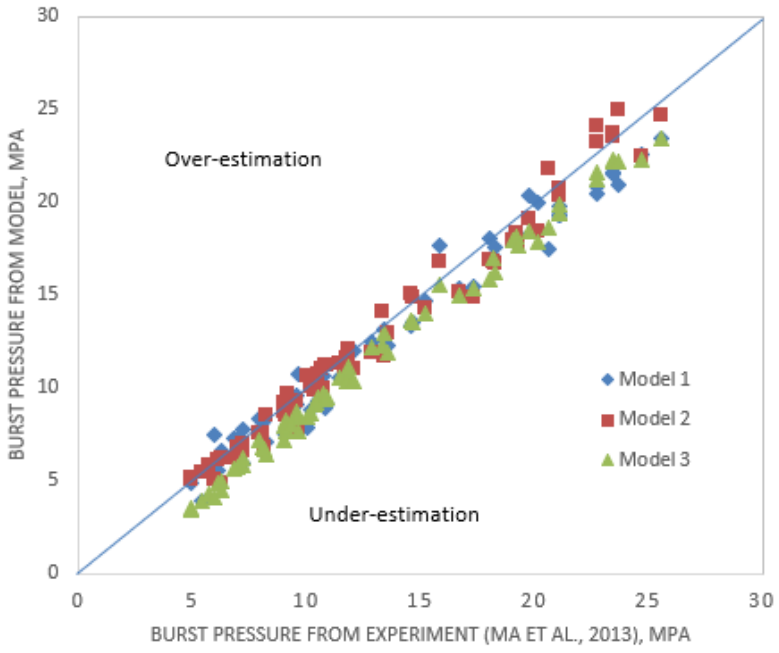

Figure 4.7. Comparison of the models with test results for high strength steel

4.6. Failure Analysis

The burst pressure models developed based on the study could be used for fitness-for-service assessments of pipelines. In this section, a failure analysis is carried out through calculating the probability of failure of a pipeline using the models. The limit state functions for the failure probability assessment can be written as follows (Eq.4.23):

$$g(X) = P - P_{op} \tag{4.23}$$

Where P is the burst pressure calculated using the models and P_{op} is the operating pressure. The failure function ($g(X) \leq 0$) is used for evaluating the probability of failure (P_f) based on Monte Carlo simulation. The parameters used in the analysis are summarized in Table 4.4.

Table 4.4. Random input variables for failure probability assessment

Parameters	**Yield Stress σ_y (MPa)**	**Thickness t (mm)**	**Diameter D (mm)**	**Internal pressure P_{op} (MPa)**	**Defect length l (mm)**	**Corrosion rate Cr (mm/year)**
Mean	452	14.6	508	8	150	0.25
COV*	0.2	0.1	0.1	0.25	0.5	0.2
Distribution	Normal	Normal	Normal	Normal	Normal	Normal

*Coefficient of variance, 1 inch = 25.4 mm, 1 MPa = 145 psi

Fig.4.8 compares the failure probability obtained using different burst pressure models. Failure probabilities over a period of 20 years of design life are calculated. As reported in Hasan et al. (2011), the P_f values obtained from the current design codes are significantly different in Fig.4.8. The failure probabilities calculated using Model 1, Model 2 and Model 3 presented in this paper are relatively close to each other. Thus, the causes

of variabilities in the existing models are minimized in the revisited models (Model 1, Model 2 and Model 3). Among these models, Model 3 provides higher failure probability and therefore can conservatively be used.

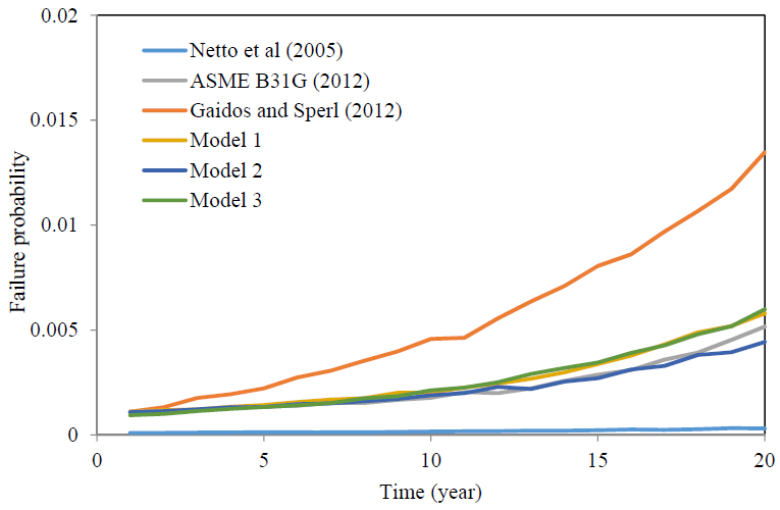

Figure 4.8. Failure probability within the design life of the analyzed pipeline

4.7. Burst Pressure Model for Cast Iron Water Main

Previous sections provide methodology for developing burst pressure models for energy pipelines with validation using test results. Test results for cast iron water main are not available. However, the study conducted for energy pipeline reveals that FE modelling can successfully be used to develop burst pressure model for cast iron water main. In this section, analysis for cast iron pipe is provided to develop a model for water mains.

4.7.1. Finite Element Analysis for Cast Iron Pipe

FE model for cast iron pipe is developed in a similar way as discussed above. Pipe diameters ranging from 127mm to 441.96mm are used based on the common pipe

diameters in the WDN at the city of Mount Pearl. Ali (2017) conducted tensile test with specimens extracted from an exhumed cast iron pipe collected from the city. The material properties from Ali (2017) are used in the analysis (Table 4.5). The results of FE analysis are shown in Table 4.6.

Table 4.5. Material properties of cast iron (After Ali, 2017)

Density (kg/m^3)	Modulus of Elasticity (GPa)	Ultimate strength (MPa)	Poisson's Ratio	Total strain at failure
7850	150.0	205	0.3	0.0039

[1] Ali, 2017.

Table 4.6. Pipe database for FE analysis with cast iron water mains

FEM No.	Diameter *D* (mm)	Wall thickness *t* (mm)	Corrosion depth *d* (mm)	Corrosion length *l* (mm)	Burst pressure *P* (MPa)
1	335.28	12.2	0	0	15.705
2	335.28	12.2	10.980	200	2.838
3	335.28	12.2	3.050	200	15.177
4	335.28	12.2	6.100	200	10.079
5	335.28	12.2	9.150	200	5.495
6	335.28	7.874	0	0	10.039
7	335.28	7.874	1.969	200	8.129
8	335.28	7.874	3.937	200	5.495
9	335.28	7.874	5.906	200	3.597
10	335.28	7.874	7.087	200	1.825
11	441.96	8.636	0	0	8.290
12	441.96	8.636	2.159	200	6.634
13	441.96	8.636	4.318	200	5.495
14	441.96	8.636	6.477	200	2.838
15	441.96	8.636	7.772	200	1.825
16	175.26	6.35	0	0	15.705
17	175.26	6.35	4.763	200	6.634
18	175.26	6.35	1.588	200	15.177

FEM No.	Diameter *D* (mm)	Wall thickness *t* (mm)	Corrosion depth *d* (mm)	Corrosion length *l* (mm)	Burst pressure *P* (MPa)
19	175.26	6.35	3.175	200	10.052
20	175.26	6.35	5.715	200	2.838
21	127	12.192	0	0	46.044
22	127	12.192	3.048	200	37.943
23	127	12.192	6.096	200	25.129
24	127	12.192	9.144	200	14.450
25	127	12.192	10.973	200	7.094
26	335.28	12.2	0	0	0.000
27	335.28	12.2	10.980	100	4.356
28	335.28	12.2	3.050	100	15.177
29	335.28	12.2	6.100	100	10.052
30	335.28	12.2	9.150	100	8.343
31	335.28	7.874	0	0	0.000
32	335.28	7.874	1.969	100	8.770
33	335.28	7.874	3.937	100	6.634
34	335.28	7.874	5.906	100	4.356
35	335.28	7.874	7.087	100	2.838
36	441.96	8.636	0	0	0.000
37	441.96	8.636	2.159	100	7.062
38	441.96	8.636	4.318	100	6.634
39	441.96	8.636	6.477	100	3.597
40	441.96	8.636	7.772	100	2.838
41	175.26	6.35	0	0	0.000
42	175.26	6.35	4.763	100	6.634
43	175.26	6.35	1.588	100	15.177
44	175.26	6.35	3.175	100	10.052
45	175.26	6.35	5.715	100	3.597
46	127	12.192	0	0	0.000
47	127	12.192	3.048	100	37.943
48	127	12.192	6.096	100	25.129
49	127	12.192	9.144	100	16.586
50	127	12.192	10.973	100	7.094

4.7.2. Development of Model for Cast Iron Pipe

With simulated burst pressures in Table 4.6, DE algorithm is conducted to obtain optimized parameters for Model 1, 2 and 3, discussed above. Table 4.7 shows the model

parameters obtained. Resulting burst pressure models for corroded cast iron pipes are shown in Equations 6.24, 6.25 and 6.26. Burst pressures calculated using the equations are then plotted against the burst pressure calculated using FE in Fig.4.9. In Fig.4.9, data points are closely scattered around the 1:1 line, the R-square values of all three models are consistently higher than 0.97. These implied that the models are reasonably fitted with simulation results. Any of these equations can therefore be used to calculate the pipe wall stress due to internal pressure as outlined in Chapter 3.

Table 4.7. The results of optimization for the model parameters for cast iron

Model	k_1	k_2	k_3	Generation	R^2
1	-0.94342	1.22143	0.10441	173	0.98659
2	-0.87921	20.72021	-8.13933	329	0.97051
3	-0.88313	0.05024	-	87	0.97082

The explicit developed models for cast iron can be expressed as:

Model 1

$$P = P_0 \times \left(1 - 0.94342 \left(\frac{d}{t} \right)^{1.22143} \left(\frac{l}{D} \right)^{0.10441} \right) \tag{4.24}$$

Model 2

$$P = P_0 \times \left(\frac{1 - 0.87921 \frac{d}{t}}{1 - 0.87921 \left(1 + 20.72021 \frac{l^2}{Dt} \right)^{-8.13933}} \right) \tag{4.25}$$

Model 3

$$P = P_0 \times \left(1 + \frac{0.88313\frac{d}{t}}{1 + 0.05024\frac{t}{l}} \right) \tag{4.26}$$

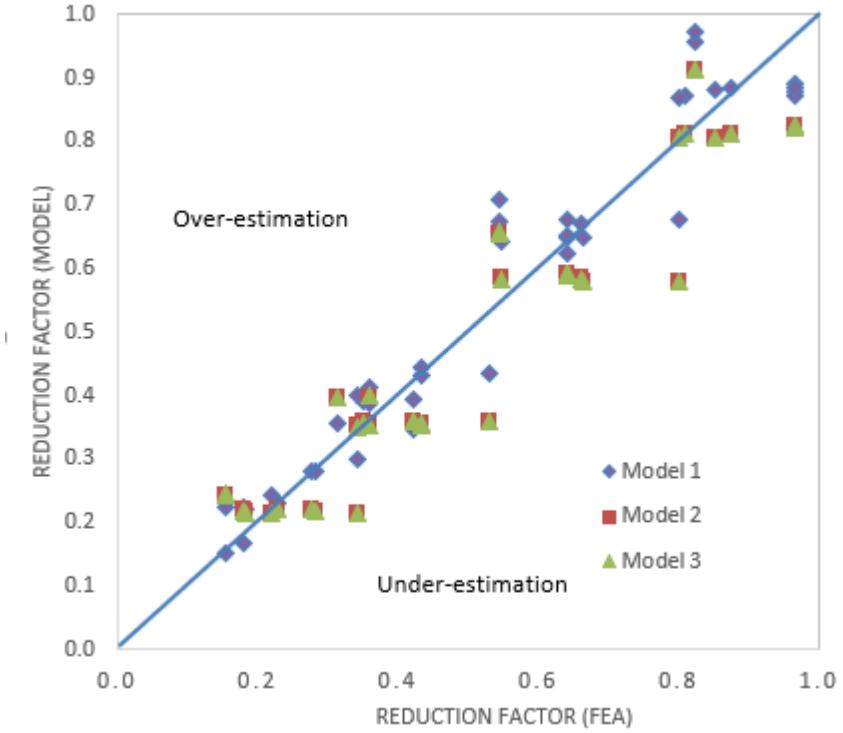

Figure 4.9. Comparison of the burst pressure models (Model 1, 2 and 3) with FE data for cast iron

4.8. Conclusion

In this chapter, burst pressure models for corroded cast iron water main are developed to facilitate calculating pipe wall stress due to internal pressure. Three existing burst pressure models for corroded energy pipeline are first revisited for a range of pipe sizes

and material strength grades. A series of FE analysis is conducted to develop a database that is used to revisit different coefficients and exponents of the models (model parameters). An optimization algorithm based on differential evolution (DE) method is used to determine the model parameters through minimization of model errors.

The study reveals that FE analysis along with optimization algorithm can suitably be used to develop improved models for burst pressure predictions. Using this approach, three models are developed based on the model structures of Netto et al. (2005), ASME B31G (2012) (or CSA Z662 2015, DNV RP-F101 2010) and Gajdoš and Šperl (2012) for high strength steel and cast iron pipe, separately.

For high strength steel pipes, the models provide the burst pressure reduction factors that match well with the values calculated using FE analysis. However, the values calculated using the existing models vary widely from the FE calculations. Among the developed models, the model based on Gajdoš and Šperl (2012) provides the most reasonable estimation of the burst pressure reduction factor for high strength steel with respect to the FE results. The models provide lower bound (conservative) values of the burst pressure with respect to the experimental burst test results available in the literature.

The FE analysis then applied to develop burst pressure model for corroded cast iron pipe. Three burst pressure models for cast iron are proposed that match reasonably with FE results.

CHAPTER 5. EFFECTS OF WATER MAIN BREAKS ON OVERALL NETWORK[4]

5.1. Introduction

In Chapters 3 and 4, a mechanics-based model for failure assessment and a framework for mechanics-based reliability assessment have been developed. This chapter focuses on developing a consequence assessment method for risk assessment of water distribution system due to water main break. A water main break may disconnect a part of the network or may reduce the redundancy of the network. To provide uninterrupted service to community, the water distribution network (WDN) is designed with an amount of redundancy using looped networks to provide alternative paths for the situations if one or more links go out of service. It is, however, difficult to assess all possible paths from the source to the demand points for a municipal WDN containing thousands of demand nodes and pipes. The performance of the WDN in providing an acceptable level of service to consumers is assessed in terms of system reliability (Tung 1985). Over the last few decades, considerable research has focused on system reliability assessments of the WDN. However, no universally accepted definition and measure of system reliability has been used. Wagner et al. (1988) developed analytical methods for system reliability assessment using network connectivity and approachability. Wagner et al. (1988) and Quimpo and

[4] This chapter is based on the published work in a peer-reviewed journal: Hieu Chi Phan, Ashutosh Sutra Dhar, Prem Thodi, and Rehan Sadiq (2018), "Probability of network disconnection of water distribution system for maintenance prioritization", Journal of Water Supply: Research and Technology-Aqua, p.jws2018097 (https://doi.org/10.2166/aqua.2018.097). The work was carried out, and the paper was drafted by the first author. The work was supervised, and the paper was reviewed by the co-authors.

Shamsi (1991) incorporated multiple connections from several source nodes to demand nodes for estimating the system reliability. The connectivity and approachability are defined as the connection of all demand nodes to the source nodes, and the connection of a demand node to its source, respectively.

Su et al. (1987) and other researchers employed hydraulic failure as the reliability measure for WDN design optimization, which is based on the measure of hydraulic availability of the system needed to provide an acceptable level of service. This approach is rigorous and provides a precise description of a WDN. However, analysis of hydraulic availability involves extensive system simulations and is therefore computer time-intensive. To overcome the computational problem, several heuristic measures of system reliability were developed (Goulter and Coals 1986, Shamir and Howard 1981, Awumah et al. 1991), which are criticized for not evaluating the hydraulic availability (Cullinane et al. 1992). Cullinane et al. (1992) attempted to balance the two types of measures where the hydraulic failure is evaluated for selected conditions. This approach still relies on heuristics and judgement. Shinstine et al. (2002) demonstrated that availability measure provides a means of examining the robustness of a WDN during design, rather than relying on implicit judgement. They employed a hydraulic simulation model (i.e., KYPIPE) to obtain the values of a pressure head at each demand node by closing a pipe or a combination of pipes, which was repeated until all the combinations of the pipes were examined. Pipes were considered as repairable components and an average time to repair of one day was assumed. In this study, a WDN containing up to 109 pipes and 89 nodes were analyzed. However, repeated hydraulic simulation of a larger WDN containing thousands of nodes would be

tedious. Aydin et al. (2014) reported 7 days of simulation of a WDN using the EPANET model. Moreover, this approach only simulates the network conditions when valves are closed immediate after pipe breaks. Water disruption due to leaks in water mains is not simulated.

Despite the limitations, the hydraulic based approach is desired for the design optimization of WDN, since it provides water availability at the demand nodes. On the other hand, for repairing deteriorating water mains in an existing WDN, the pipe breaks causing isolation of part of the system should be given priority. If isolated from the network, the demand nodes will not have any available supply. The focus of the present study is the prioritization of water mains for repair/maintenance and to identify the pipes and combinations of pipes causing isolation (disconnection) of parts of the WDN. The failure probability of the system is defined as the probability of disconnection. Although breaks of other pipes may also cause water to be unavailable at certain demand nodes due to low pressure, this is not considered here, to avoid computationally expensive hydraulic simulations.

To identify a pipe and combinations of pipes causing isolation, the minimal cut-set method is used. In the conventional minimal cut-set method, pipes causing system failure are rigorously examined, requiring complex and extensive computation. Yannopoulos and Spiliotis (2013) employed graph theory using a connectivity matrix to identify minimal cut-sets. The computational time required in this method is also significantly high. To overcome this computational limitation, this study employs Complex Network Analysis (CNA) to find the minimal cut-sets of the network. CNA has been used for the

quantification of structural properties of networks and to improve understanding of network connectivity and robustness. Complex network models have been applied in various areas including WDNs (Yazdani and Jeffrey, 2010, 2011a, 2011b; Nazempour et al., 2016). Yazdani and Jeffrey (2010) discussed the metrics for CNA to evaluate the robustness and vulnerability characteristics of a WDN. Among several metrics for CNA, Algebraic Connectivity (AC) has been proposed and analyzed by Fiedler (1973). AC is a well-known measure for evaluating the well-connectedness of a graph (Fiedler, 1973; Capocci et al., 2005; Ghosh and Boyd, 2006; Newman, 2006, Yazdani and Jeffrey, 2011a, b). The network with higher AC is more robust and more tolerant to the breakage of links. AC provides information on graph partitioning that is closely related to the disconnection of nodes due to pipe breaks (Phan et al., 2017a). Fiedler (1973) pointed out that an event of disconnection in a system would lead to the increase of AC. On the other hand, decrease of AC corresponds to a reduction of redundancy in the network (Phan et al., 2017a). AC has been used to develop a framework to evaluate the redundancy or robustness of WDNs (Fiedler, 1973; Yazdani and Jeffrey, 2010; Phan et al., 2017a). However, no such comprehensive modeling has ever been performed to take advantage of the characteristics of the AC for network reliability assessment.

The novelty of the current study is the development of a method for finding minimal cut-sets of complex WDNs using AC. The proposed approach is computationally more efficient than the existing methods of finding minimal cut sets. A reliability framework is then developed based on AC and the failure probability of pipe components. The proposed method is applied to a real water distribution network.

5.2. Reliability with Minimal Cut-sets

This study assumes that network disconnection is equivalent to system failure and is denoted as an event, *E*. The probability of system failure can be determined using the minimal cut-set approach (Tung, 1985; Yannopoulos and Spiliotis, 2013). The minimal cut-set is a combination of a minimum number of component failures that lead to system failure (i.e., disconnection, in the current study). If E_k is an event of system failure due to a set of *k* pipes, *k* ranges from 1 to m-1 where *m* is the number of pipes in the network, the relationship between event *E* and events E_k can be written as:

$$E = E_1 \cup E_2 \cup \ldots \cup E_{m-1} \tag{5.1}$$

Because the events E_k are mutually exclusive, then:

$$P(E) = \sum_{k=1}^{m} P(E_k) \tag{5.2}$$

Where, $P(E)$ is the probability of system failure and $P(E_k)$ is the probability of event E_k to occur.

A variable, *pk* is defined as the number of minimal cut-sets consisting of *k* pipes in the network, and event E_k is the union of *pk* events corresponding to *pk* minimal cut-sets:

$$E_k = E_{k.1} \cup E_{k.2} \cup \ldots E_{k.pd} \cup \ldots \cup E_{k.pk} \tag{5.3}$$

$$P(E_k) = 1 - \prod_{pd=1}^{pk} \left(1 - P(E_{k.pd})\right) \tag{5.4}$$

$E_{k.pd}$ is the event of the pd^{th} minimal cut-set to occur, where *pd* ranges from 1 to *pk*. The relationship of system failure and the event of minimal cut-sets occurring is provided in the fault tree analysis diagram shown in Fig.5.1.

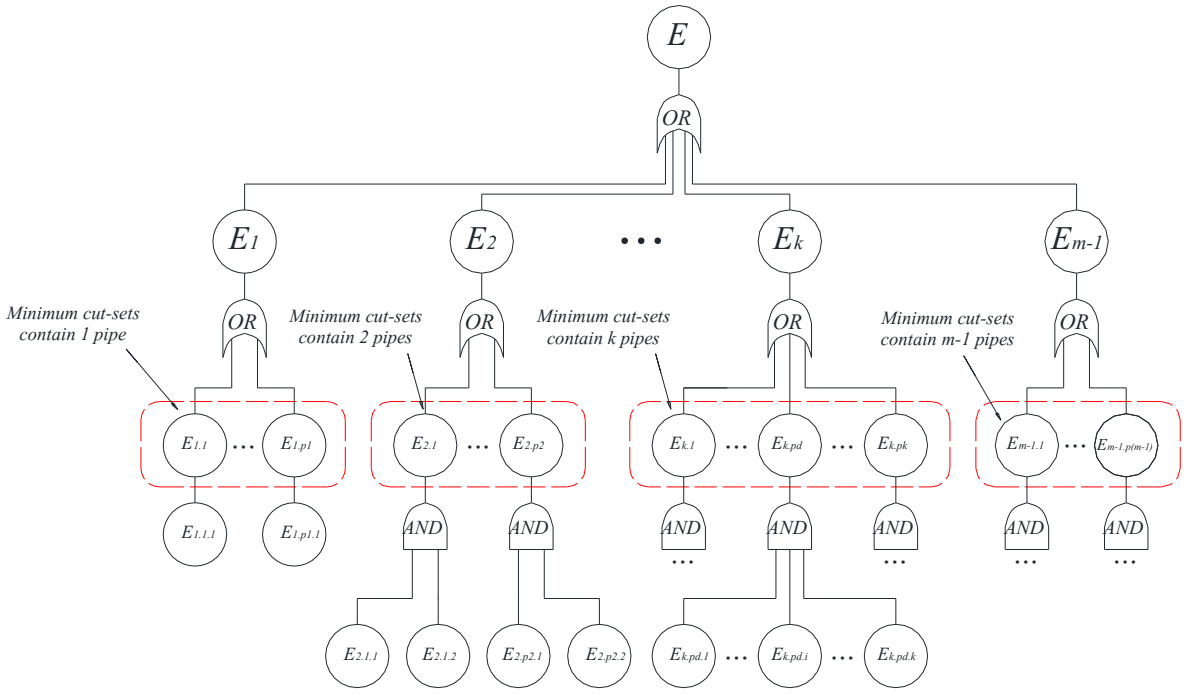

Figure 5.1. FTA of the event of disconnection occurrence in the network

Here, $E_{k.pd}$ is the intersection of *k* basic events $E_{k.pd.i}$ with i = [1:k]. In other words, $E_{k.pd.i}$ is the event of the i^{th} pipe break in the pd^{th} minimal cut-set, and thus:

$$E_{k.pd} = E_{k.pd.1} \cap E_{k.pd.pd.2} \cap \dots \cap E_{k.pd.i} \dots \cap E_{k.pd.k} \tag{5.5}$$

$$P(E_{k.pd}) = \prod_{i=1}^{k} P(E_{k.pd.i}) \tag{5.6}$$

Eq.5.4 could be rewritten as:

$$P(E_k) = 1 - \prod_{pd=1}^{pk} (1 - \prod_{i=1}^{k} P(E_{k.pd.i})) \tag{5.7}$$

Since $E_{k.pd.i}$ is the event of an individual pipe breakage, the probability of these basic events can be found directly using the component reliability model.

From Eq.5.2 and 4.7, the probability of disconnection (i.e. system failure) in the network can be estimated as:

$$P(E) = \sum_{k=1}^{m}\left[1 - \prod_{pd=1}^{pk}\left(1 - \prod_{i=1}^{k} P\left(E_{k.pd.i}\right)\right)\right] \quad (5.8)$$

The failure probability of a simple hypothetical network with its connection of nodes and lengths of pipes as presented in Fig.5.2 is examined using this approach. For the system failure probability assessment, reliability of the components (the pipes in the current study) in the network is required. Researchers have investigated several risk factors, including age, diameter, length, pipe material, corrosiveness of soil, and operating pressure for the prediction of water main breaks and developed relationships with the time-to-failure (Goulter and Coals 1986, Kleiner et al. 2010). The major challenge with this approach is the lack of availability of data to develop the model. Municipalities often lack resources to collect data, except for break records. Historic break records are therefore used to predict subsequent breaks using a homogeneous or non-homogeneous Poisson model (Goulter and Kazemi 1988, Kleiner et al. 2010). While failure probability assessment using a mechanics-based method is discussed in Chapter 3, the historic break record-based model is considered here for the hypothetical network as an example. The reliability model is developed using the average break per year (Br) of the network, which is readily available to a city. The average break rate for each pipe segment is assumed to be proportional to the length of the segment. The event of a water main break is assumed to be a Poisson process,

which is commonly used to forecast the break patterns in individual water mains (e.g. Goulter and Coals, 1986; Kleiner et al., 2010; Yannopoulos and Spiliotis, 2013). A homogeneous Poisson process with a constant annual failure rate is considered. Note that the annual break rate is not necessarily constant for a WDN. In this case, a non-homogeneous Poisson model or other models can be developed for pipe break assessments. The development of a component failure model is not within the scope of the current study.

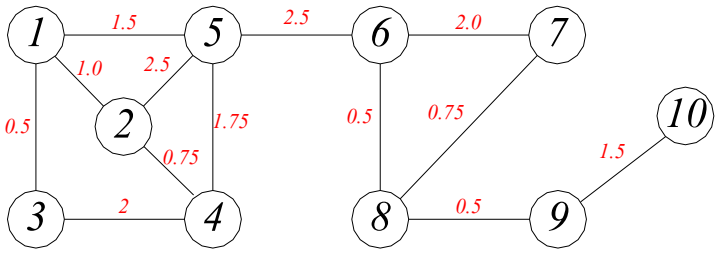

Figure 5.2. Example of a hypothetical network

Based on these assumptions, the average annual break rate for pipe linking node i and node j (from now on, written as pipe ij) can be found as follows:

$$\lambda_{ij} = \frac{Br}{l_{total}} l_{ij} \tag{5.9}$$

Where, Br is the average annual break rate in the WDN, l_{total} is total length of pipes in the network, l_{ij} is length of pipe ij and λ_{ij} is break rate of pipe ij.

Since the pipe breaking is assumed to be a Poisson process, the annual pipe failure probability can be estimated using an exponential model with a constant failure rate. This comes from the assumption that the average annual break rate is a constant. Therefore, the

component reliability of pipe ij at time t, $R_{ij}(t)$, is the probability of a pipe to function at a desired level within the period of time [0:t], where:

$$R_{ij}(t) = e^{-\lambda_{ij}t} \tag{5.10}$$

Thus,

$$P_{ij}(t) = 1 - e^{-\lambda_{ij}t} \tag{5.11}$$

For the hypothetical network in Fig.5.2, the average break per year (Br) is randomly chosen as 3 breaks per year. From Eq.5.9 and 4.10, the failure probability of each pipe within 1 month (t = 1/12) is calculated and given in Table 5.1. Consequently, the network disconnection probability is found as 0.063 with the details of calculating process given in Table 5.2. E_5 (empty) and E_{13} (empty) in Table 5.2 indicate that there are no minimal cut-sets with 5 and 13 pipes, respectively.

In Table 5.1, the pipe is named for the first and second nodes that it links. For example, pipe 5-6 means the pipe connects nodes 5 and 6. The numbers alongside in Fig.5.2 indicate the assumed geometric length of the corresponding pipe. For example, pipe 5-6 has 2.5 units length.

Table 5.1. Failure probability of pipes in a period of 1 month

Pipe	Length	λ_{ij}	$P_{ij}(t)$*
1-2	1.0	0.169014	0.014085
1-3	0.5	0.084507	0.007042
1-5	1.5	0.253521	0.021127
2-4	0.75	0.126761	0.010563
2-5	2.5	0.422535	0.035211
3-4	2.0	0.338028	0.028169
4-5	1.75	0.295775	0.024648
5-6	2.5	0.422535	0.035211
6-7	2.0	0.338028	0.028169
6-8	0.5	0.084507	0.007042
7-8	0.75	0.126761	0.010563
8-9	0.5	0.084507	0.007042
9-10	1.5	0.253521	0.021127

*t = 1 month

It can be observed from Table 5.2 that $P(E_1) \gg P(E_2) \gg P(E_3) \gg P(E_4)$. In general, $P(E_k) \gg P(E_h)$ (where h>k). This is due to the fact that $P(E_h)$ requires an intersectional condition for h (i.e., larger than k) simultaneous pipe breaks. Similarly, the intersectional condition indicates the fact that $P(E_{k-1}) \ll P(E_k)$, since the failure probability of each component is less than 1. The difference of $P(E_k)$ and $P(E_h)$ is more significant when components $P(E_{k.pd.i})$ in Eq.5.7 are relatively small. The average failure probability, $P_{Br.av}$, is useful to quantify this difference. The average failure probability can be obtained by taking the ratio of expected pipe breaks per total number of pipes in the network. This ratio is positively correlated with the breakage probability of the pipe components. Assuming that the pipe break is a Poisson process, the average failure probability within a period Δt can be written as:

$$P_{Br.av}(\Delta t) = \frac{Br \times \Delta t}{m} \tag{5.12}$$

Where: Br is the average annual break rate in the WDN and m is the number of pipes in the network.

Table 5.2. Calculations of disconnection probability of network in a period of 1 month

Min. cut-sets contain k Pipes E_k	**pk**	**Min. cut-set ($E_{k.pd}$)**	**Pipes in the min. cut-set $E_{k.pd}$ ($E_{k.pd.[pd.1]}$; … ; $E_{k.pd.[pd.k]}$)**	**$P(E_{k.pd})$**	**$P(E_k)$**
E_1	3	$E_{1.1}$	5-6	0.035211	0.0622
		$E_{1.2}$	8-9	0.007042	
		$E_{1.3}$	9-10	0.021127	
E_2	4	$E_{2.1}$	1-3; 3-4	0.000198	7.6849×10^{-4}
		$E_{2.2}$	6-7; 6-8	0.000198	
		$E_{2.3}$	6-7; 7-8	0.000297	
		$E_{2.4}$	6-8; 7-8	7.439×10^{-5}	
E_3	6	$E_{3.1}$	1-2; 1-3; 1-5	2.0955×10^{-6}	4.3219×10^{-5}
		$E_{3.2}$	1-2; 1-5; 3-4	8.3820×10^{-6}	
		$E_{3.3}$	1-2; 2-4; 2-5	5.2387×10^{-6}	
		$E_{3.4}$	1-3; 2-4; 4-5	1.8336×10^{-6}	
		$E_{3.5}$	1-5; 2-5; 4-5	1.8336×10^{-6}	
		$E_{3.6}$	2-4; 3-4; 4-5	7.3342×10^{-6}	
E_4	5	$E_{4.1}$	1-2; 1-3; 2-5; 4-5	8.6082×10^{-8}	7.8458×10^{-7}
		$E_{4.2}$	1-2; 1-5; 2-4; 4-5	7.7474×10^{-8}	
		$E_{4.3}$	1-2; 2-5; 3-4; 4-5	3.4433×10^{-7}	
		$E_{4.4}$	1-3; 1-5; 2-4; 2-5	5.5339×10^{-8}	
		$E_{4.5}$	1-5; 2-4; 2-5; 3-4	2.2136×10^{-7}	
E_5 (empty)	0	-	-		0
			…		
E_{13} (empty)	0	-	-		0
			Sum:		0.0630

If the first component in Eq.5.2 (i.e., $P(E_1)$) significantly overwhelms the summation of the others, then network disconnection probability $P(E)$ can be approximated by $P(E_1)$. That is:

$$P(E) \approx P(E_1) \tag{5.13}$$

To investigate the relationship of $P_{Br.av}$ and the difference between $P(E_1)$ and $P(E)$, the network in Fig.5.2 has been investigated by changing the average break (Br) within a fixed period of time, Δt. Fig.5.3 compares the results. Fig.5.3a shows that $P(E)$ is very close to $P(E_1)$. This is supported by Fig.5.3b, in which the ratio between $P(E_1)$ and $P(E)$ is consistently larger than 0.89. This demonstrates that $P(E_1)$ accounts for more than 89 percent of $P(E)$ in all cases. It also implies that the approximation in Eq.5.13 can be more accurate with small $P_{Br.av}$. In other words, the smaller the $P_{Br.av}$, the closer the distance between $P(E_1)$ and $P(E)$ becomes. It is observed from Fig.5.3 that $P(E_1)$ can be used to predict $P(E)$ within an acceptable small value of $P_{Br.av}$. In the case of a WDN, containing thousands of pipes combining with relatively small Br, the system $P_{Br.av}$ is expected to be small. This leads to the approximation presented in Eq.5.13 being reasonable.

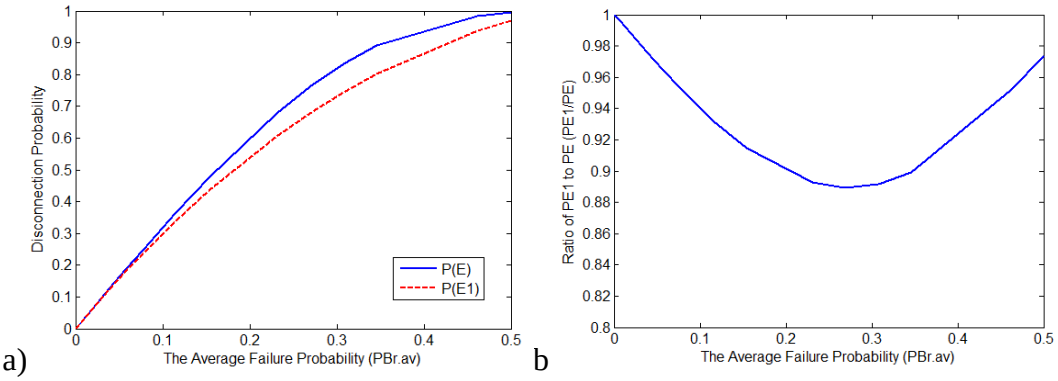

Figure 5.3. The difference between P(E) and P(E1) with the change of PBr.av. a) Comparison of $P(E)$ and $P(E_1)$, b) Ratio of $P(E_1)/P(E)$

5.3. Algebraic Connectivity

One of the major limitations of using the minimal cut-set approach for evaluating the disconnection probability of a large network is the high computational cost needed to determine all minimal cut-sets. Although applying the approximation presented in Eq.5.13, the computational cost can be significantly reduced. The conventional approach to solve the minimal cut-set problem is to count all the paths connecting two different nodes of the network. Yannopoulos and Spiliotis (2013) used the connectivity matrix from graph theory to record all the paths. If any element of the connectivity matrix is zero, then there is a disconnection between the concerned nodes. Subsequently, the minimal cut-sets are found by removing (idealized for breaking) a set of pipes and recalculating the resulting connectivity matrix. If the connectivity matrix of the break-containing network comprises zero elements, then a disconnection occurs. However, computational cost of such an approach may be significantly increased when the size of the network is large. In the following sections, the characteristic of the algebraic connectivity is investigated to determine the minimal cut-sets for a single pipe break and multiple pipe breaks.

5.3.1. AC for Single Pipe Breaks

Algebraic Connectivity (AC) is a parameter used in graph theory to determine the strength of connection between the nodes in a network. Mathematically, it is defined as the second smallest Eigenvalue of the Laplacian matrix of the connected graph (Fiedler, 1973). Municipal WDNs can be considered as graphs of connected network, where a number of pipes connect the nodes at their intersections. Then, the graph of WDN can be described

as G=G(V,P), where *V* is a set of *n* nodes (intersections) and *P* is a set of *m* pipes. An adjacent matrix A of G is used to describe the link between the nodes, where:

$$A = a_{ij} \tag{5.14}$$

$a_{ij} = 1$, if there is a link (pipe) between node i and node j.

$a_{ij} = 0$, if there is no link (pipe) between node i and node j.

The node-degree matrix is a diagonal matrix, which contains the information about the number of connections (node-degree) at each node, and is defined as:

$$D = diag(d_i)$$

d_i = number of connection (node-degree) of node i, where:

$$d_i = \sum_{j=1}^{n} a_{ij}$$

Then, the Laplacian matrix is given by Eq.5.15:

$$L = D - A \tag{5.15}$$

The Laplacian matrix L for the undirected network is usually symmetrical and the sum of rows (and columns) is zero. This characteristic leads to the fact that the first (i.e. smallest) Eigen-value (λ_1) of the matrix is zero, corresponding to the Eigen vector of $(1,1,...,1)^T$. The second smallest Eigenvalue (λ_2) of the Laplacian matrix is the AC, which is greater than 0 if G is a connected graph. The Eigenvalues of a network with *n* nodes of connected graph are: $\lambda_1 = 0 \leq \lambda_2 = \mathrm{AC} \leq \lambda_3 \leq \cdots \leq \lambda_n$.

A network with higher AC implies that the network is better connected (Newman 2010; Costa et al., 2007; Yazdani and Jeffrey 2010 and 11a). The addition of links to a network has been observed to increase the AC, as reported in Ghosh and Boyd (2006) and Phan et al. (2017a). Ghosh and Boyd (2006) have reported a method to maximize the AC with a set of pipes to increase the redundancy of the network when the number of nodes remains the same. On the contrary, the process of pipe breakage may be considered as a reverse process of decreasing the AC with the break or removal of pipes from the network. As long as the disconnection has not occurred, the AC tends to decrease, implying that the redundancy of the network is reduced after a break event. This indicates if a break does not isolate a node or cluster of nodes, the AC will decrease from the value prior to the break.

However, when a node or a cluster of nodes is isolated due to pipe breakage, the Laplacian matrix of the network becomes a combination of two (or more) non-connected sub-networks. Then, the AC will be higher. For example, assume a network has two clusters; Cluster 1 includes nodes from 1 to i-1, and Cluster 2 includes nodes from i+1 to n. The clusters of nodes are only linked by i^{th} node. If links to this node are all broken, then the network Laplacian matrix will have the following form:

$$L = \begin{matrix} \\ \\ \\ \\ Node\ 1\ to\ i-1 \\ Node\ i \\ Node\ i+1\ to\ n \end{matrix} \begin{matrix} \begin{bmatrix} [Laplacian\ Matrix\ of\ Cluster\ 1] & [0] & [0] \\ [0] & 0 & [0] \\ [0] & [0] & [Laplacian\ Matrix\ of\ Cluster 2] \end{bmatrix} \\ Node\ 1\ to\ i-1 \quad Node\ i \quad Node\ i+1\ to\ n \end{matrix} \tag{5.16}$$

The separation above is called graph partitioning. In the case of graph partitioning, the AC of the network is a combination of the isolated clusters. Fiedler (1973) mathematically proved that:

$$\lambda_2(G) \leq \lambda_2(G_{rn}) \leq \lambda_2(G_{rp}) \quad (5.17)$$

Where: $\lambda_2(\mathrm{G})$ is the AC of the connected network, $\lambda_2(\mathrm{G_{rn}})$ is the AC of the network after the disconnection with removal of nodes, and $\lambda_2(\mathrm{G_{rp}})$ is the AC of the network after the disconnection with removal of pipes.

The disconnection may be viewed as the direct failure of the network, considering the system failure as the state of not properly serving water to every demand node (i.e. the communities). The reduction of redundancy might lead to the disabling of service to demand nodes but might not directly result in a network failure event. Thus, the AC will change with the removal of a pipe in the network, where:

1. AC will increase (ΔAC is positive) if an isolation of nodes occurs, and

2. AC will decrease (ΔAC is negative) if the redundancy is reduced.

Now, if the removal of a pipe leads to disconnection of the network (e.g., AC increases), such a pipe is considered as a minimal cut-set. Thus, observing the change in AC by removing pipes one by one within the network, all minimal cut-sets can be determined.

For illustration, the AC for a hypothetical network shown in Fig.5.2 is estimated to demonstrate the numerical values of the parameter in describing robustness of the network.

The network consists of 10 nodes and 13 links (i.e. pipes) with the AC of 0.19781 (i.e. AC_{intact}=0.19781). It is representative of a WDN connecting two distinct communities. Community 1 contains nodes 1 to 5 and Community 2 contains nodes 6 to 10. The communities are connected by pipe 5-6. In other words, pipe 5-6 has a high betweenness.

Table 5.3 ranks 13 events corresponding to the removals of 13 pipes from the network. The difference between AC before and after removal of a pipe is presented in a descending order. There are 3 events with AC increases, resulting in the network disconnection. These are events 1.1, 1.2 and 1.3, with the removals of pipes 5-6, 8-9 and 9-10, respectively. These three pipes are the minimal cut-sets that contain only one break corresponding to events $E_{1.1}$, $E_{1.2}$ and $E_{1.3}$, shown in Table 5.2.

As seen in Fig.5.2, the removal of pipes 5-6, 8-9 and 9-10 will result in the disconnection of a node or cluster of nodes. Removal of pipe 5-6 caused the highest increase (i.e. ranked first) since it has high betweenness. Pipe 9-10 has the least increase because the removal of 9-10 leads to the isolation of a single node (node 10). Phan et al. (2017a) have concluded from a previous study that the size and number of disconnected clusters greatly affect the increase of the AC.

The other 10 events (i.e., event 1.4 to 1.13) in Table 5.3 show a decrease of the AC with removal of a single pipe, indicating no disconnection. However, the redundancy of the network is decreased, and thus the change in the AC shows a positive correlation to redundancy. Similar observations were reported in previous studies (Yazdani and Jeffrey, 2011a and b). These 10 events can further be divided into two groups; the first group

consisted of events 1.4 to 1.10 with the removal of pipes in Community 1. The second group is the events 1.11 to 1.13 with the removal of pipes in Community 2 which has a higher absolute change in AC (ΔAC) compared to the first group. This difference is because Community 2 (with AC=0.5188) has less redundancy compared to Community 1 (with AC=2.000).

Table 5.3. AC with removal of a link

Sub-Event	Removed Pipe ID	AC	Change in AC $\Delta AC = AC - AC_{intact}$	Type of Network Struct. Change	Grouped as	Note
1.1	5-6	0.518806	0.32100	Disconnection	Group 1	$E_{1.1}$
1.2	8-9	0.351227	0.15342	Disconnection	Group 1	$E_{1.2}$
1.3	9-10	0.266187	0.06838	Disconnection	Group 1	$E_{1.3}$
1.4	1-2	0.197626	-0.00018	Less redundancy	Group 2	
1.5	2-4	0.197626	-0.00018	Less redundancy	Group 2	
1.6	1-3	0.193938	-0.00387	Less redundancy	Group 2	
1.7	3-4	0.193938	-0.00387	Less redundancy	Group 2	
1.8	2-5	0.186393	-0.01141	Less redundancy	Group 2	
1.9	1-5	0.182328	-0.01548	Less redundancy	Group 2	
1.10	4-5	0.182328	-0.01548	Less redundancy	Group 2	
1.11	7-8	0.181990	-0.01582	Less redundancy	Group 2	
1.12	6-7	0.167151	-0.03066	Less redundancy	Group 2	
1.13	6-8	0.134125	-0.06368	Less redundancy	Group 2	

From the analysis it can be observed that the ΔAC can be used for:

1. Identifying the disconnection and reduction of redundancy by observing the sign of ΔAC, where a positive sign (+) denotes network disconnection and a negative sign (-) indicates reduction of redundancy;

2. Identifying the components causing most significant disconnection based on the highest positive ΔAC;

3. Identifying the components causing the most significant decrease in redundancy, based on the highest negative ΔAC.

The AC based method to determine the minimal cut-set involving a single pipe break, as discussed above, is based on solving the Eigenvalue problem. This is basically different from the method of counting paths as described in Yannopoulos and Spiliotis (2013). To identify whether a single pipe or a set of pipes breaking is a minimal cut-set or not, the method reported in Yannopoulos and Spiliotis (2013) requires finding the associated connectivity matrix B, as presented below:

$$B = AA^1 + AA^2 + \cdots + AA^{n-1} \quad (5.18)$$

Where: AA is the adjacent matrix A (see Eq.5.14) with the removal of the concerned pipe or set of pipes.

Since the computational cost of multiplying two matrices with size *n x n* is $O(n^3)$ for a naive algorithm, the computational cost of the last component of matrix B will be $O(n^4)$. Even for the improved algorithm proposed by Coppersmith and Winograd (1990), the

computational cost of estimating A^{n-1} will be approximately (n-2) × $O(n^{2.375477})$ = $O(n^{3.375477})$. However, using the Eigenvalue problem, it can be reduced to $O(n^2)$ for each step of the interaction, for calculating only Eigenvalues (Flannery et al., 1992), compared to the cost of $O(n^3)$ otherwise. Thus, calculating the last component in Eq.5.18 itself is more computationally expensive than the Eigenvalue problem. Consequently, this method of counting paths is more computationally expensive than the method based on the Eigenvalue problem. Using the available functions of Matlab^R software to solve the Eigenvalue problem consisting of 5000 nodes and 5000 pipes, which is close to the size of the WDN in the city of Mount Pearl in Newfoundland and Labrador, the time required for the Eigenvalue problem is just 130 seconds and calculating component AA^{n-1} only takes 430 seconds.

5.3.2. AC for Multiple Pipe Breaks

However, for multiple breaks, it is challenging to compare ACs. Firstly, the number of computations increases significantly since many more sets of pipes are to be considered when the size of minimal cut-sets (i.e. number of pipes in the minimal cut-set) is large. For example, if finding the minimal cut-sets containing one pipe break requires to solve *m* Eigenvalue problems, approximately *m(m-1)/2* Eigenvalue problems need to be solved to determine all the minimal cut-sets containing two simultaneous pipe breaks. Secondly, a combination of breaks can lead to a "noisy" situation, in which both the disconnection and reduction of redundancy may occur. Once this "noise" happens, the ΔAC may decrease (e.g., $E_{2.3}$ in Table 5.2) or increase (e.g., $E_{2.1}$ in Table 5.2), depending on the network

structure. If ΔAC decreases, it may fail to recognize the disconnection. This is further demonstrated below through application of the hypothetical network in Fig.5.2.

Table 5.4 presents the ACs for all possible minimal cut-sets of the network shown in Fig.5.2. In Table 5.4, minimal cut-set $E_{2.3}$ lead to disconnection of node 7; however, the change in AC is negative. Thus, the ΔAC based method would fail to identify $E_{2.3}$. This phenomenon is termed herein as "noise". The reason for the negative ΔAC is that the increase of AC due to disconnection of node 7 is less than the decrease of AC due to loss of redundancy.

Note that all the pipes within the set of a minimal cut-set must break simultaneously to cause disconnection of the network or to increase the AC. Removal of only one pipe from the set does not lead to disconnection or an increase in AC. Thus, the AC of a network with removal of a pipe from the set of a minimal cut-set is always lower than the AC of the network with removal of all pipes in the minimal cut-set. This characteristic can be used to eliminate the noise, as discussed below.

To implement this, when ΔAC decreases with a set of *b* breaks, the AC of the network is calculated with removal of each of the pipes within the set, i.e. AC_u* for removing u^{th} pipe (u=[1:b]). If the largest AC_u* is less than the AC with removal of the full set of pipes, then disconnection occurs. For example, removal of the set of pipes 6-7 and 6-8 causes a negative ΔAC value in Table 5.4, with an AC of 0.1823. The AC of the network with the break of pipes 6-8 and 6-7 (AC_1* and AC_2*) are 0.1341 and 0.1672, respectively. These two values are lower than the AC of the event $E_{2.3}$ (0.1823). Therefore, the set of pipes 6-

7 and 7-8 is a minimal cut-set that leads to disconnection. In this manner, the noise removal is applied to the network (Fig.5.2) and the minimal cut-sets of the network based on the change in AC are successfully determined and tabulated in Table 5.4.

Table 5.4. Minimal cut-sets and associated AC values

Min. cut-set ($E_{k.pd}$)	**Pipes in the min. cut-set $E_{k.pd}$ ($E_{k.pd.[pd.1]}$;…; $E_{k.pd.[pd.k]}$)**	**AC**	**ΔAC**
$E_{1.1}$	5-6	0.5188	0.3210
$E_{1.2}$	8-9	0.3512	0.1534
$E_{1.3}$	9-10	0.2662	0.0684
$E_{2.1}$	1-3; 3-4	0.2230	0.0252
$E_{2.2}$	6-7; 6-8	0.5858	0.3880
$E_{2.3}$	6-7; 7-8	0.1823	-0.0155
$E_{2.4}$	6-8; 7-8	0.4384	0.2406
$E_{3.1}$	1-2; 1-3; 1-5	0.2051	0.0073
$E_{3.2}$	1-2; 1-5; 3-4	0.2509	0.0531
$E_{3.3}$	1-2; 2-4; 2-5	0.2104	0.0126
$E_{3.4}$	1-3; 2-4; 4-5	0.2509	0.0531
$E_{3.5}$	1-5; 2-5; 4-5	0.4131	0.2153
$E_{3.6}$	2-4; 3-4; 4-5	0.2051	0.0073
$E_{4.1}$	1-2; 1-3; 2-5; 4-5	0.3004	0.1026
$E_{4.2}$	1-2; 1-5; 2-4; 4-5	0.3004	0.1026
$E_{4.3}$	1-2; 2-5; 3-4; 4-5	0.2137	0.0159
$E_{4.4}$	1-3; 1-5; 2-4; 2-5	0.2137	0.0159
$E_{4.5}$	1-5; 2-4; 2-5; 3-4	0.3004	0.1026

5.4. Reliability Assessment Using AC

The exact solution of the network disconnection probability can be obtained theoretically by rigorously examining the minimal cut-sets using FTA, as discussed above. However, this process requires tedious and complex computations for a large-scale network. Therefore, a practical approach is required, using with assumptions to overcome

the difficulties. This section develops a framework to estimate network disconnection probability based on the change of AC. It is revealed earlier that a single event-based failure probability provides a reasonable approximation of the system failure probability (i.e., $P(E) \approx P(E_1)$). Both single event-based and multiple-event-based failure probabilities are considered here for the AC based reliability assessment. For the failure probability of the pipe components, a constant failure rate-based model, a failure function (i.e., exponential function) and Monte Carlo simulation (MCS) are considered.

5.4.1. Single Event Based Approximate Failure Probability

When the pipe breaking is assumed as a Poisson process with a constant failure rate, which depends on the length of the components, the mean pipe failure rate of a component can be related to the length of the component using Eq.5.9. It can be expressed for the minimal cut-set containing one pipe as:

$$-\lambda_{1.pd} = -\frac{Br}{l_{total}} l_{1.pd} \tag{5.19}$$

Where: $l_{1.pd}$ is the length of pipe corresponding to the pd^{th} minimal cut-set containing only one pipe.

Approximating P(E) ≈ P(E1), as described in Eq.5.13, the failure probability of the system can be defined as:

$$P(E) \approx P(E_1) = 1 - \prod_{pd=1}^{p1}\left(1 - P\left(E_{1.pd}\right)\right) = 1 - \prod_{pd=1}^{p1}\left(e^{-\lambda_{1.pd} \times t}\right)$$

$$= 1 - e^{t\sum_{pd=1}^{p1}\left(-\lambda_{1.pd}\right)} \tag{5.20}$$

Substituting Eq.5.19 with Eq.5.20:

$$P(E,t) \approx 1 - e^{\left(-\frac{Br \times t}{l_{total}} \sum_{pd=1}^{p1} (l_{1.pd})\right)} \quad (5.21)$$

For a group of pipes with minimal cut-set, the total length of the group is given by

$$l_{g1} = \sum_{pd=1}^{p1} (l_{1.pd}) \quad (5.22)$$

Using the length of the group of pipes, the failure probability of the system can be defined as:

$$P(E,t) \approx 1 - e^{\left(-\frac{l_{g1} \times Br \times t}{l_{total}}\right)} \quad (5.23)$$

However, the pipe breaking is not necessarily a Poisson process with or without a constant failure rate. Particularly, the WDN is a system containing a mixture of pipes ranging from newly installed segments to wear-out segments. The age-dependent degradation of WDN pipe segments is an unavoidable mechanism, because these structures are exposed directly to a hazardous environment, leading to corrosion and cracking. Once a pipe is at its wear-out stage, the assumption of a constant break rate may no longer be adequate. The degrading pipe segments would need a more precise failure function with sufficient input data to describe the failure process with an increasing failure probability. For any other component failure model, the failure probability of the system can be defined based on the assumption of P(E) ≈ P(E1) as:

$$P(E,t) \approx P(E_1,t) = \left[1 - \prod_{pd=1}^{pk} \left(1 - P\left(E_{1.pd.[pd.1]}, t\right)\right)\right] \quad (5.24)$$

A detailed failure probability estimation procedure using either Poisson process-based failure functions or any other failure functions are illustrated in Fig.5.4.

5.4.2. Multiple Event Based Failure Probability

Fig.5.5 illustrates the detailed procedure of calculating system failure probability considering rigorous multiple events (i.e., minimal cut-sets). As discussed earlier, "noise" may appear in the failure probability assessment for minimal cut-set containing multiple pipes. Thus, there can be some disconnection events with negative ΔAC. A sub-algorithm (Fig.5.5) discussed in Section "AC for multiple pipe breaks" can be applied to avoid the noise problem. For calculation of failure probability of the components, application of a Monte Carlo (MC) simulation is used.

The methods discussed above are applied to the network presented in Fig.5.2 through development of codes using Matlab^R software. The calculated failure probabilities are compared in Fig.5.6. For the failure function, an equivalent exponential model is considered for illustration. The failure probability based on rigorous investigation of the network using FTA (without the use of AC) is also calculated and included in the figure. Among AC based methods, the approximate failure probabilities calculated using a Poisson process based and exponential component failure model are the same in Fig.5.6, since equivalent reliability models are used for the components. In the developed framework, different reliability models can be used (e.g. Weibull or lognormal distribution) instead of an exponential model, if the distribution is known.

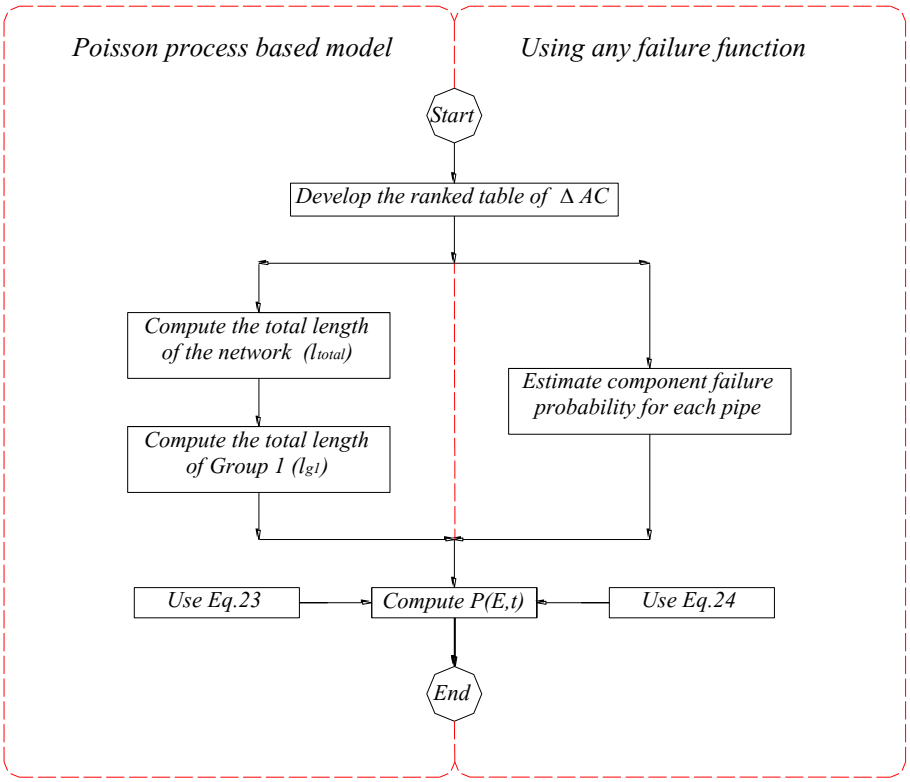

Figure 5.4. Flow chart for single event based approximate failure probability (P(E) ≈ P(E1))

The MC simulation conducted using 10000 trials each time provides multiple event-based failure probabilities, which is very close to the failure probabilities calculated using single event-based approximation. Note that the MC simulation without the "noise" removal sub-algorithm fails to predict the failure probability (Fig.5.6).

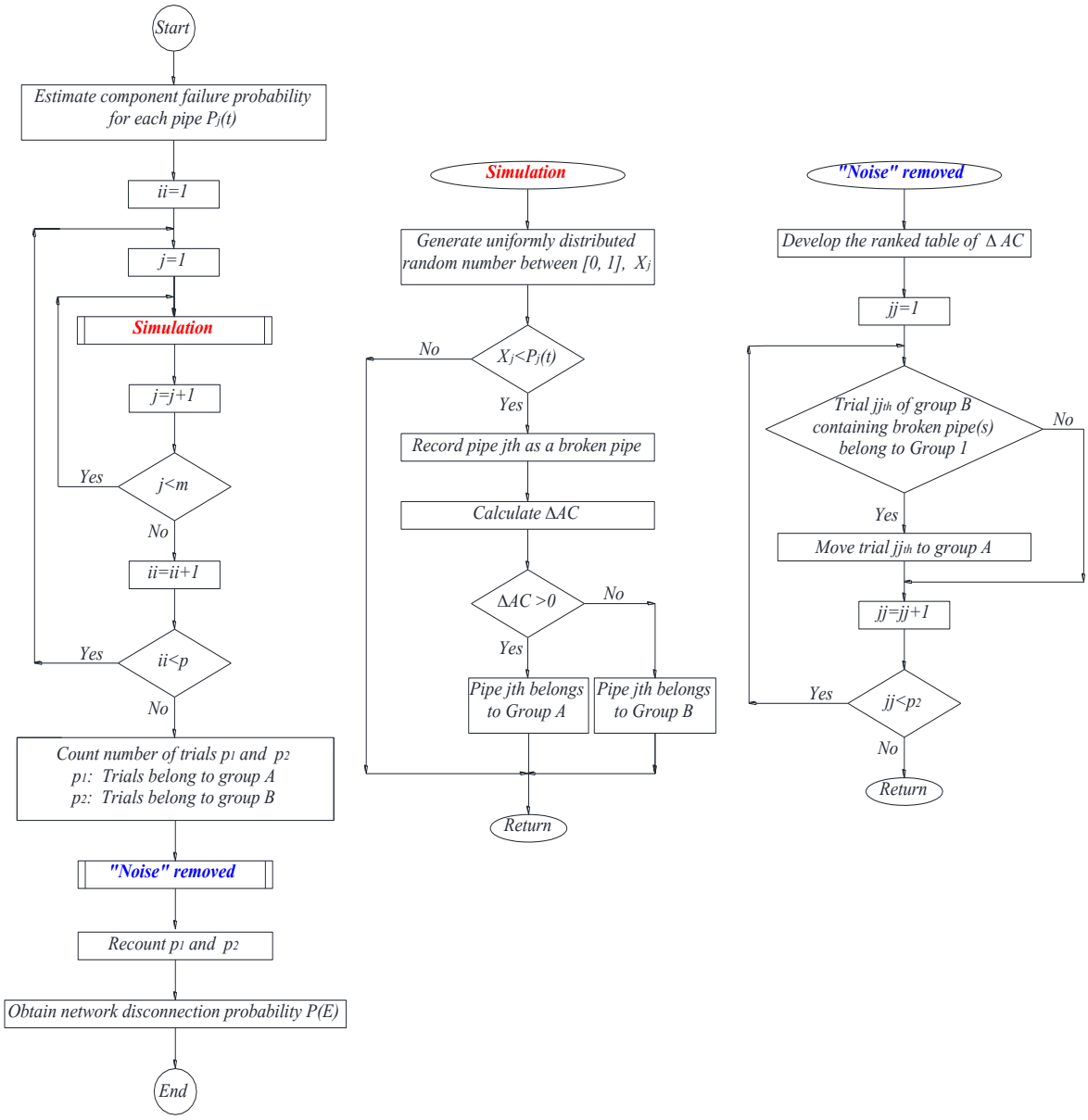

Figure 5.5. Flow chart for multiple event-based failure probability calculation

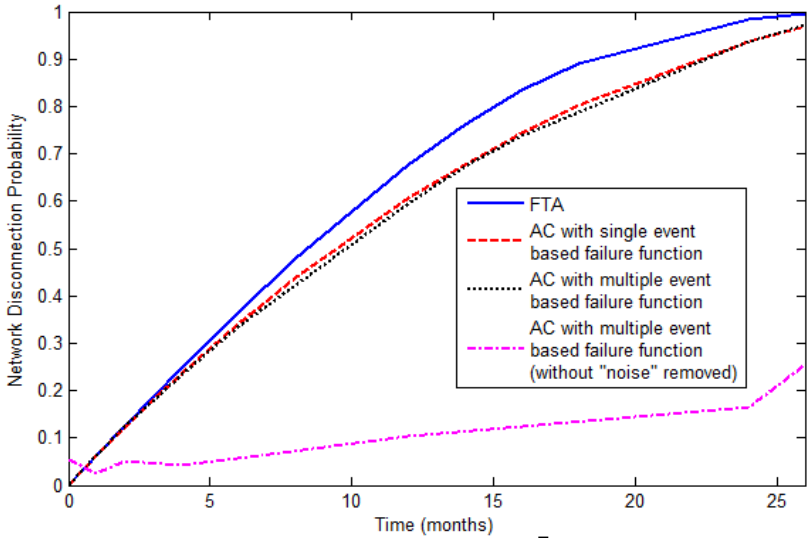

Figure 5.6. Comparison of network disconnection probability with different approaches

In Fig.5.6, the failure probability calculated using the FTA and AC methods is not significantly different. The network disconnection probability reaches close to one hundred percent after 26 months, according to the rigorous FTA solution. The AC based method with reliability algorithms predicts the failure probability as 97 percent (after 26 months).

5.5. A Case Study of the City of Mount Pearl

The developed method is applied to the network in the city of Mount Pearl, which is a community with a population of approximately 25,000. The water main system contains 130km of pipe network (see schematic shown in Fig.5.7). Thus, on average, 192 people are served by each kilometer of water main, which is comparable to common WDNs in the USA and Canada, which serve 164 people per kilometer (Folkman, 2018). Diameters of the pipes in the city range from 150 to 450mm. Water is bought from St John's – a neighbor city – to two water tanks located at the North (S1) and South West (S2) parts of the city.

The water distribution system to support the entire city is based on gravity flow. The locations of the sources are ignored in this study, for simplification. However, they could be useful for further study, which defines system failure as the disconnection of the source to nodes or reachability of the network. A sample of a raw database for the network is presented in Table 5.5. The table is included to show the typical WDN data that can be used for the AC based method. After reorganizing the database, it is found that the WDN of the city of Mount Pearl contains 4848 nodes and 5046 pipes (Table 5.5).

This pipe system generally comprises ductile iron (91%), cast iron pipe (5%) and other materials (4%). Based on the annual water main break records of the city, the annual break rate is 6.931 breaks/year/100km. This break rate is comparable to the average break rate of 6.77 breaks/year/100km reported in Folkman (2018). It is understood that the break rate based on limited records is not sufficient for failure assessment but is acceptable for the purpose of illustration.

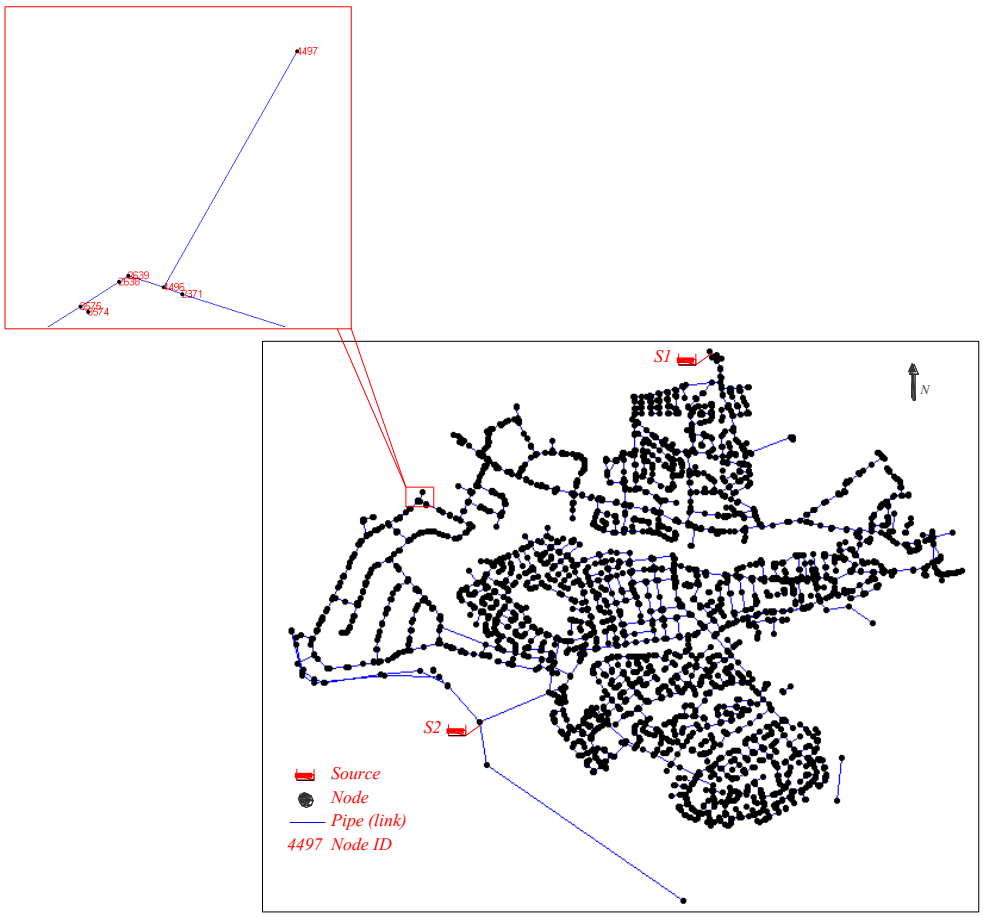

Figure 5.7. Schematic of water main network in city of Mount Pearl

Table 5.5. Water main database for city of Mount Pearl

Node ID	Shape	Pipe ID	Material	Diameter (mm)	X	Y
1	Point	1	Ductile Iron	150	320991.62230	5264475.70150
2	Point	1	Ductile Iron	150	321007.09150	5264498.97460
3	Point	2	Ductile Iron	200	321048.28280	5265709.24110
…	…	…	…	…	…	…
8564	Point	9474	Ductile Iron	150	320423.51620	5263016.32110

Table 5.6. Complex network system parameters for the city of Mount Pearl (After Phan et al. 2017a)

Parameter	Equation	Calculated value	Reference values*
Total length	$l_{total} = \sum_{i=1}^{n}\sum_{j=1}^{n} l_{ij}$	129.837 (km)	
Number of pipes	-	5046	769-3065
Number of nodes	-	4848	755-2799
Link-per-node	$e = \frac{m}{n}$	1.041	1.01-1.10
Average node degree	$k_a = \frac{2m}{n}$	2.082	2.04-2.23
Link density	$q = \frac{2m}{n(n-1)}$	4.29×10^{-4}	7.83×10^{-4}– 2.7×10^{-3}
Independent loop	$f = m - n + 1$	197	-
Meshedness coefficient	$r_m = \frac{f}{2n-5}$	0.0203	9.97×10^{-3} – 5.86×10^{-2}
Threshold for random removal of node	$f_c = 1 - \frac{1}{\frac{mean(k^2)}{k_a} - 1}$	0.1770	0.22 – 0.42
Route factor	$g = \frac{1}{1-n}\sum_{i=1}^{n-1} \frac{\varepsilon_{s,i}}{\delta_{s,i}}$	1.7560	1.45 -1.67
Characteristic path length	$l = \frac{1}{1-n}\sum_{i\neq j} d_{ij}$	88.378	25.94 – 51.44
Algebraic connectivity	-	1.5625×10^{-5}	6.09×10^{-5}– 2.43×10^{-4}
Spectra gap	-	2.55×10^{-2}	9.08×10^{-3}– 7.27×10^{-2}

* From Yazdani and Jeffrey (2011a)

Phan et al. (2017a) calculated different parameters used in complex network analysis to assess the robustness and redundancy of the network for the WDN of the city. Yazdani and Jeffrey (2011a) provided a summary of the parameters used to assess the redundancy and robustness of networks. The parameters calculated for the network in the city of Mount Pearl are provided in Table 5.6 and are compared with values for different other cities as reported in Yazdani and Jeffrey (2011a). In Table 5.6, the parameters for the city of Mount Pearl are mostly within the ranges of those for the other cities, indicating that the

redundancy, connectivity and robustness of the city network are similar to those for other cities reported in Yazdani and Jeffrey (2011a). The redundancy, connectivity and robustness parameters of the Mount Pearl network range from the average to lower bound values of the parameters in the networks reported in Yazdani and Jeffrey (2011a). The low well-connectivity can be observed since the network contains high betweenness pipes, the removal of which could lead to the separation of the network.

5.5.1. Identification of the Critical Pipes

For identification of critical pipes using AC, the pipes can be ranked according to the change in AC (ΔAC) with and without removal of a pipe from the network. Sample results of ranking of the pipes in the city of Mount Pearl's WDN are presented in Table 5.7. The histogram of the ΔAC is presented in Fig.5.8. According to this table, there are 2061 out of 5046 pipes belonging to Group 1 that directly lead to disconnection, and the remaining pipes belonging to Group 2 cause a reduction of redundancy. From Fig.5.8, the ΔAC generally ranges from -2.5×10^{-6} to 2.5×10^{-6} with some outliers that have significantly high positive values of up to 40×10^{-5}. This sudden jump in ΔAC marks the most critical pipes, the failures of which would lead to an overall structural change in the network (i.e. disconnection on a large scale). Group 2 does not contain such outliers. Even though Group 2 has no outliers, it is helpful to understand the reduction of redundancy on a macro scale. To investigate the groups of pipes further, a set of the top 50 ranked pipes from Group 1 is analyzed in more detail. The most important pipes of Group 2 (first 100 ranked pipes) have also been analyzed as, illustrated in Fig.5.9.

The critical pipes in the network are also identified using the Shortest Path (SP) method for comparison. In the SP method, the shortest path to all pairs of nodes within the network is investigated. The method is thus computationally more demanding than the AC based method. A pipe component appearing in the highest number of the shortest path is most critical, since water is expected to flow through this pipe component to a maximum number of destinations. The pipes are therefore ranked according to the number of their appearances on the shortest paths. The pipes with higher rank are more critical. Fig.5.10 shows the top 100 highest ranked pipes (shown in pink color) in the city of Mount Pearl's network. As seen in the figure, the critical pipes connect the northern and southern communities. The highest ranked pipe is the one laid between the Southern community, S1, and Northern community, S2 (Fig.5.10). Note that the sub-communities are not disconnected with removal of the pipe, since there are several other paths (redundancy) to connect the two sub-communities. An alternative path is shown as bold black lines in Fig.5.10. Thus, the SP method provides information for the important pipes (critical pipes), which may or may not lead to the separation of part(s) of the network. The method cannot be applied to identify the pipes that may lead to network disconnections.

The top ranked pipes based on the ΔAC (Fig.5.9) matched well with the shortest path results presented in Fig.5.10. Thus, the ΔAC could effectively classify the critical pipes in Group 1 and Group 2. The ranked ΔAC table can also be used to identify the alternate path of connecting two points, which cannot be obtained from the shortest path method.

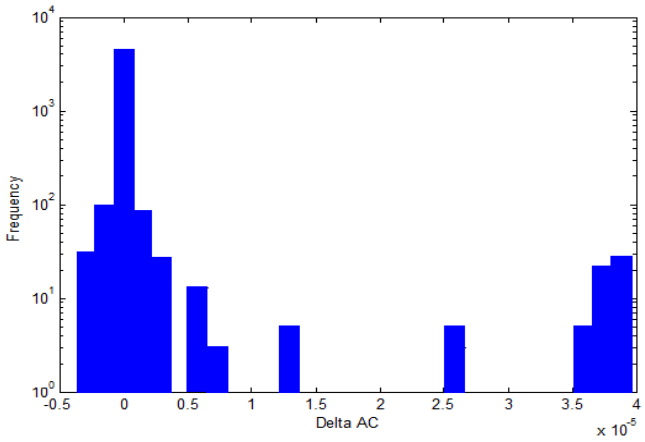

Figure 5.8. Histogram of the ΔAC with single break from Table 5.7

Table 5.7. The changes of AC for the city of Mount Pearl WDN

Removed pipe ID	AC	Δ AC = AC-AC$_{intact}$	Type of network structural change	Grouped as
1734-1735	5.52×10^{-5}	3.96×10^{-5}	Disconnection	Group 1
1734-3518	5.52×10^{-5}	3.96×10^{-5}	Disconnection	Group 1
1733-3518	5.52×10^{-5}	3.95×10^{-5}	Disconnection	Group 1
...	...	...	...	...
2373-2631	1.21×10^{-5}	-3.56×10^{-6}	Less redundancy	Group 2
1655-2631	1.21×10^{-5}	-3.57×10^{-6}	Less redundancy	Group 2
1655-1656	1.21×10^{-5}	-3.57×10^{-6}	Less redundancy	Group 2

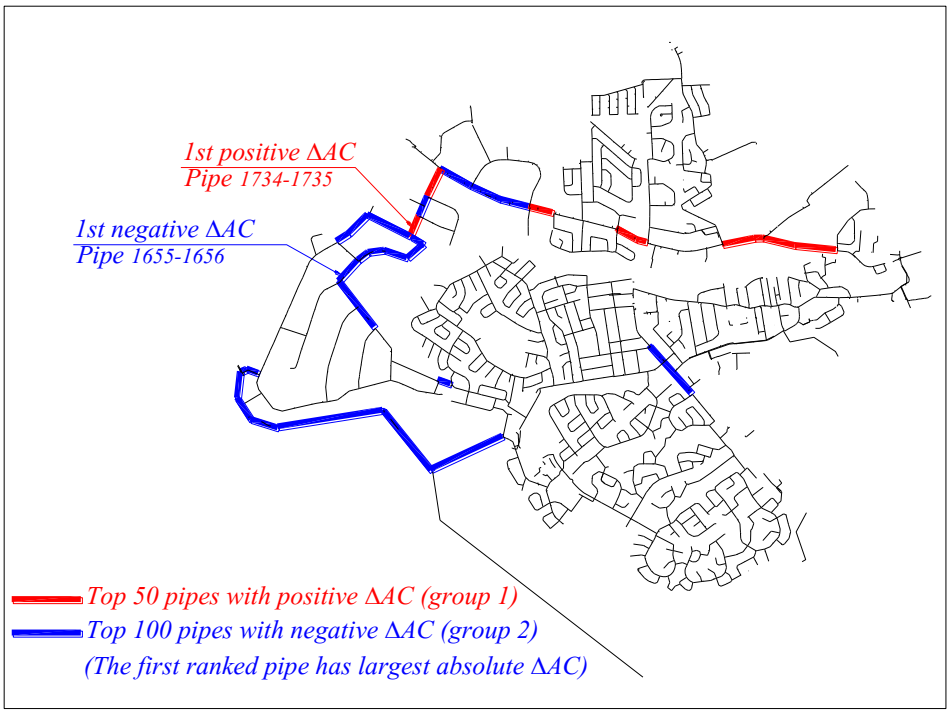

Figure 5.9. Top ranked pipes of Group 1 and Group 2

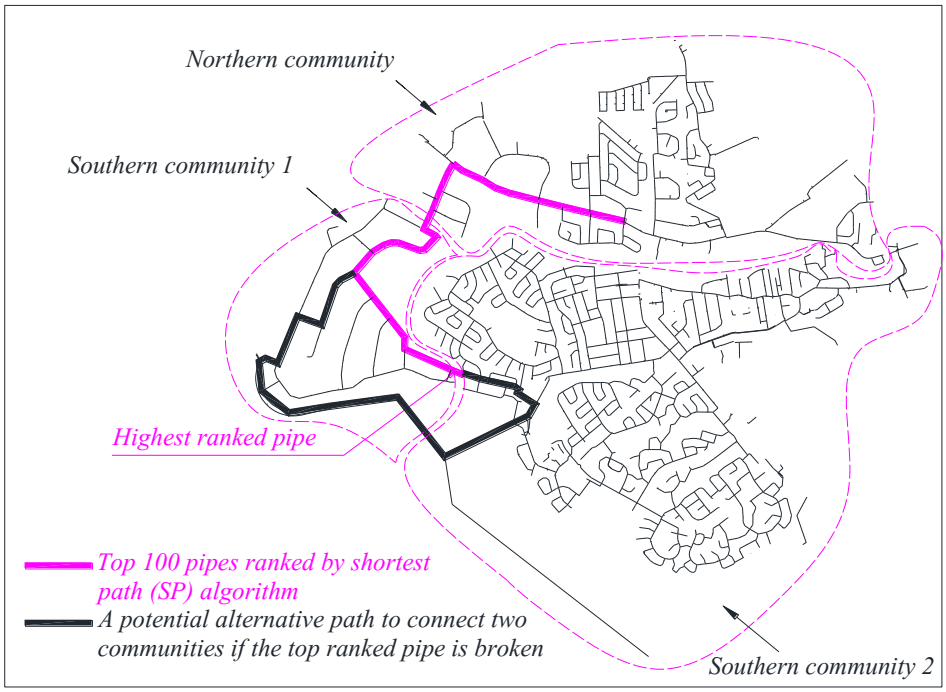

Figure 5.10. Results for shortest path analysis

5.5.2. Estimating the System Disconnection Probability

Disconnection probability of the city of the Mount Pearl WDN is analyzed using the methods discussed above. The results are presented in Table 5.8 and Fig.5.11. Time periods of 1, 2, 6 and 12 months are used in the analysis. From Table 5.8, the $P_{Br.av}$ of the network is significantly low compared with the example in Fig.5.2. Thus, the calculated failure probabilities using the single event-based approach and the multiple even based approach are almost the same in Fig.5.11.

Table 5.8. Comparison of failure probabilities

Δt (month)	**Average number of breaks**	**$P_{Br.av}$**	**$P(E_1, \Delta t)$ Single event based**	**$P(E, \Delta t)$ Multiple event based**
1	0.716	1.486×10^{-4}	0.243	0.229
2	1.518	2.973×10^{-4}	0.427	0.436
6	4.479	8.918×10^{-4}	0.812	0.814
12	8.834	17.836×10^{-4}	0.964	0.973

5.6. Conclusion

In an existing water distribution system, pipe breaks causing isolation of part of the system should be avoided, to provide uninterrupted service to the dwellers. Studying the disconnection probability of WDN is therefore important for optimizing repair/maintenance prioritization planning. A pipe or combination of pipes causing network isolation can be identified using the minimal cut-sets method. In the conventional minimal cut-set method, pipes causing system failure (i.e., isolation) are rigorously examined to determine a combination of the minimal number of components' failure leading to the system failure. The process of finding minimal cut-sets is very complex and

requires extensive computation. This chapter presents a method of finding minimal cut-sets using algebraic connectivity (AC) for complex network analysis. The AC based approaches reduced the amount of computation required compared to the existing methods including the graph theory used in Yannopoulos and Spiliotis (2013). The AC is a network parameter which is determined by solving Eigenvalue problems that avoids the counting the paths, as described in Yannopoulos and Spiliotis (2013). The decrease of AC due to a pipe break indicates a reduction of redundancy and the increase of AC indicates disconnection (isolation) of parts of the network. For the events with multiple pipe breaks, some break might cause an increase in AC while others might cause a decrease in AC, resulting in a "noisy" situation. A methodology is developed to eliminate the "noise" for multiple pipe breaks through scrutinizing the pipes in the minimal cut sets. A failure probability estimation framework is developed using the AC based minimal cut-sets.

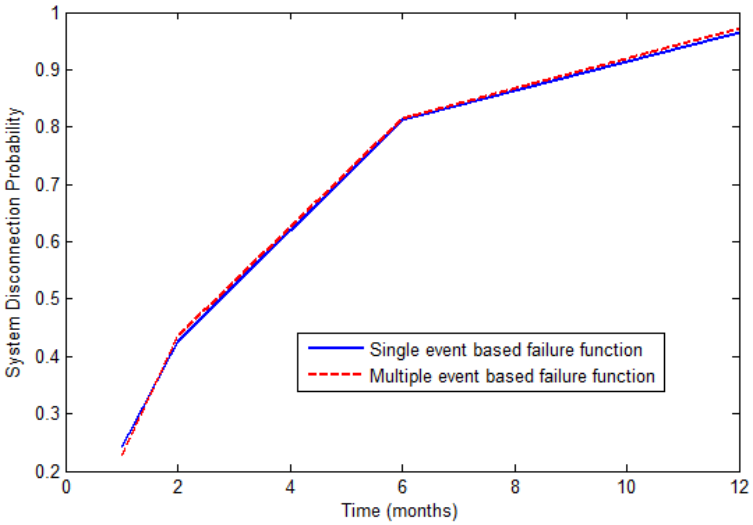

Figure 5.11. System disconnection probability

The proposed method employs removal of pipes one by one from the network and subsequent estimation of the change in AC (ΔAC) for estimating the network failure probability and ranking pipes within the network according to their importance level. Based on these steps, the critical pipes in the network can be identified. The suitability of the proposed method is demonstrated through application, first to a simple hypothetical network and then to a medium sized real water distribution system. The study reveals that the single event based approximate failure probability can reasonably be used for system probability assessment, saving extensive computational time. The critical pipes identified using the AC based method are validated through comparison with the results of the shortest path (SP) method. The SP method is a distance related measurement in CNA, which is useful for identifying high betweenness pipes or nodes (Newman 2010). However, the SP method cannot be used for identification of network isolation.

The proposed reliability model presented in this chapter considers the probability of disconnection only. Hydraulic availability of the demand nodes is not considered. Thus, lower bound values of the system failure probability are obtained. The developed model examines constant annual break rate-based component failure functions. Further observation on the properties of the AC and the effects of individual pipe failure on the overall network are discussed in Chapter 6.

CHAPTER 6. RISK ASSESSMENT OF WDN DUE TO WATER MAIN BREAKS[5]

6.1. Introduction

Water distribution network (WDN) is a valuable infrastructure that is essential for the human community. WDNs are often operated in highly hazardous environments, resulting in corrosion and breaks. Maintenance of the infrastructure is required to reduce the frequency of water main breaks and hence to protect the public health and safety. The annual maintenance cost of a WDN is often significant (Fares and Zayed, 2010). A strategy with risk based prioritizing or ranking pipes/components within a WDN can provide a proper maintenance plan with optimal utilization of resources. Risk is mathematically defined as the multiplication of failure probability and consequence. Quantifications of the probability and consequence of water main failure are very complex, as these depend on a number of uncertain factors. Fuzzy techniques are often successfully used for risk estimation especially when the inputs contain the uncertainty (Fares and Zayed, 2010). Yan and Vairavamoorthy (2003) used a fuzzy technique to combine numerical inputs (i.e. diameter, age and material) and linguistic inputs (i.e. road loading, soil condition and the surrounding environment). Based on this combination, crisp indicators for pipe conditions are obtained for prioritizing pipe inspections. Kleiner et al. (2004) introduced a fuzzy-based failure probability assessment and then used a risk matrix for estimating the time-dependent risk. However, the consequences in Kleiner et al. (2004) are arbitrarily assumed.

[5] This chapter is based on an article submitted for publication in a peer-reviewed journal: Hieu Chi Phan, Ashutosh Sutra Dhar, Guangji Hu, Rehan Sadiq (2018), "Managing Water Main Breaks in Distribution Networks – A Risk-Based Decision Making". The work was carried out, and the paper was drafted by the first author. The work was supervised, and the paper was reviewed by the co-authors.

Fares and Zayed (2010) proposed a hierarchical fuzzy expert system and Fuzzy Inference System (FIS) to evaluate the risk score by considering various environmental, physical, and operational deterioration factors and post-failure consequences. However, the 16 sub-factors in this approach require subjective assessments. The relationship between pipe age and break records was considered separately without properly modelling.

However, estimating the overall consequence of failure by a non-fuzzy method is difficult. It is hard to unify different types of consequences into a general unit even though many studies attempted to convert different consequences into one outcome. Moglia et al. (2006) provided a decision support system for prioritization of water pipelines based on the risk of a pipe failure with the consequence in terms of cost. Roger (2011) proposed using a simple scoring system involving pipe diameter, material, age and break history factors to rank pipes within a network. Baah et al. (2015) also used a system of 11 factors to produce the general consequence based on pipe diameters, burial depths and other parameters.

Both of these approaches involve different types of consequence parameters. Combining various types of consequences into an aggregated one is important for simplifying the consequence estimating process. A fuzzy inference system (FIS) could be used to combine various consequences using a reasoning framework. In this method, different types of inputs (in crisp or fuzzy form) are converted by a combination of a fuzzy knowledge base (i.e. fuzzy rules and membership functions of fuzzy sets used in rules) and an inference engine, to obtain a crisp and aggregated output. The inputs could be in different units such as currency, importance level, and scores. Fares and Zayed (2010)

conducted a FIS analysis to aggregate the factors of cost of repair, damage to the surroundings, loss of production, traffic disruption and type of service area in a consequence model. Roozbahani et al. (2013) aggregated consequences of unsafe water supply, economical losses, negative social impacts and human losses into a unified consequence. In the application of FIS, the definitions of fuzzy rules and membership functions play important roles in the consequence assessment.

Determining consequence parameters for a WDN, where the pipes are interacting with each other, is a challenging task. The interaction of pipes within a network was discussed in many reliability studies as the connectivity and the reachability (Tung, 1985; Wagner et al., 1988; Quimpo and Shamsi, 1991), which are defined as the connection of all demand nodes to the source nodes and the connection of a demand node to its source, respectively. The interaction of pipes can be modelled as the effects of a pipe's breaking on the whole network's integrity using graph theory. The complex network analysis in graph theory has recently been used for the assessment of well-connectedness of a WDN (Yazdani and Jeffrey, 2010, 2011a, 2011b; Yannopoulos and Spiliotis, 2013; Nazempour et al., 2016; Phan et al. 2018a). Phan et al. (2018a) proposed a method of using Algebraic Connectivity (AC) to estimate the disconnection probability of the network.

AC is a parameter that measures the well-connectedness of a graph (Fiedler, 1973; Capocci et al., 2005; Ghosh and Boyd, 2006; Newman, 2006, Yazdani and Jeffrey, 2011a, b). A network with a higher AC is more robust or more tolerant to breakage of pipes. Phan et al. (2018a) took the advantage of the property of AC and observed the change of a network's connectivity with and without a single water main break to highlight the

important pipes within the network. This approach considers only the effects on network connectivity as the consequence and does not account for other consequences such as the economic consequence and the impact of service disruption to the community. For example, the impact of water service disruption within a school zone is different from the impact of service disruption to a hospital. This effect can be determined by incorporating an importance factor for the pipes based on their location. As for the economic consequence, pipe diameter can be used as the consequence parameter, as the breaking of a larger diameter pipe is expected to have a higher cost than the breaking of a smaller diameter pipe. This research develops a risk-based prioritization method of water mains in a WDN, combining the impact on system connectivity with other consequences. An FIS is developed to obtain an aggregated consequence and then, a simple risk based prioritizing plan.

6.2. Algebraic Connectivity

As discussed in Chapter 5, AC is defined as the second smallest Eigen-value of the Laplacian matrix (Fiedler, 1973). If a municipal Water Distribution Network (WDN) is modeled as a graph of G=G(V,P), where V is a set of n nodes (intersections) and P is a set of m pipes, then an adjacent matrix A of G is used to describe the link between the nodes, where:

$$A = a_{ij} \tag{6.1}$$

$a_{ij} = 1$ if there is a link (pipe) between node i and node j.

$a_{ij} = 0$ if there is no link (pipe) between node i and node j.

The node-degree matrix is a diagonal matrix, which contains the information about the number of connections (node-degree) at each node, and is defined as:

$$D = diag(d_i) \tag{6.2}$$

d_i: number of connections (node-degree) of node i, where:

$$d_i = \sum_{j=1}^{n} a_{ij} \tag{6.3}$$

Then, the Laplacian matrix is given by Eq.6.4:

$$L = D - A \tag{6.4}$$

The Laplacian matrix, L, for the undirected network is usually symmetric and the sum of rows (and columns) is zero. This characteristic leads to the fact that the first (i.e. smallest) Eigen-value (λ_1) of the matrix that corresponds to the Eigen vector of $(1,1,...,1)^T$ is zero. The second smallest Eigen-value (λ_2) of the Laplacian matrix is the AC, which is greater than 0 if G is a connected graph. The Eigen-values of a network with n nodes of connected graph are: $\lambda_1 = 0 \leq \lambda_2 = AC \leq \lambda_3 \ldots \leq \lambda_n$.

If the AC of the network with the removal of the i^{th} pipe and the intact network are denoted as AC_i and AC_o, respectively, the changing AC (ΔAC) due to the removal of the i^{th} pipe can be found as:

$$\Delta AC_i = AC_i - AC_o \tag{6.5}$$

ΔAC_i was used to rank water mains in a WDN according to their impacts on the robustness of the network and the potential of causing isolation (disconnection) (Phan et al., 2018a). In this method, the topology of WDN (measured as ΔAC) was considered for ranking the importance of pipes (called herein a topological consequence). The AC approach is different from the existing pipe ranking method, which measures the importance of pipes based on hydraulic availability. Yoo et al. (2014) employed a method for priority determination of water mains considering hydraulic importance. They employed the original water flows within the segment of the WDN, consisting of a set of pipes that was disconnected by a water control valve after failure of a particular pipe, including the failed pipe (in the event of a failure) to define a hydraulic importance factor (HIF), after Walski (1993) and Jun et al. (2008). The HIF for a pipe is defined as (Eq.6.6):

$$HIF_i = \frac{(Q_i + Q_{i,seg})}{Q_{sum}} \tag{6.6}$$

Where Q_i and $Q_{i,seg}$ are the flows in the i^{th} pipe and in the pipes within the affected segment, respectively, if the i^{th} pipe breaks. Q_{sum} is the summation of flow in all pipes within the WDN. HIF_i reflects the hydraulic importance of the i^{th} pipe, where a higher HIF_i value indicates a higher importance of the pipe.

The capability of priority determination using AC is examined with the comparison of priority determined using the hydraulic importance (Yoo et al., 2014) for a hypothetical series-parallel system, shown in Fig.6.1. The network is organized with a combination of pipes at different importance levels. Sub-system 1 has pipes 1-2 and 9-12 in series. It is also in parallel with pipes 2-10-11-9 and Sub-system 2. In Subsystem 2, pipes 4-7 and 5-6

are parallel. Node 1 is a source and node 2 is an isolated destination. As seen in the figure, pipe 1-2 is most important as failure of this pipe would cause complete disruption of water service. Pipe 10-11 is relatively less important since its failure will not cause any disruption of service at any of the nodes except node 11. However, the redundancy of the network will be reduced due to the failure of pipe 10-11.

AC and HIF of the pipes in the network shown in Fig.6.1 are calculated for comparison. AC is calculated through development of a Matlab^{R} code. For HIF, hydraulic analysis is performed to calculate the flow in each of the pipes in the intake network using EPAnet software (Shang et al., 2008). The HIF is then calculated using Eq.6.6. A Breadth-First search algorithm (Moore, 1959) was used to identify the affected segment for any breakage of pipe.

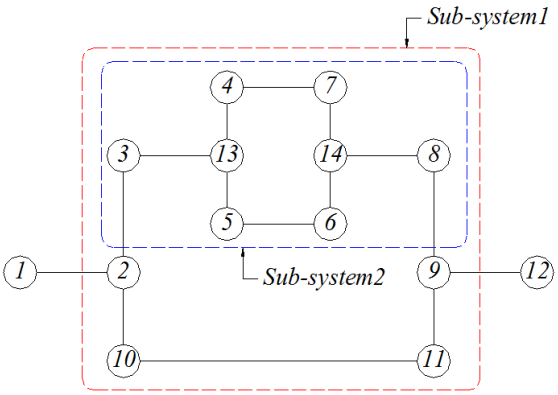

Figure 6.1. A hypothetical water distribution network

Table 6.1 shows a comparison of ranking of the pipes according to AC and HIF. In this table, the group of pipes having positive ΔAC (group 1) is placed first, followed by the group of pipes with the corresponding negative ΔAC (group 2). In groups 1 and 2, pipes

are ranked in the descending and ascending order according to the ΔAC values, respectively. This order implied that disconnection is more important than reduction of redundancy, and that the important level of a pipe within a group is positively correlated to its corresponding absolute ΔAC. In Table 6.1, the ΔAC is ranked from pipes [1-2; 9-12], pipe 10-11 to pipe [4-7; 5-6] in descending order.

As seen in Table 6.1, the rankings of pipes according to HIF and AC are different, even though these are common for some pipes, particularly the most critical pipes (i.e., 1-2). The AC-based approach ranks pipes 1-2 and 9-12 at the same level, while the HIF approach ranks pipe 9-12 in the 6^{th} place, while pipe 1-2 is ranked it in the first place. This is because the AC-based approach focuses on the topological changes of the system regardless of the direction of flow, while the HIF-based method accounts for the direction of the flow. Failure of pipes 9-12 located on the downstream side has less impact on the upstream pipes. Thus, the major difference between the hydraulic and the AC based approaches is that the hydraulic method considers the direction of flow while the AC based method focuses on the change of network well-connectedness due to a pipe breakage. One of the limitations of the hydraulic based method is that it requires a detailed hydraulic analysis of complex WDN. Additionally, the hydraulic-based prioritization does not provide any indication of whether a pipe break would cause disconnection. In comparison, a positive increase of AC indicates that the failure of the pipe would lead to disconnection in the network. AC is therefore employed here to account for the topological consequence.

Table 6.1. Important level of pipe in the hypothetical network

Removed Pipe ID	AC*	ΔAC	Type of Network Structural Change	Group	HIF	ΔAC Rank	Hydraulic Rank*
1-2	0.27716	0.00921	Disconnection	1	1.0000	1	1
9-12	0.27716	0.00921	Disconnection	1	0.1480	1	6
3-13	0.07608	-0.19187	Less Redundancy	2	0.3890	3	3
8-14	0.07608	-0.19187	Less Redundancy	2	0.1297	3	7
2-3	0.08154	-0.18640	Less Redundancy	2	0.4535	5	2
8-9	0.08154	-0.18640	Less Redundancy	2	0.0065	5	13
9-11	0.09453	-0.17342	Less Redundancy	2	0.0835	7	10
2-10	0.09453	-0.17342	Less Redundancy	2	0.1480	7	4
10-11	0.09679	-0.17116	Less Redundancy	2	0.1670	9	5
6-14	0.18639	-0.08156	Less Redundancy	2	0.0326	10	14
5-13	0.18639	-0.08156	Less Redundancy	2	0.0977	10	8
7-14	0.18639	-0.08156	Less Redundancy	2	0.0326	10	14
4-13	0.18639	-0.08156	Less Redundancy	2	0.0977	10	8
4-7	0.22429	-0.04366	Less Redundancy	2	0.0651	14	11
5-6	0.22429	-0.04366	Less Redundancy	2	0.0651	14	11

* If two or more pipes have the same value, they are placed in the same order number, but the next order number is skipped.

6.3. Risk Assessment Methodology

Risk calculation requires development of models for failure probability and consequence assessments. A simple failure probability model for the pipes in a WDN can be established based on break records, pipe age and other information or using a mechanics based stochastic method discussed in Chapter 3. However, it is difficult to estimate the consequence, since a general rule of consequence applicable for all water main systems is not available (Walski and Pelliccia, 1982). Relative consequence is therefore used to rank the pipes based on their corresponding consequence. Roger (2011) proposed an implicit risk table for pipes based on the sum-up score, in which the final score is linearly added

from diameter, installation date, material and break records. Baah et al. (2015) conducted a risk analysis based on a composed consequence of different types of impact factors, including location factors (i.e. factor related to the location of pipe with respect to other construction, buildings, area etc.) and size factor (i.e. diameter). Although these studies employ relative consequences to compare the risk of failure among pipes in the network, the scoring system requires subjective judgement. This study proposes using a FIS for consequence assessment accounting for the topological consequence (using AC) with other consequences based on available information. Fig.6.2 presents the framework for the risk assessment. As shown in the figure, the failure probability of each pipe at time *t* is established while the relative consequences corresponding to the break of each pipe are fuzzified and aggregated to obtain a crisp overall consequence. After calculation of the risk, the priority order of each individual pipe in the network is determined for prioritization planning.

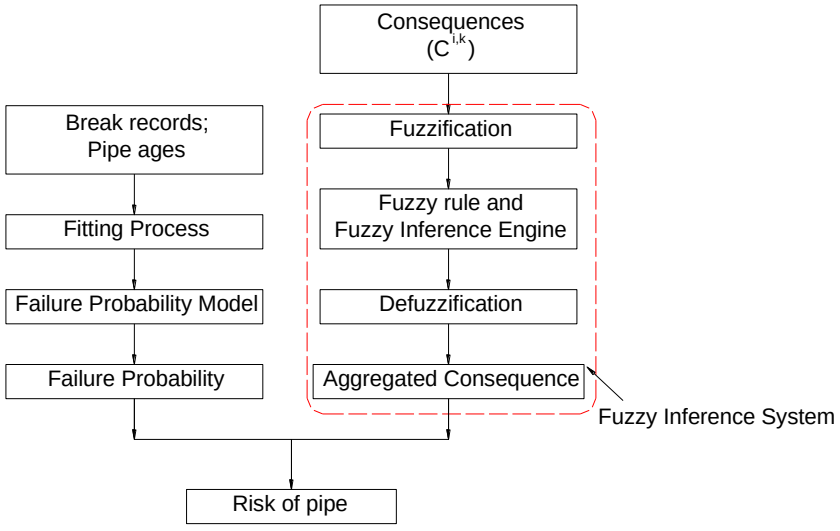

Figure 6.2. Flowchart of evaluating risk for each pipe

6.4. Failure Probability Modeling

A number of different approaches, including physical and statistical models, are proposed in the literature for failure probability modelling of a WDN (Rajani and Kleiner, 2001; Kleiner and Rajani, 2001). A statistical fitting process can be conducted based on the pipe age and break records of the network. This is a simple approach, which can be improved using different techniques. For example, where the data are annually collected, an updating step using Bayesian theory could be applied to train the model with new break records. The failure probability model can also be developed using a mechanically based approach if the information on the pipe degradation is available (Phan et al., 2018b).

The Weibull distribution for failure probability modeling is used because of its flexible property and suitability for a WDN (Large et al., 2014). It is widely used for modeling pipe breakage (e.g. Sadiq et al.,2004; Rogers, 2011; Park et al., 2015; Phan et al., 2018b). Sadiq et al. (2004) observed various distributions to define the failure probability for a water main and the Weibull distribution was found to fit well with the simulated data. Nonetheless, Park et al. (2015) conducted a statistical goodness of fit test on different distributions and the Weibull distribution was found to have an insignificant difference from lognormal, gamma and logistic distributions.

The probability density function according to Weibull distribution is given by Eq.6.7:

$$f_i(t) = \frac{\beta_i}{\eta_i}\left(\frac{t-\gamma_i}{\eta_i}\right)^{\beta_i - 1} e^{-\left(\frac{t-\gamma_i}{\eta_i}\right)^{\beta_i}} \tag{6.7}$$

Reliability and failure probability functions are defined as:

$$R_i(t) = e^{-\left(\frac{t-\gamma_i}{\eta_i}\right)^{\beta_i}} \tag{6.8}$$

$$F_i(t) = 1 - e^{-\left(\frac{t-\gamma_i}{\eta_i}\right)^{\beta_i}} \tag{6.9}$$

Where $R_i(t)$ is reliability and $F_i(t)$ is failure probability at time t; β_i is shape parameter, η_i is a scale parameter and γ_i is the location parameter indicating the year of construction; t is the current observing year. Thus, $(t- \gamma_i)$ is the age of the i^{th} pipe. The parameters can be determined using a fitting process with available data.

6.5. Relative Consequences

The selection of consequence parameter depends on the available information about the pipes and the water distribution system. Information about pipe diameters is generally available to the municipalities, where the diameter is a common factor appearing in various cost models (Walski and Pelliccia, 1982; Kim and Mays, 1994; Loganathan et al., 2002; Dandy and Engelhardt, 2006; Montalvo et al., 2008; Alvisi and Franchini, 2009; Marchionni et al. 2016) or mentioned as an important factor of consequence (Male et al., 1990; Li et al. 2014). The failures of large diameter pipes incur more significant consequences in the form of financial losses, social impact and environmental impact (Ji et al 2017). Diameter is not only related directly to the cost for repair/replacement of a pipe but also partly implies to the volume of water transported. Thus, it provides an indication of the volume of water that may be affected by the failure. While the diameter-related consequences account for the cost of failure without concerning the interaction of

pipes within the network, the ΔAC could be used to account for the topological consequence. In addition, location parameters could be used, if the information is available, to account for the consequence based on the location of the pipes.

Because the aim of prioritizing is comparing a pipe with others to choose the most significant pipe set, the ratio of input parameter with the maximum value can be used to obtain the relative magnitude of the input values for each pipe, up to the maximum one in the network. For example, the crisp input for diameter and topological (AC) consequences of the i^{th} pipe can be calculated as (Eqs.5.10 and 5.11):

$$C^{i,dia} = \frac{D_i}{D_{max}} \tag{6.10}$$

$$C^{i,sys} = \frac{\Delta AC_i}{\Delta AC_{max}} \tag{6.11}$$

Where: $C^{i,dia}$ and $C^{i,sys}$ are the diameter-related and system-related consequences of the i^{th} pipe; D_i and D_{max} are the diameters of the i^{th} pipe and the maximum diameter of all pipes in the network, ΔAC_i and ΔAC_{max} are the change of AC for the i^{th} pipe and the maximum change in AC of all pipes in the network.

6.5.1. Fuzzification of Consequences

Assuming that the severity level of consequence of a pipe failure can linguistically be evaluated as *Low, Medium Low, Medium, Medium High and High*, a set of Triangular Fuzzy Numbers, $A^{i,k}$, with the 5 grades or subsets $A_j^{i,k}$ (j=1,2,…,5), can be used correspondingly. If the consequence of the failure of the i^{th} pipe is denoted as $C^{i,k}$ (k can

both be diameter and system-related consequence), then $C^{i,k}$ can be a member of subset $A_j^{i,k}$ at a certain degree of membership $\mu_j\ (C^{i,k})$ which ranges between [0, 1].

In this study, the subset $A_j^{i,k}$, which corresponds to the linguistic severity grade of consequence, is assumed as a triangular fuzzy number (TFN) and shown in Table 6.2. The TFN can be assigned subjectively or obtained from expert elicitation. Note that the maximum of $C^{i,k}$ is 1 for all k and that the fuzzy set A can be generally used for diameter, location and system related consequences.

Fig.6.3 illustrates the relationship of uncertain relative consequence $C^{i,k}$, subset $A_j^{i,k}$ and the membership function $\mu_j\ (C^{i,k})$. For example, if the i^{th} pipe has the system related consequence $C^{i,k}$ of 0.7, the corresponding $\mu_3\ (C^{i,k})$ and $\mu_4\ (C^{i,k})$ are 0.2 and 0.8, respectively. The other $\mu_j\ (C^{i,k})$ (j=1, 2, 4, 5) are equal to zero. That is:

$$A^{i,k} = \left[\mu_1\left(C^{i,k}\right), \mu_2\left(C^{i,k}\right), \mu_3\left(C^{i,k}\right), \mu_4\left(C^{i,k}\right), \mu_5\left(C^{i,k}\right)\right] = [0,0,0.2,0.8,0]$$

Table 6.2. Triangle fuzzy numbers and their corresponding qualitative scale of fuzzy set A

Subset	Qualitative scale	TFN
A_1	Low	(0, 0, 0.25)
A_2	Medium Low	(0, 0.25, 0.5)
A_3	Medium	(0.25, 0.5, 0.75)
A_4	Medium High	(0.5, 0.75, 1)
A_5	High	(0.75, 1, 1)

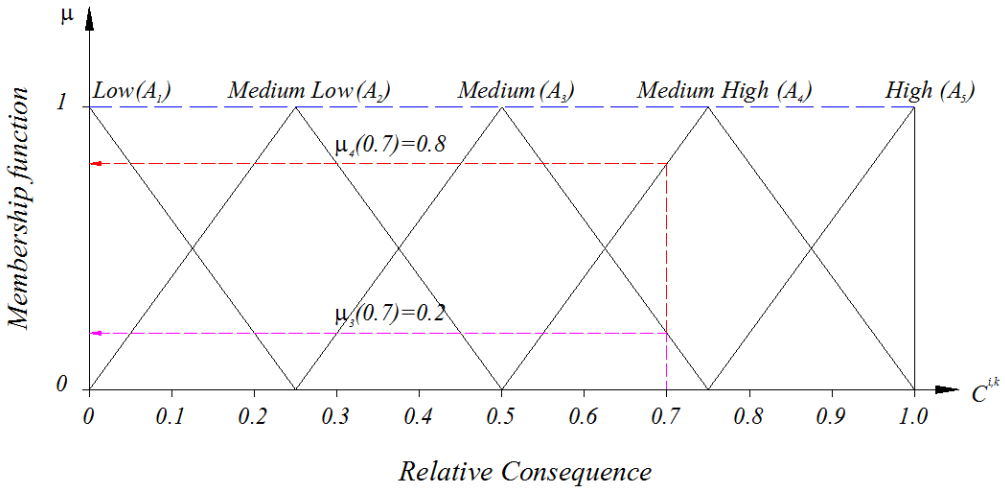

Figure 6.3. The 5-grade fuzzy subsets A for relative consequence

The membership function μ corresponding to the k[th] relative consequence of the i[th] pipe, $C^{i,k}$, is given in Eq.6.12:

$$\mu_1\left(C^{i,k}\right) = \begin{cases} 1 - 4C^{i,k} & 0 \le C^{i,k} \le \frac{1}{4} \\ 0, & \frac{1}{4} \le C^{i,k} \le 1 \end{cases}$$

$$\mu_j\left(C^{i,k}\right) = \begin{cases} 0, & 0 \le C^{i,k} \le \frac{j-2}{6} \\ 4C^{i,k} - (j-2), & \frac{j-2}{4} \le C^{i,k} \le \frac{j-1}{4} \\ j - 4C^{i,k}, & \frac{j-1}{4} \le C^{i,k} \le \frac{j}{4} \\ 0, & \frac{j}{4} \le C^{i,k} \le 1 \end{cases} \quad \text{j=2, 3, 4} \qquad (6.12)$$

$$\mu_5\left(C^{i,k}\right) = \begin{cases} 0, & 0 \le C^{i,k} \le \frac{3}{4} \\ 4C^{i,k} - 3, & \frac{3}{4} \le C^{i,k} \le 1 \end{cases}$$

6.5.2. Fuzzy Inference System for Aggregating Consequences

Once the relative consequences are fuzzified, the aggregation process can be conducted based on a set of fuzzy rules with a fuzzy set for aggregated consequence (Hu et al., 2018). In this study, the fuzzy set for aggregated consequence is assumed to be the same as the relative consequence, as illustrated in Fig.6.3. A fuzzy rule is presented with the combination of the linguistic expressions and logic operations such as AND or OR as in the example below.

Rule p: IF (diameter-related Consequence) is High OR (system-related Consequence) is High, THEN (Aggregated Consequence for Rule p) is High.

A set of m fuzzy rules R = $[R_1 , \ldots, R_p , \ldots, R_m]$ is evaluated and a set of output consequences corresponding to each rule, $[C_1^i, \ldots, C_p^i, \ldots, C_m^i,]$, is found. The output consequences are then aggregated to obtain the fuzzy form of the aggregated consequence. The aggregated consequence for the ith pipe, C_A^i is then obtained by a defuzzification method to produce a crisp value. In this study, the Center of Gravity defuzzification method is used.

Fig.6.4 illustrates a simple example of the aggregating process. For simplicity purpose, a fuzzy set of 3 grades corresponding to Low, Medium and High is applied. Fig.6.4a defines the grades (i.e., severity) of two assumed relative consequences used for illustrating the FIS. A set of 3 fuzzy rules is used:

Rule 1: IF Consequence 1 is Low OR Consequence 2 is Low, then Aggregated Consequence is Low;

Rule 2: IF Consequence 1 is Medium OR Consequence 2 is Low, then Aggregated Consequence is Medium;

Rule 3: IF Consequence 1 is High OR Consequence 2 is Medium, then Aggregated Consequence is High.

As an example, the ith pipe with Consequence 1 = 0.7 and Consequence 2 = 0.35, the membership functions, μ_j ($C^{i,k}$), corresponding to Low, Medium and High grades are 0, 0.05 and 0.25 (i.e., $A^{i,1} = [0,0.5,0.25]$) for Consequence 1 and 0.125, 0.625 and 0 (i.e., $A^{i,2} = [0.125,0.625,0]$) for Consequence 2 (Fig.6.4a). The corresponding membership function for the aggregated consequence can be found using the highest value of the consequence (i.e., the OR operation) as shown by the dotted line in the Rule Output column of Fig.6.4b. Fig.6.4c shows the membership value of aggregated consequence obtained using superposition of the rule outputs in Fig.6.4b. Consequently, the aggregated consequence is obtained as the center of gravity of the shaded area in Fig.6.4c, which is 0.594 in the figure for the case considered, indicating a medium aggregated consequence.

a)

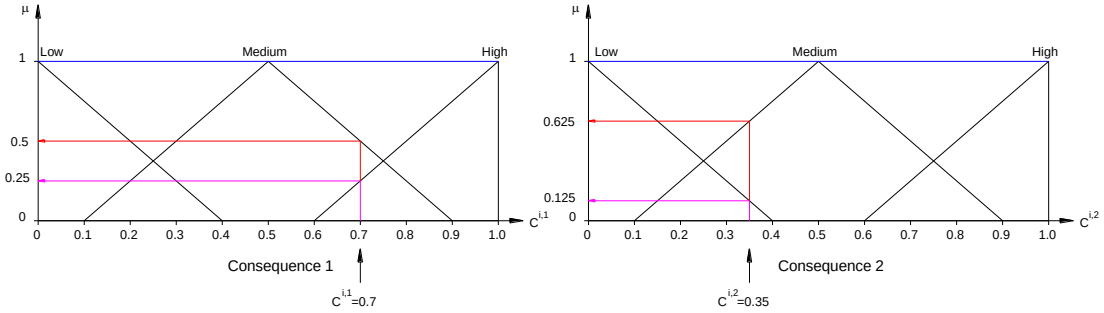

b)

Rule	Consequence 1	Consequence 2	Rule Output
Rule 1	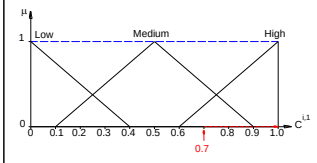	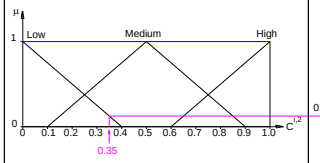	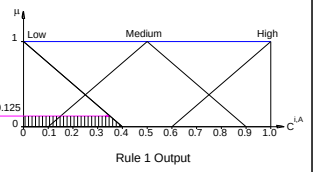
Rule 2	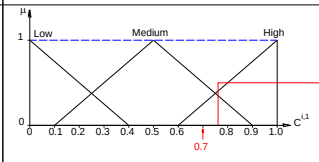	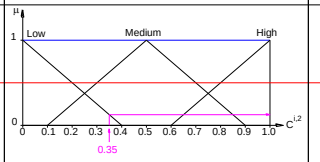	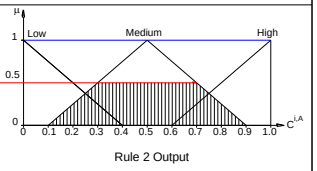
Rule 3	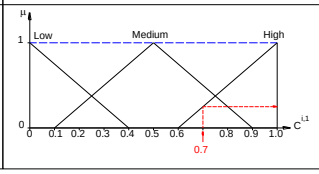	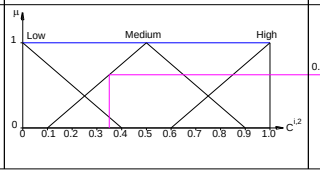	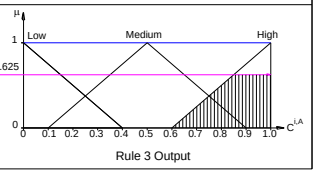

c)

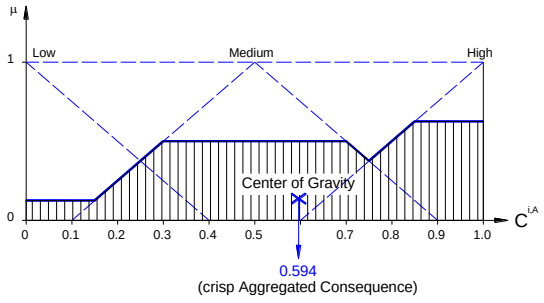

Figure 6.4. Example of the aggregation process for consequences. a) The 3-grade fuzzy subsets A for Consequence 1 and 2; b) Aggregating process table; c) Aggregated consequence

6.6. Case study

The proposed method was applied for the WDN of the City of Mount Pearl, a community with a population of approximately 25,000 in Newfoundland and Labrador, Canada. The water main system consists of 107 km of pipes (Fig.6.5). The diameters of the pipes range from 150 to 450 mm (Fig.6.6a) and the age of the pipes varies from less than 20 years to over 50 years (Fig.6.6b). Water is brought from a neighboring city to a water tank located in the South-West of the community. The water distribution system to support the entire city is based on gravity flow. Topologically, the network is divided into 2 communities, the southern and the northern. These communities are linked by a bridge pipe (bolded in Fig.6.5). The northern community is mostly used for residential services, and the southern community is used for both industrial (the western part) and residential (the eastern part) purposes.

6.6.1. AC and HIF Based Ranking

The water mains of Mount Pearl's WDN were ranked using ΔAC and HIF-based approaches. Table 6.3 presents the typical data with GIS coordinates for the WDN, showing up to 8558 nodes and 9474 pipes. These raw data required filtering for analysis, as there exist duplicated points and pipes or gaps between pipes at the connections. Filtered data were analyzed to calculate ΔAC using the developed Matlab^{R} code. The hydraulic analysis was conducted using EPAnet 2.0 software through development of an interface in the Python programming language. For the hydraulic analysis, parameters such as elevation, node demand etc. vary significantly from network to network. For the example

presented here it is assumed that all demand nodes are at an elevation of 0 m and the elevation of the tank is at 50 m with the water level at 100 m. The demand for each node is assumed to be the same.

Table 6.3. Data of WDN at the city of Mount Pearl

Node ID	Pipe ID	Material	Diameter (mm)	Year	Street name	X (coordinate)	Y (coordinate)
1	1	DI	150	1971	Spruce Avenue	320991	5264475
2	1	DI	150	1971	Spruce Avenue	321007	5264498
3	2	DI	200	2012	Stonegate Crescent	321048	5265709
4	2	DI	200	2012	Stonegate Crescent	321046	5265710
…	…	…	…	…	…	…	…
8557	9474	DI	150	2016	Third Street	318867	5263849
8558	9474	DI	150	2016	Third Street	318866	5263854

DI: Ductile Iron

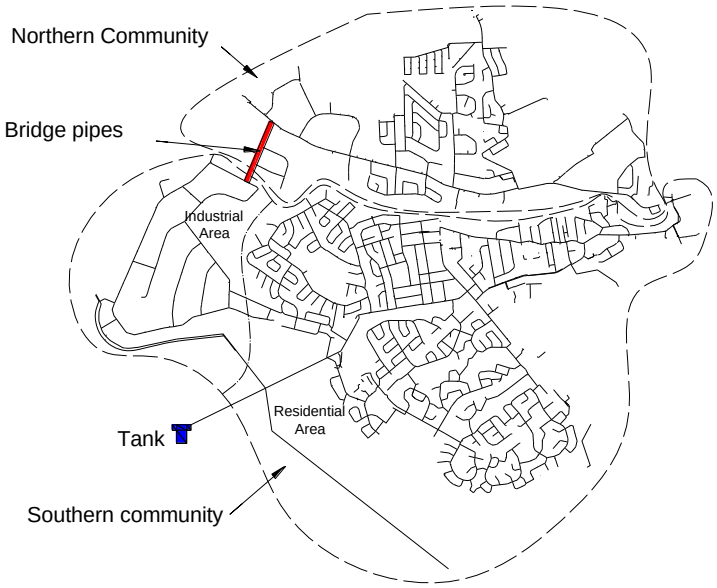

Figure 6.5. WDN of the city of Mount Pearl

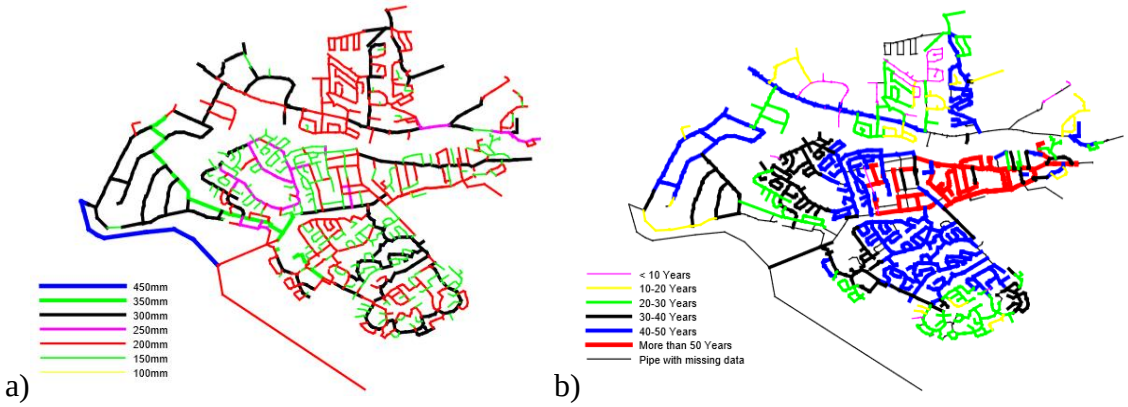

Figure 6.6. a) Pipe diameter and b) Pipe age distributions of WDN from city of Mount Pearl

Fig.6.7 plots the ΔAC and HIF for the city water mains. As seen in Fig.6.7, both the hydraulic and AC based approaches successfully highlight the most important pipes (pipes with the high absolute magnitude of ΔAC and HIF) which connect northern and southern communities. In general, the ΔAC based ranking reasonably corresponds to the HIF based ranking of the pipes. A similar result from AC based analysis and from the "shortest path" algorithm was reported earlier in Phan et al. (2018a) to highlight the most important pipes. These two methods are not directly providing a powerful value for evaluating the topology change of the network after a break appeared. The ΔAC based method can be used to assess the network connectivity directly and finally yield a parameter to relatively estimate the important of pipe in the network.

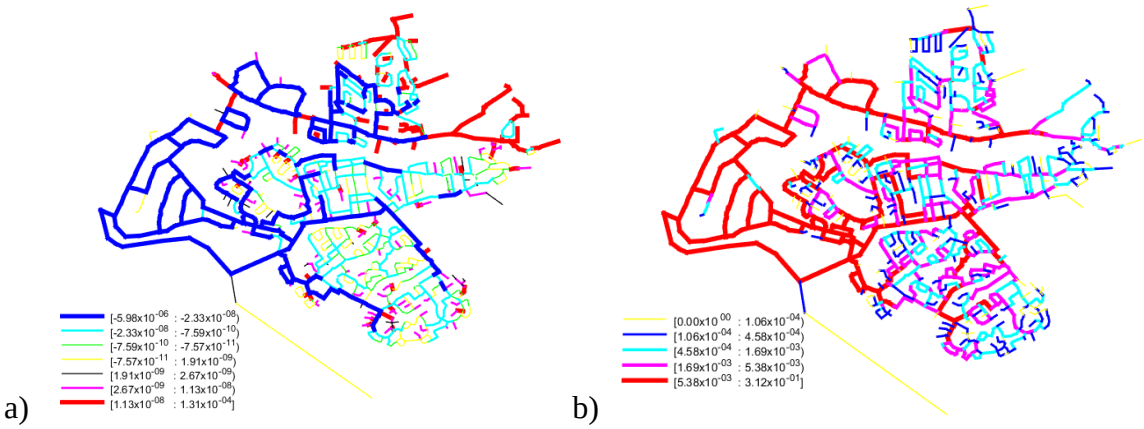

Figure 6.7. a) ΔAC and b) HIF maps of WDN at the city of Mount Pearl

6.6.2. Failure Probability

The failure probability model of pipes in the city of Mount Pearl was established based on materials, break records and the ages of the pipes. Water main break data are collected from the city for development of the failure probability model. Fig.6.8 shows the CDF of the failure probability for the two types of pipe materials mostly used in the city (i.e., cast iron and ductile iron). After 35 years of age, the failure probability of both cast iron and ductile iron pipes significantly increases with different rates. In less than 60 years, cast iron pipes appear to reach the failure probability limit of 1 while the ductile iron pipes reach the failure probability of 1 after 90 years of age. The Weibull function is fitted with the CDF in Fig.6.8. The details of Weibull parameters for different cases obtained through curve fitting with the CDF in Fig.6.8 using least-squares method are given in Table 6.4. Based on these parameters and age, i.e. $(t- \gamma_i)$, the failure probability of each pipe per kilometer is calculated. The calculated failure probability of the pipes in the city's WDN corresponding to the year of 2018 and 2028 are shown in Fig.6.9. The maximum

probability of failure of the pipes appears to be low (5.14×10^{-5}/m and 1.06×10^{-4}/m in 2018 and 2028, respectively). These failure probabilities are estimated based on limited pipe break data from the City of Mount Pearl and require updating using additional information when information will be available.

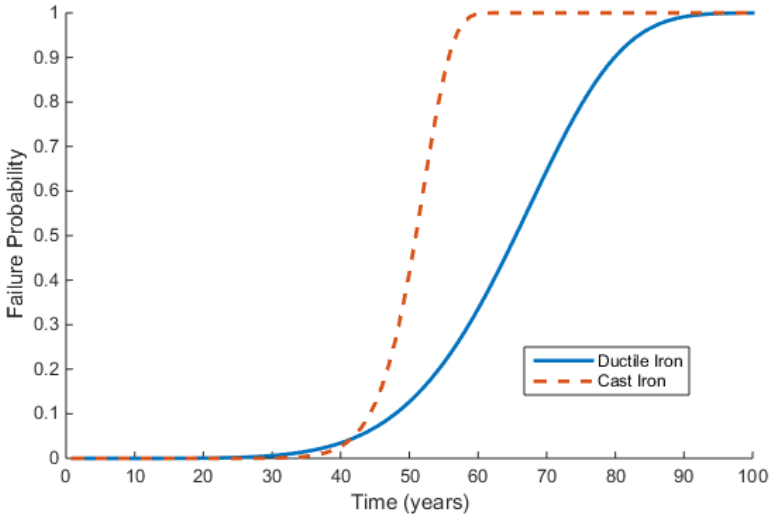

Figure 6.8. CDF of water mains based on statistical failure records

Table 6.4. Parameters of fitted Weibull distribution with different materials

Model type	**β***	**η***
Ductile Iron	13.41778	52.36
Cast Iron	6.04686	69.59

* In Eqs. 6.7, 6.8 and 6.9

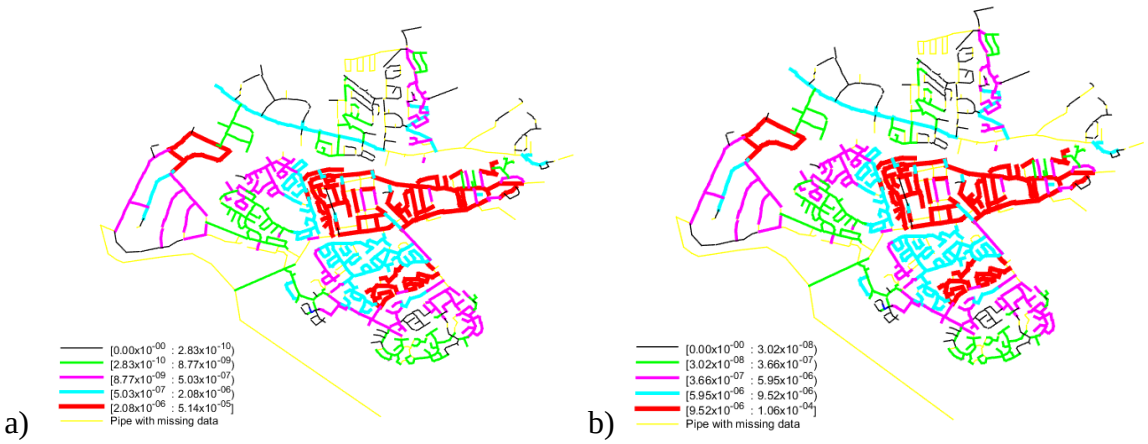

Figure 6.9. Failure probability per km length of pipe in a) 2018 and b) 2028

Table 6.5. Consequence assessment

Pipe ID Node i	Pipe ID Node j	Year Installed	Material	Diameter (mm)	$C^{ij,dia}$	ACij	ΔAC_{ij}	$C^{ij,sys}$
0	1	2012	Ductile Iron	200	0.4444	1.8579×10^{-5}	1.1462×10^{-7}	0.0009
1	2	2002	Ductile Iron	200	0.4444	1.8596×10^{-5}	1.3107×10^{-7}	0.0010
2	12	1987	Ductile Iron	200	0.4444	1.8415×10^{-5}	-4.9676×10^{-8}	-0.0004
…	…	…	…	…	…	…	…	…
*879	*1907	1991	Ductile Iron	300	0.6667	1.4904×10^{-4}	1.3057×10^{-4}	1.0000
…	…	…	…	…	…	…	…	…
**2611	**3766	1993	Ductile Iron	450	1.0000	1.6512×10^{-5}	-1.9528×10^{-6}	-0.0150
3987	166	1987	Ductile Iron	200	0.4444	1.8314×10^{-5}	-1.5032×10^{-7}	-0.0012
3988	167	1987	Ductile Iron	200	0.4444	1.7364×10^{-5}	-1.1008×10^{-6}	-0.0084
3989	223	1987	Ductile Iron	300	0.6667	1.8383×10^{-5}	-8.1560×10^{-8}	-0.0006

*: Maximum $C^{ij,sys}$; **: Maximum $C^{ij,dia}$

6.6.3. Consequence Assessment

The diamater and topological consequences calculated for the city of Mount Pearl's water mains are shown in Table 6.5. Based on the calculated relative consequence, the

membership functions are defined as shown in Fig.6.3. The two types of consequences were classified into 5 catagories, including Low, Low-Medium, Medium, Medium-High and High, and then the two consequence categories were aggregated to one output.

Table 6.6 presents the rule set used for calculation of aggregated consequence using FIS. Aggregated Consequences are grouped into 5 categories, 1, 2, 3, 4 and 5, corresponding to Low, Low-Medium, Medium, Medium-High and High. An "AND" operation is used in the rule set to yield aggreagted consequence. For example, rule 14 in Table 6.6 with [3,4] means "IF the System-related Consequence is Medium (3) AND Diameter-related Consequence is Medium-High (4) then the Aggregated Consequence is Medium-High (4)", which is A_4 according to Table 6.2.

Table 6.6. Rules for FIS

Rule number	Input relative Consequences	Aggregated Consequence	Corresponding Subset (in Table 6.2)
1	[1,1]	1	A_1
2	[1,2]	1	A_1
3	[1,3]	2	A_2
4	[1,4]	3	A_3
5	[1,5]	5	A_5
6	[2,1]	1	A_1
7	[2,2]	2	A_2
8	[2,3]	2	A_2
9	[2,4]	3	A_3
10	[2,5]	5	A_5
11	[3,1]	2	A_2
12	[3,2]	2	A_2
13	[3,3]	3	A_3
14	[3,4]	4	A_4
15	[3,5]	5	A_5
16	[4,1]	3	A_3

Rule number	Input relative Consequences	Aggregated Consequence	Corresponding Subset (in Table 6.2)
17	[4,2]	3	A_3
18	[4,3]	4	A_4
19	[4,4]	4	A_4
20	[4,5]	5	A_5
21	[5,1]	3	A_3
22	[5,2]	3	A_3
23	[5,3]	4	A_4
24	[5,4]	4	A_4
25	[5,5]	5	A_5

The aggregated consequence calculated for the water mains for the city's WDN is plotted in Fig.6.10. The aggregated consequence ranges from 0.08 to 0.92. The most significant consequences are again for the pipes as those connecting northern and southern communities (the bridge pipes). The less significant pipes are those in small streets that deliver water to households.

Figure 6.10. Aggregated consequence of WDN at the city of Mount Pearl

6.6.5. Risk Assessment

Based on the failure probability and the aggregated consequence, the failure risks of pipes in the WDN are calculated. Since the failure probability is a function of age, the risks corresponding to a particular year are calculated. A map of pipe risk is shown in Fig.6.11 for two different years separated by a decade (i.e., 2018 and 2028). The risk ranges from 0 to 9.82×10^{-6}/m in the year of 2018, and from 0 to 20.10×10^{-6}/m in 2028. The maximum calculated risk value of the network is, thus, almost double after a decade.

This time dependent feature of the risk map provides a tool for prioritizing pipes in the network for maintenance. It is to be noted that, the failure probability models were developed for the pipes using limited available data that predict lower failure probability. As a result, estimated risks are also less. However, this chapter presents a framework for risk calculation and can be used with updating of failure probability models when additional information will be available.

Even though a risk map is successfully developed, as in Fig.6.11, choosing a risk threshold for maintenance scheduling is difficult which requires a subjective decision that depends on the decision makers. A method for selecting thresholds is currently not available for WDN. In Chapter 3 a relationship is developed between risk thresholds versus corresponding failure probabilities to provide a guideline when choosing the threshold for decision making (Phan et al, 2018b). In this method, a number of risk thresholds are arbitrarily chosen and the maximum failure probabilities corresponding to these risks are calculated to develop the relationships. A system risk and a system failure probability are

considered in that study (Phan et al. 2018b). A similar relationship is developed here, however, with consideration of risks and failure probabilities of each pipe component. Furthermore, to provide a guideline for understanding the maintenance/replacement works for pipes with highest risks, a relationship of risk threshold and corresponding total length of pipes having risks higher than the threshold is provided.

To develop these relationships, various risk thresholds are first chosen and the set of pipes which have risk higher than the threshold is selected. The total length of the pipes with higher risks is calculated. The maximum failure probabilities of all other remaining pipes are then found. The risk threshold against maximum failure probability and the total pipe lengths with risks higher than threshold are plotted in Fig.6.12. As shown in the figures, the risk of the WDN can be reduced from 9.82×10^{-6}/m to 3.51×10^{-6}/m through replacing about 5.57km of pipe. The corresponding failure probability reduce from 5.14×10^{-5}/m to 1.83×10^{-5}/m. Thus, the developed relationship could be used for carefully selecting the risk threshold for maintenance prioritization planning.

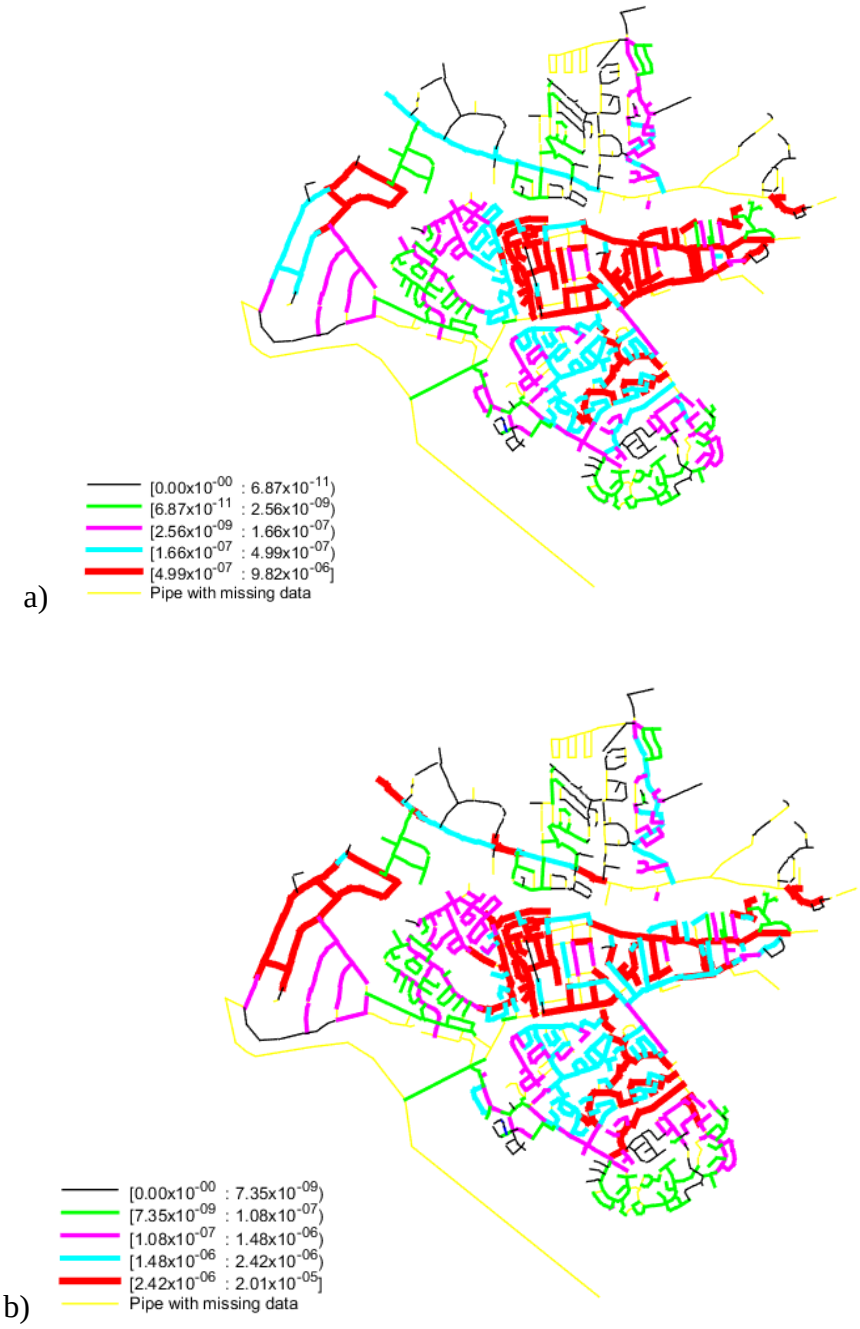

Figure 6.11. Risk maps of WDN at the city of Mount Pearl in the year of a) 2018 and b) 2028

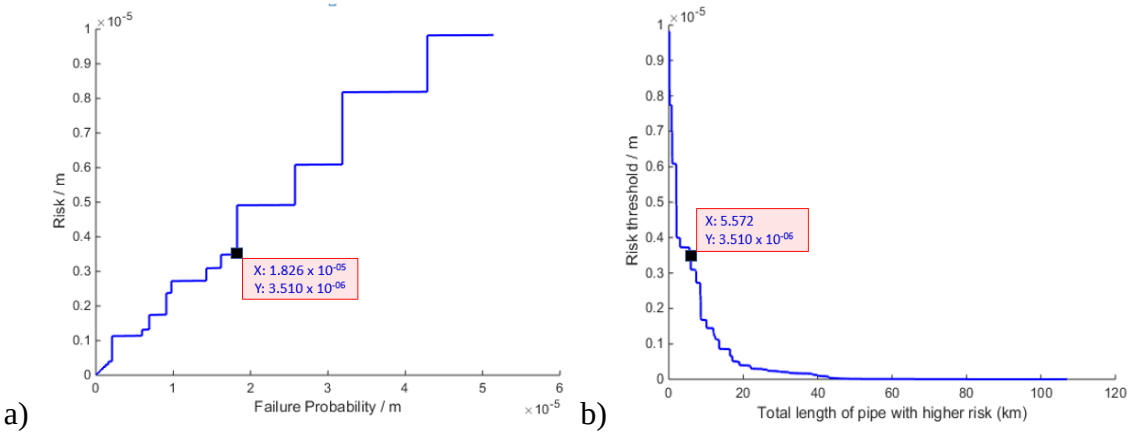

Figure 6.12. Relationship of a) Risk versus maximum failure probability in the year 2018 and b) Risk versus total length of need-to-replaced pipe

6.7. Conclusion

This chapter presents a simple risk assessment framework for developing a prioritizing plan for maintenance of a WDN. While the failure probability of water mains can be estimated based on break records or any other method for risk assessment, the determination of consequences of water main breaks is a challenging task. In this study, the use of AC from complex network analysis is proposed to consider the topological consequences that account for redundancy reduction and network isolation due to water main breaks. To demonstrate the capability of using AC, pipes in a water distribution network are ranked using AC and using a hydraulic importance factor calculated using hydraulic analysis. The AC based ranking was found to reasonably correspond to hydraulic importance-based ranking, particularly for the most critical pipes, indicating that the change in AC can be related to the topological consequence. A pipe diameter related consequence is proposed to account for the economic consequence. A break of a large

diameter pipe is expected to have a higher economic consequence than small diameter pipes, justifying the use of diameter for economic consequence. A fuzzy inference system is proposed here to combine different consequences to obtain aggregated consequences for risk calculation. The application of the risk calculation method is demonstrated considering an AC based consequence and a diameter-based consequence. However, the developed framework would be useful to account for any other consequence (e.g. location factor) if information is available. Based on the risk level of each pipe, a risk map for prioritizing water mains is developed for decision making. A relationship for risk, total length of pipe with higher risk can be developed for decision maker for selecting the risk threshold knowing the corresponding failure probability.

CHAPTER 7. CONCLUSION AND FUTURE WORK

7.1. Introduction

Water mains represent a significant part of the modern asset which are used to provide portable water to the communities. The water mains in municipalities are aging and experiencing leaks and breakages. Maintaining the integrity of the aging water mains has been a challenge for municipalities. A reliability and risk-based maintenance planning can be used to maintain the infrastructure with optimum utilization of resources. However, reliability and risk assessments for complex water distribution network are computationally challenging. Researchers are employing different approaches for reliability and risk assessment of WDN. Different limitations of these approaches are identified. This thesis develops an improved framework for prioritizing plan for water main maintenance considering reliability and risk modelling.

7.2. Contribution of the Thesis

In this thesis, reliability assessment method of water mains is developed accounting for the physical failure mechanism of pipelines. A method for overall reliability assessment of complex WDN is then developed using the parameter from graph theory. Risk assessment methods for WDN are also developed considering the effect on individual pipes as well as the WDN system. The following presents the specific findings from the research:

- Develop a framework for mechanics-based reliability/risk assessment for WDN

A method for prioritizing water mains for maintenance considering failure probability and risk of pipeline system is developed. For reliability assessment, a mechanics-based model of corroded water main is used, which would be useful for municipalities with no available prior break data. The pipe failure probability model is established based on a stochastic degradation analysis using MC simulation to develop a Weibull failure distribution function. A method is proposed for updating the model using expert opinions on the pipe conditions after an inspection and/or maintenance (repair/replacement) work without any requirement for data mining exercise. The model would thus be useful for existing and repaired/renewed pipe components. A risk assessment method is proposed for calculation of risk for small pipeline systems. The system failure of the pipeline network is defined using FTA applicable for small network.

Thresholds for the reliability and risk are found to govern the decision process in the reliability and risk-based approaches. In this regard, a careful determination of the thresholds is required to optimize the decision process considering both the reliability and the risk. To this end, a relation has been developed between the risk and the reliability for a system defined using FTA. The thresholds can rationally be chosen based on this relation.

- Development of a mechanics-based failure assessment model

For mechanics-based reliability assessment of water mains, a remaining strength assessment method for corroded pipelines is required. While stress assessment methods for

intake pipeline are available in AWWA design code, a method for assessment of corroded water main is not available. Remaining strength assessment methods available for energy pipelines are examined here to develop a stress calculation method for corroded water main due to internal pressure. Three existing burst pressure models for corroded energy pipeline are first revisited for a range of pipe sizes and material strength grades. A series of FE analysis is conducted to develop a database that is used to revisit different coefficients and exponents of the models (model parameters). An optimization algorithm based on differential evolution (DE) method is used to determine the model parameters through minimization of model errors.

Existing models for energy pipelines are examined with the results of FE analysis to revisit the existing models. FE analyses are then used to develop burst pressure models for corroded cast iron water mains.

- Effects of water main breaks on overall network

Studying the disconnection probability of WDN is important for optimizing repair/maintenance prioritization planning. The conventional method of finding a pipe or combination of pipes causing network isolation is very complex and requires extensive computation. This study presents a novel method for finding minimal cut-sets using Algebraic Connectivity (AC) determined by solving Eigenvalue problems of the Laplacian matrix.

It is observed that the decrease of AC due to a pipe break indicates a reduction of redundancy and the increase of AC indicates disconnection (isolation) of parts of the

network. A failure probability estimation framework is developed using this property of the AC to find the minimal cut-sets. This method is found to provide significant saving of computational time in determining the cut-sets.

It is also revealed that the importance level of pipe to the network corresponds with the change in AC, and the pipes in the network can be ranked according to this importance level. The critical and high betweenness pipes identified using the AC based method are validated through comparison with the results of the Shortest Path method.

- Risk assessment of WDN due to water main breaks

A framework for risk assessment of complex WDN is developed for prioritizing plan for maintenance. For determination of consequence of water main breaks, the use of Algebraic Connectivity (AC) from complex network analysis is proposed as the topological consequences of redundancy reduction and network isolation due to water main breaks. Pipes in a WDN are ranked using the changing amount of AC before and after break has occurred. This approach was found to reasonably correspond to hydraulic importance-based ranking, particularly for the most critical pipes, indicating that the change in AC can be related to the topological consequence. A pipe diameter related consequence is proposed to account for the economic consequence. The Fuzzy Inference System is proposed to aggregate different consequences to the final consequences for risk assessment. A risk map for prioritizing water mains is developed for decision making based on the risk level of each pipe. A relationship for risk, total length of pipe with higher risk can be developed for

decision maker for selecting the risk threshold knowing the corresponding failure probability.

7.3. Limitations of the study

This research develops a framework for reliability/risk-based maintenance planning of water distribution network. The following presents some limitations of the study that might be addressed through future research.

- In the mechanics-based reliability assessment model developed, a stochastic method using Monte Caro simulation is used for corrosion prediction. However, a corrosion monitoring program can be undertaken to develop more realistic corrosion model using realistic data for reliability assessment of the pipes.

- The mechanics-based model for corroded water mains is developed considering the internal pressure only, while conventional method of stress calculation (neglecting localized corrosion) is used for the external loads. Although internal pressure typically dominates the stresses in pressure pipes, a stress calculation method for external loads can be developed considering local corrosions.

- The AC can only assess the topological consequence. The effects of the location of water source and the direction of the water flow cannot be accounted using the AC.

- Although there is no limitation in term of the size of the WDN for application of AC, it may require tedious work to define the nodes and the network for large water distribution system.

7.4. Recommendations for Future Research Work

The thesis develops a framework for prioritizing water mains for maintenance considering reliability and risk levels. The framework can be applied to develop reliability and risk assessment methods for water mains. The following presents a list area for potential further work.

- In the current research, a framework for failure probability assessment considering physical failure mechanism is proposed. In this method, corrosion models available from published literature are employed. It is recommended to conduct a corrosion study with both cast iron and ductile pipes to develop improved corrosion models for water mains. Using the corrosion models, new failure probability models can be developed for municipal WDN. It is also recommended to inspect the municipal water mains based on the assessment of the failure probability and update the model for future failure probability assessment. For updating the failure models, a Bayesian updating process can be used.

- Understanding the physical failure mechanism of municipal water mains is area of study required for the development of failure assessment model. The physical failure models used in the current study are based on conventional stress assessment methods without detail understanding of the soil-pipe interaction. However, water mains are buried structures whose behavior is governed by the interaction between the pipe and the soil. It is recommended to perform detail pipe soil interaction analyses to develop improved physical model for failure assessment of water main. In this regard, fracture mechanics approach should be applied accounting for the reduction of fracture toughness due to long

exposure of water mains in corrosive environment (known as stress corrosion cracking). The modelling work should be supplemented by experimental work to validate the developed model.

- Further research is expected to develop more rational method of consequence assessment of water main breaks for risk calculation. In this thesis, Algebraic Connectivity is used as a parameter for the assessment of consequence on overall network and hypothetical approaches are used to account for other consequence. It is recommended to investigate the other consequences using real-time data from the municipalities. This method should be examined through application to different WDNs.

References

Alidoosti, A., Yazdani, M., Fouladgar, M. M. and Basiri, M.H., 2012. Risk assessment of critical asset using fuzzy inference system. Risk Management, 14(1), pp.77-91.

Ali, I., 2017. Mechanical properties of an exhumed cast iron pipe material (Doctoral dissertation, Memorial University of Newfoundland).

Alvisi, S. and Franchini, M., 2009. Multiobjective optimization of rehabilitation and leakage detection scheduling in water distribution systems. Journal of water resources planning and management, 135(6), pp.426-439.

ASME B31G, 2012. Revision of ASME B31G-2009 - Manual for Determining the Remaining Strength of Corroded pipelines, a Supplement to ANSI/ASME B31 Code for Pressing Piping. An American National Standard, New York.

Atkinson, S., Farmani, R., Memon, F. A. and Butler, D., 2014. Reliability Indicators for Water Distribution System Design: Comparison. J. Water Resour. Plann. Manage., ASCE, 140(2), 160-168.

Awumah, K., Goulter, I. and Bhatt, S., 1991. Entropy-based redundancy measures in water distribution network design. Hydr. Engrg., ASCE, 117(5): 595-614.

AWWA M45, 2014. Fiberglass Design Manual. American Water Works Association. Denver, Colorado.

Baah, K., Dubey, B., Harvey, R. and McBean, E., 2015. A risk-based approach to sanitary sewer pipe asset management. Science of the Total Environment, 505, pp.1011-1017.

Aydin, N. Y., Mays, L.W. and Schmitt, T., 2014. Sustainability assessment of urban water distribution system. Water Resources Management, 28(2014): 4373-4384.

Balkaya, M., Moore, I. D., and Sağlamer, A., 2011. Study of Non-uniform Bedding Support Because of Erosion under Cast Iron Water Distribution Pipes. Journal of geotechnical and geo-environmental engineering, 138(10), 1247-1256.

Bao, Y. and Mays, L. W., 1990. Model for water distribution system reliability. Journal of Hydraulic Engineering, 116(9), pp.1119-1137.

Barone, G. and Frangopol, D. M., 2014. Reliability, risk and lifetime distributions as performance indicators for life-cycle maintenance of deteriorating structures. Reliability Engineering & System Safety, 123, pp.21-37.

Bromley, J., Jackson, N. A., Clymer, O. J., Giacomello, A. M. and Jensen, F. V., 2005. The use of Hugin® to develop Bayesian networks as an aid to integrated water resource planning. Environmental Modelling & Software, 20(2), pp.231-242.

Capocci, A., Servedio, V. D., Caldarelli, G. and Colaiori, F. 2005. Detecting communities in large networks. Physica A: Statistical Mechanics and its Applications, 352(2): 669-676.

Chen, Y., Zhang, H., Zhang, J., Li, X. and Zhou, J., 2015. Failure Analysis of High Strength Pipeline with Single and Multiple Corrosions. Materials and Design, vol.67, pp. 552–557.

Cheng, T. and Pandey, M. D., 2012. An accurate analysis of maintenance cost of structures experiencing stochastic degradation. Structure and Infrastructure Engineering, 894, 329-39.

Chookah, M., Nuhi, M. and Modarres, M., 2011. A probabilistic physics-of-failure model for prognostic health management of structures subject to pitting and corrosion-fatigue. Reliability Engineering and System Safety 96 (2011), 1601–1610.

Coppersmith, D. and Winograd, S., 1990. Matrix multiplication via arithmetic progressions. Journal of symbolic computation, 9(3): 251-280.

Coronin, S. A., 2000. Assessment of Corrosion Deffects in Pipelines. Doctorate thesis in Mechanical Enigneering, University of Waterloo, Canada.

CSA Z662, 2015. Oil and Gas Pipeline Systems. Canadian Standard Association.

Cosham, A. and Hopkins, P., 2004. The assessment of corrosion in pipelines – guidance in the pipeline defect assessment manual (PDAM). Pipeline Pigging and Integrity Management Conference, May 17-18, 2004, Amsterdam, The Netherlands.

Costa, L. D. F., Rodrigues, F. A., Travieso, G. and Villas, B. P. R., 2007. Characterization of complex networks: A survey of measurements. Advances in physics, 56(1), pp.167-242.

Cullinane, M. J., 1986. Hydraulic reliability of urban water distribution systems. In Water Forum'86: World Water Issues in Evolution. ASCE. 1264-1271.

Cullinane, M. J, Lansey K. E., and Mays L. W., 1992. Optimization-availability-based design of water-distribution networks. J. Hydraul. Eng., 118(3): 420-441.

Dandy, G. C. and Engelhardt, M. O., 2006. Multi-objective trade-offs between cost and reliability in the replacement of water mains. Journal of water resources planning and management, 132(2), pp.79-88.

Dassault Systemes (2014) "ABAQUS/CAE User's Guide", Dassault Systemes Simulia Corp., Providence, RI, USA.

Deuerlein, J., Wolters, A., Roetsch, D. and Simpson, A.R., 2009. Reliability analysis of water distribution systems using graph decomposition. In World Environmental and Water Resources Congress 2009: Great Rivers (pp. 1-11).

Diniz, J. L. C., Vieira. R. D., Castro. J. T., Benjamin. A. C. and Freire, J. L. F., 2006. Stress and strain Analysis of Pipelines with Localized Metal Loss. Experimental Mechanics, vol.46 (6), pp.765-775.

DNV RP-F101, 2010. Corroded Pipeline. Det Norske Veritas, Hovik, Norway, Standard No. DNV RP-F101.

Doyle, G., Seica, M. V. and Grabinsky, M.W., 2003. The role of soil in the external corrosion of cast iron water mains in Toronto, Canada. Canadian geotechnical journal, 40(2), pp.225-236.

Ebeling, C. E., 2010. An Introduction to Reliability and Maintainability Engineering, Waveland Press, inc. Long Grove Illinois, Illinois.

Fahimi, A., Evans, T. S., Farrow, J., Jesson, D. A., Mulheron, M. J. and Smith, P. A., 2016. On the residual strength of aging cast iron trunk mains: Physically-based models for asset failure. Materials Science and Engineering: A, 663, pp.204-212.

Fares, H. and Zayed, T., 2010. Hierarchical fuzzy expert system for risk of failure of water mains. Journal of Pipeline Systems Engineering and Practice, 1(1), pp.53-62.

Fekete, G. and Varga. L., 2012. The effect of the width to length ratios of corrosion defects on the burst pressures of transmission pipelines. Engineering Failure Analysis, Elsevier, vol.21, pp. 21-30.

Fiedler, M. 1973. Algebraic connectivity of graphs. Czechoslovak mathematical journal, 23(2): 298-305.

Flannery, B. P., Press, W. H., Teukolsky, S. A. and Vetterling, W., 1992. Numerical recipes in C. Press Syndicate of the University of Cambridge, New York, 24.

Folkman, S., 2018. Water main break rates in the USA and Canada: a comprehensive study. Utah State University, Utah, USA.

Fujiwara, O. and De Silva, A. U., 1990. Algorithm for reliability-based optimal design of water networks. Journal of Environmental Engineering, 116(3), 575-587.

Gajdoš, Ľ., and Šperl, M., 2012. Determination of burst pressure of thin-walled pressure vessels. Engineering Mechanics, 67, 323-333.

Gheisi, A. R. and Naser, G., 2013. On the significance of maximum number of components failures in reliability analysis of water distribution systems. Urban Water Journal, 10(1), pp.10-25.

Ghosh, A. and Boyd, S. 2006. Growing well-connected graphs. Proceedings of the 45th IEEE Conference on Decision and Control, IEEE, San Diego, CA, USA, 6605-6611.

Goulter, I. C. and Coals, A. V., 1986. Quantitative approaches to reliability assessment in pipe networks. Journal of Transportation Engineering, 112(3): 287-301.

Goulter, I. C. and Kazemi, A., 1988. Spatial and temporal groupings of water main pipe breakage in Winnipeg. Can J Civ Eng, 15:91–97.

Grigg, N. S., Fontane, D. G. and Van Zyl, J., 2013. Water distribution system risk tool for investment planning. Water Research Foundation.

Harvey, R., 2015. An Introduction to Asset Management Tools Municipal Water, Wastewater and Stormwater Systems, a white paper prepared for the Canadian Water Network research project, The School of Engineering at the University of Guelph, Ontario, Canada.

Hasan, M., Khan, F. and Kenny, S., 2011. Identification of the cause of variability of probability of failure for burst models recommended by codes/standards. Journal of Pressure Vessel Technology, 133(4), p.041101.

Hickey, H. E., 2008. Water supply systems and evaluation methods – Volume I: Water Supply system concept. Federal Emergency Management Agency (FEMA), Washington D.C.

Hu, G., Kaur, M., Hewage, K. and Sadiq, R., 2018. An integrated chemical management methodology for hydraulic fracturing: A fuzzy-based indexing approach. Journal of Cleaner Production, 187, pp.63-75.

Hu, G., Ouache. R., Phan, H. C., Gandhi, H., Hewage, K. and Sadiq, R., 2018. Hydraulic fracturing flowback water storage failure assessment: a modified fuzzy fault tree analysis. Submitted.

Hu, Y., Wang, D., and Chowdhury, R., 2013. Long Term Performance of Asbestos Cement Pipe, Project #4093, Water Research Foundation, Denver, Colorado.

Jenkins, L., Gokhale, S. and McDonald, M., 2015. Comparison of Pipeline Failure Prediction Models for Water Distribution Networks with Uncertain and Limited Data. J. Pipeline Syst. Eng. Pract. 10.1061/(ASCE)PS.1949-1204.00001814, 04014012.

Ji, J., Robert, D. J., Zhang, C., Zhang, D. and Kodikara, J., 2017. Probabilistic physical modelling of corroded cast iron pipes for lifetime prediction. Structural Safety, 64, pp.62-75.

Jun, H., Loganathan, G. V., Kim, J. H. and Park, S., 2008. Identifying pipes and valves of high importance for efficient operation and maintenance of water distribution systems. Water resources management, 22(6), pp.719-736.

Kabir, G., Tesfamariam, S., Francisque, A. and Sadiq, R., 2015. Evaluating risk of water mains failure using a Bayesian belief network model. European Journal of Operational Research, 240(1), pp.220-234.

Kabir, G., Tesfamariam, S., Loeppky, J. and Sadiq, R., 2016. Predicting water main failures: A Bayesian model updating approach. Knowledge-Based Systems, 110, pp.144-156.

Kiefner, J. F., Vieth, P. H., 1989. A Modified Criterion for Evaluating the Strength of Corroded Pipe. Final Report for Project PR 3-805 to the Pipeline Supervisory Committee of the American Gas Association, Battelle, Ohio.

Kim, J. H. and Mays, L. W., 1994. Optimal rehabilitation model for water-distribution systems. Journal of Water Resources Planning and Management, 120(5), pp.674-692.

Kleiner, Y., Nafi, A. and Rajani, B., 2010. Planning renewal of water mains while considering deterioration, economies of scale and adjacent infrastructure. Water Science and Technology: Water Supply, 10(6), pp.897-906.

Kleiner, Y. and Rajani, B., 2001. Comprehensive review of structural deterioration of water mains: statistical models. Urban water, 3(3), pp.131-150.

Kleiner, Y. and Rajani, B., 2010. I-WARP: Individual water main renewal planner. Drinking Water Engineering and Science, 3(1), pp.71-77.

Kleiner, Y., Rajani, B. and Krys, D., 2012. Performance of ductile iron pipes. I: Characterization of external corrosion patterns. Journal of Infrastructure Systems, 19(1), 108-119.

Kleiner, Y., Sadiq, R. and Rajani, B., 2004. Modeling failure risk in buried pipes using fuzzy Markov deterioration process. In Pipeline Engineering and Construction: What's on the Horizon? (pp. 1-12).

Large, A., Gat, Y. L., Elachachi, S. M., Renaud, E. and Breysse, D., 2014. Decision support tools: Review of risk models in drinking water network asset management. In Vulnerability, Uncertainty, and Risk: Quantification, Mitigation, and Management (pp. 587-597).

Li, F., Ma, L., Sun, Y. and Mathew, J., 2014. Group maintenance scheduling: A case study for a pipeline network. In Engineering Asset Management 2011 (pp. 163-177). Springer, London.

Lindhe, A., 2008. Integrated and Probabilistic Risk Analysis of Drinking Water Systems, Thesis for the Degree of Licentiate of Engineering, Chalmers University of Technology, Goteborg, Sweden.

Liu, D., Zhou, W. and Pan, X., 2016. Risk evaluation for city gas transmission and distribution system based on information revision. Journal of Loss Prevention in the Process Industries 41 (2016), 194-201.

Loganathan, G. V., Park, S. and Sherali, H. D., 2002. Threshold break rate for pipeline replacement in water distribution systems. Journal of water resources planning and management, 128(4), pp.271-279.

Ma, B., Shuai, J., Liu, D. and Xu, K., 2013. Assessment on failure pressure of high strength pipeline with corrosion defects. Engineering Failure Analysis, Vol.32, pp. 209–219.

Male, J. W., Walski, T. M. and Slutsky, A. H., 1990. Analyzing water main replacement policies. Journal of Water Resources Planning and Management, 116(3), pp.362-374.

Marchionni, V., Cabral, M., Amado, C. and Covas, D., 2016. Estimating water supply infrastructure cost using regression techniques. Journal of Water Resources Planning and Management, 142(4), p.04016003.

Martin, O., Nilsson, K. And Jaksic, N., 2007. On plastic collapse analysis of KBS-3 canister Mock-up. JRC Scientific and Technical Report, EUR 23224 EN-2007, Joint Research Centre, Institute for Energy, European Commission, Patten, Netherlands.

Mohebbi, H. and Li, C. Q., 2011. Experimental investigation on corrosion of cast iron pipes. International Journal of Corrosion, doi:10.1155/2011/50651.

Mondal, B.C. and Dhar, A.S., 2015. Corrosion effects on the strength of steel pipes using FEA. 34th International Conference on Ocean, Offshore and Arctic Engineering, St. John’s, NL, May 31- June 5, 2015.

Mondal, B. C. and Dhar, A. S., 2016a. Burst pressure assessment for pipelines with multiple corrosion defects. Annual Conference of the Canadian Society of Civil Engineering (CSCE), London, June 1-4, 2016.

Mondal, B.C. and Dhar, A.S., 2016b. Finite-Element Evaluation of Burst Pressure Models for Corroded Pipelines", Journal of Pressure Vessel Technology, ASME, Vol. 139, 021702-1.

Montalvo, I., Izquierdo, J., Pérez, R. and Tung, M. M., 2008. Particle swarm optimization applied to the design of water supply systems. Computers & Mathematics with Applications, 56(3), pp.769-776.

Moore, E. F., 1959. The shortest path through a maze. In Proc. Int. Symp. Switching Theory, 1959 (pp. 285-292).

Moglia, M., Burn, S. and Meddings, S., 2006. Decision support system for water pipeline renewal prioritization. Journal of Information Technology in Construction (ITcon), 11(18), pp.237-256.

Mughabghab, S. F. and Sullivan, T. M., 1989. Evaluation of the pitting corrosion of carbon steels and other ferrous metals in soil systems, Waste Manage. 9 (1989) 239–251.

Muhlbauer, W. K., 2004. Pipeline risk management manual: Ideas, techniques, and resources. Elsevier.

Nazempour, R., Monfared, M. A. S. and Zio, E., 2016. A complex network theory approach for optimizing contamination warning sensor location in water distribution networks. arXiv preprint arXiv:1601.02155.

Newman, M. E., 2006. Finding community structure in networks using the Eigen-vectors of matrices. Physical review E, 74(3):036104.

Newman, M., 2010. Networks: an introduction. Oxford University Press, England.

Netto, T. A., Ferraz, U. S. and Estefen, S. F., 2005. The effect of corrosion defects on the burst pressure of pipelines. Journal of constructional steel research, 61(8), pp.1185-1204.

NIPP 2013: Partnering for Critical Infrastructure Security and Resilience. US department of homeland security.

Nishiyama, M. and Filion, Y., 2013. Review of statistical water main break prediction models. Canadian Journal of Civil Engineering, 40(10), pp.972-979.

Oh, C. K., Kim, Y. J., Baek, J. H., Kim, Y. P. and Kim, W. S., 2007. Ductile failure analysis of API X65 pipes with notch-type defects using a local fracture criterion., Journal of Pressure Vessels and Piping, Elsevier, Vol. 84, pp.5512–525.

Park, H., Ting, S., and Jeong, H., 2015. Procedural Framework for Modeling the Likelihood of Failure of Underground Pipeline Assets. J. Pipeline Syst. Eng. Pract., 10.1061/(ASCE)PS.1949-1204.0000222, 04015023.

Park, S., Vega, R., Choto, Z. and Grewe, M., 2010. Risk-based Asset Prioritization of Water Transmission/Distribution Pipes for the City of Tampa. Florida Water Resources Journal, December 2010 issue, 22-28.

Phan, H. C. and Dhar, A. S., 2016. Pipeline Maintenance Prioritization Considering Reliability and Risk: A Concept Methodology. Journal of Advances in Civil and Environmental Engineering. 3(1): 13-30.

Phan, H. C., Dhar, A. S. and Sadiq, R., 2017a. Complex network analysis for water distribution systems by incorporating the reliability of individual pipes. 6th CSCECRC International Construction Specialty Conference, CSCE 2017 Annual General Conference. Vancouver, BC, May 31 - June 3, 2017.

Phan, H. C., Dhar, A. S. and Mondal, B. C., 2017b. Revisiting burst pressure models for corroded pipelines. Canadian Journal of Civil Engineering, 44(7), pp.485-494.

Phan, H. C., Dhar, A. S., Thodi, P. and Sadiq, R., 2018a. Probability of network disconnection of water distribution system for maintenance prioritization. Journal of Water Supply: Research and Technology-Aqua, 67(3), pp.252-269.

Phan, H. C., Dhar, A. S. and Sadiq, R., 2018b. Prioritizing Water Mains for Inspection and Maintenance Considering System Reliability and Risk. Journal of Pipeline Systems Engineering and Practice. 18:9(3):04018009.

Phan, H. C., Dhar, A. S., Sadiq, R. and Hu, G., 2018c. Managing Water Main Breaks in Distribution Networks – A Risk-Based Decision Making. Submitted.

Qing, A., 2009. Differential evolution: fundamentals and applications in electrical engineering. John Wiley & Sons.

Quimpo, R. G. and Shamsi, U. M., 1991. Reliability-based distribution system maintenance. Journal of Water Resources Planning and Management, 117(3), 321-339.

Rajani, B. and Kleiner, Y., 2001. Comprehensive review of structural deterioration of water mains: physically based models. Urban water, 3(3), pp.151-164.

Rajani, B. and Tesfamariam, S., 2007, June. Estimating time to failure of cast-iron water mains. In Proceedings of the Institution of Civil Engineers-Water Management, 160, 2:83-88.

Rajani, B., Makar, J., McDonald, S., Zhan, C., Kuraoka, S., Jen, C. K. and Veins, M., 2000. Investigation of grey cast iron water mains to develop a methodology for estimating service life. Denver, CO: American Water Works Association Research Foundation.

Rogers, P. D., 2011. Prioritizing Water Main Renewals: Case Study of Denver Water System. J. Pipeline. Syst. Eng. Pract. 2011.2:73-81.

Roozbahani, A., Zahraie, B. and Tabesh, M., 2013. Integrated risk assessment of urban water supply systems from source to tap. Stochastic environmental research and risk assessment, 27(4), pp.923-944.

Ross, S. M., 1985. Introduction to probability models (No. 519.2 R826 1985). Academic Press.

Rossum, J. R., 1969. Prediction of pitting rates in ferrous metals from soil parameters, J. Am. Water Works Assoc. 61 305–319.

Sadiq, R., Rajani, B. and Kleiner, Y., 2004. Probabilistic risk analysis of corrosion associated failures in cast iron water mains. Reliability Engineering & System Safety, 86(1), pp.1-10.

Sadiq, R., Saint-Martin, E. and Kleiner, Y., 2008. Predicting risk of water quality failures in distribution networks under uncertainties using fault-tree analysis. Urban Water Journal, 5(4), pp.287-304.

Sahraoui, Y., Khelif, R. and Chateauneuf, A., 2013. Maintenance planning under imperfect inspections of corroded pipelines. International journal of pressure vessels and piping, 104, pp.76-82.

Scheidegger, A., Leitão, J. P. and Scholten, L., 2015. Statistical failure models for water distribution pipes–A review from a unified perspective. Water research, 83, pp.237-247.

Shang, F., Uber, J. G., Rossman, L. A., Janke, R. and Murray, R., 2008. EPANET multi-species extension user's manual. Risk Reduction Engineering Laboratory, US Environmental Protection Agency, Cincinnati, Ohio.

Shamir, U., and Howard, C. D., 1981. Water supply reliability theory. Am. Water Works Assoc, 73(7): 379-384.

Shinstine, D. S., Ahmed, I. and Lansey, K. E., 2002. Reliability/availability analysis of municipal water distribution networks: Case studies. Journal of water resources planning and management, 128(2), 140-151.

Sridhar, N., Dunn, D. S., Anderko, A. M., Lencka, M. M., and Schutt, H. U., 2001. Effects of water and gas compositions on the internal corrosion of gas pipelines-modeling and experimental studies. Corrosion, 57(3), 221.

St. Clair, A. M. and Sinha, S., 2014. Development of a standard data structure for predicting the remaining physical life and consequence of failure of water pipes. Journal of Performance of Constructed Facilities, 28(1), pp.191-203.

Storn, R., and Price, K., 1997. Differential Evolution – A simple and efficient heuristic for global optimization over continuous spaces. Journal of Global Optimization, Vol.11, pp. 341-359.

Storn. R., 2008. Differential Evolution Research – Trends and Open Questions, Advances in Differential Evolution. Springer-Verlag Berlin Heidelberg, pp. 1-31.

Swankie, T., Chauhan, V., Owen, R., Bood, R. and Gilbert, G., 2012, September. Assessment of the remaining strength of corroded small diameter (below 6") pipelines and pipework. In 2012 9th International Pipeline Conference (pp. 673-682). American Society of Mechanical Engineers.

Su, Y. C., Mays, L. W., Duan, N. and Lansey, K. E., 1987. Reliability-based optimization model for water distribution systems. Journal of Hydraulic Engineering, 113(12), pp.1539-1556.

Tchorzewska-Cieslak, B., 2011. Matrix method for estimating the risk of failure in the collective water supply system using fuzzy logic. Environment Protection Engineering, 37(3), pp.111-118.

Tee, K. F. and Khan, L. R., 2012, July. Risk-cost optimization and reliability analysis of underground pipelines. In Proceedings of the 6th International ASRANet Conference, London, UK (pp. 2-4).

Tee, K. F., Khan, L. R. and Chen, H. P., 2013. Probabilistic failure analysis of underground flexible pipes. Structural engineering and mechanics, 47(2), pp.167-183.

Thodi, P. N., Khan, F. I. and Haddara, M. R., 2010. The Development of Posterior Probability Models in Risk-Based Integrity Modeling. Risk analysis, 30(3), pp.400-420.

Tung, Y. K., 1985. Evaluation of water distribution network reliability. In Hydraulics and hydrology in the small computer age, Speciality conference, ASCE, 359-364.

Wagner, J. M., Shamir, U. and Marks, D. H., 1988. Water distribution reliability: analytical methods. Journal of Water Resources Planning and Management, 114(3), pp.253-275.

Walski, T. M. and Pelliccia, A., 1982. Economic analysis of water main breaks. Journal (American Water Works Association), pp.140-147.

Walski, T. M., 1993. Water distribution valve topology for reliability analysis. Reliability engineering & system safety, 42(1), pp.21-27.

Wang, C. W., Niu, Z. G., Jia, H. and Zhang, H. W., 2010. An assessment model of water pipe condition using Bayesian inference. Journal of Zhejiang University-SCIENCE A, 11(7), pp.495-504.

Wang, N. and Zarghamee, M., 2013. Evaluating Fitness-for-Service of Corroded Metal Pipelines: Structural Reliability Bases. J. Pipeline Syst. Eng. Pract., 10.1061/(ASCE)PS.1949-1204.0000148, 04013012.

Watson, T. G., Christian, C. D., Mason, A. J., Smith, M. H. and Meyer, R., 2004. Bayesian-based pipe failure model. Journal of Hydroinformatics, 6(4), pp.259-264.

Wu, W., Cheng, G., Hu, H. and Zhou, Q., 2013. Risk analysis of corrosion failures of equipment in refining and petrochemical plants based on fuzzy set theory. Engineering Failure Analysis, 32, pp.23-34.

Velazquez, J. C., Caleyo, F., Valor, A. and Hallen, J. M., 2009. Predictive model for pitting corrosion in buried oil and gas pipelines, Corrosion, 65:332–342.

Vincenzi, L., Roeck, G. D. and Savoia, M., 2013. Comparison between coupled local minimizers method and differential evolution algorithm in dynamic damage detection problems. Advances in Engineering Software, Vol. 65 (2013), pp. 90–100

Yan, J. M. and Vairavamoorthy, K., 2003. Fuzzy approach for pipe condition assessment. In New pipeline technologies, security, and safety (pp. 466-476).

Yannopoulos, S. and Spiliotis, M., 2013. Water distribution system reliability based on minimum cut–set approach and the hydraulic availability. Water Resources Management, 27(6), 1821-1836.

Yazdani, A. and Jeffrey, P. 2010. Robustness and vulnerability analysis of water distribution networks using graph theoretic and complex network principles. Water Distribution Systems Analysis, 933-945.

Yazdani, A. and Jeffrey, P., 2011a. Complex network analysis of water distribution systems. Chaos: An Interdisciplinary Journal of Nonlinear Science, ASCE,21(1): 933-945.

Yazdani, A. and Jeffrey, P., 2011b. Applying network theory to quantify the redundancy and structural robustness of water distribution systems. Journal of Water Resources Planning and Management, 138(2): 153-161.

Yoo, D. G., Kang, D., Jun, H. and Kim, J.H., 2014. Rehabilitation priority determination of water pipes based on hydraulic importance. Water, 6(12), pp.3864-3887.

Zhou, W. and Huang. X. G., 2012. Model error assessments of burst capacity models for corroded pipes. International Journal of Pressure Vessels and Piping Vol. 99-100, pp. 1-8.

Zhou, W. and Zhang, S., 2015. Impact of model errors of burst capacity models on the reliability evaluation of corroding pipelines. Journal of Pipeline Systems Engineering and Practice, 7(1), p.04015011.

Zhu, X. and Leis, B. N., 2012. Evaluation of burst pressure prediction models for line pipes. International Journal of Pressure Vessels and Piping, vol. 89, pp. 85-97.

Zhuang, B., Lansey, K. and Kang, D., 2012. Resilience/availability analysis of municipal water distribution system incorporating adaptive pump operation. Journal of Hydraulic Engineering, 139(5), pp.527-537.